



FIRE-RES

Innovative technologies & socio-ecological-economic solutions for fire resilient territories in Europe

D2.3 QUALITY STANDARD FOR WUI ARCHITECTURE AND LANDSCAPE DESIGN

www.fire-res.eu

fire-res@ctfc.cat

Project Acronym: FIRE-RES

Project name: Innovative technologies and socio-ecological-economic solutions for fire resilient territories in Europe

Call ID: H2020-LC-GD-1-1-2020 (Preventing and fighting extreme wildfires with the integration and demonstration of innovative means)

Work Package: 2

Task Number: 2.1

Lead beneficiary: Centre National de la Recherche Scientifique (CNRS)

Contributing beneficiary(ies): Centre National de la Recherche Scientifique (CNRS), Instituti SistemasCoplejos de Ingenieria (ISCI), Instituti Superior de Agronomia (ISA), Cabildo Insular de Gran Canaria (CIGC).

Publication

Publication date: 25/11/2024

Authors: Virginie Tihay Felicelli, CNRS; Anthony Graziani, CNRS; Toussaint Barboni, CNRS; Yolanda Perez-Ramirez, CNRS; Paul-Antoine Santoni, CNRS.

Abstract: The document provides a state-of-the-art review of the regulations or recommendations for fuel management and home hardening to prevent wildland fire in the WUI. The section on architectural design presents the study on the vulnerability of joinery to hedge fires. The landscaping section first presents the study on the influence of fuel moisture content on the ignition and burning of shrubs. This is followed by the numerical study of the effectiveness of fuel management in two case studies in Portugal and Chile.

Key words: joinery, landscaping, WUI, forest fire prevention

Quote as: Virginie Tihay Felicelli, Anthony Graziani, Toussaint Barboni, Yolanda Perez-Ramirez, Paul-Antoine Santoni, D2.3 Quality standard for WUI architecture and landscape design, DOI: 10.5281/zenodo.13941898

DOI: [10.5281/zenodo.13941898](https://doi.org/10.5281/zenodo.13941898)

Dissemination level

[X] PU- Public: must be available in the website

[] CO- Confidential: Only for members of the Consortium and the Commission Services

[] CI – Classified: As referred in to Commission Decision 2001/844/EC

Document history

Edition	Date	Status	Author
Version 1	15/10/2024	Draft	Virginie Tihay Felicelli (CNRS), Anthony Graziani, (CNRS), Toussaint Barboni, (CNRS), Yolanda Perez-Ramirez CNRS; Paul-Antoine Santoni (CNRS)
Version 2	28/10/2024	Revision	Eva Samblàs Vives (CIGC)
Version 3	16/11/2024	Revision	José Borges (ISA)
Version 4	19/11/2024	Revision	Mar Viana (IDAEA)
Version 5	25/11/2024	Revised Version	Virginie Tihay Felicelli (CNRS), Anthony Graziani, (CNRS), Toussaint Barboni, (CNRS), Yolanda Perez-Ramirez CNRS; Paul-Antoine Santoni (CNRS)

Copyright © All rights reserved. This document or any part thereof may not be made public or disclosed, copied or otherwise reproduced or used in any form or by any means, without prior permission in writing from the FIRE-RES Consortium. Neither the FIRE-RES Consortium nor any of its members, their officers, employees or agents shall be liable or responsible, in negligence or otherwise, for any loss, damage or expense whatever sustained by any person as a result of the use, in any manner or form, of any knowledge, information or data contained in this document, or due to any inaccuracy, omission or error therein contained.

All Intellectual Property Rights, know-how and information provided by and/or arising from this document, such as designs, documentation, as well as preparatory material in that regard, is and shall remain the exclusive property of the FIRE-RES Consortium and any of its members or its licensors. Nothing contained in this document shall give, or shall be construed as giving, any right, title, ownership, interest, license or any other right in or to any IP, know-how and information.

The information and views set out in this publication does not necessarily reflect the official opinion of the European Commission. Neither the European Union institutions and bodies nor any person acting on their behalf, may be held responsible for the use which may be made of the information contained therein.

Table of contents

1. INTRODUCTION	1
2. CASE STUDY IN THE LIVING LABS	2
2.1. Chile	3
2.2. Portugal	4
2.3. Canary Islands	6
3. ARCHITECTURE DESIGN	8
3.1. Guidelines, standards and regulations	8
3.1.1. <i>Global overview</i>	8
3.1.2. <i>Focus on the living labs</i>	15
3.2. Materials and methods	19
3.3. Results and discussion	25
3.3.1. <i>Description of the hedge burning and flame geometry</i>	25
3.3.2. <i>Heat fluxes and damage</i>	29
3.3.3. <i>Smoke analysis</i>	35
4. LANDSCAPE DESIGN	39
4.1. Guidelines, standards and regulations	39
4.2. Plant moisture content	42
4.2.1. <i>Materials and methods</i>	42
4.2.2. <i>Results and discussion</i>	44
4.3. Numerical study	48
4.3.1. <i>Materials and methods</i>	48
4.3.2. <i>Validation setup at field scale: the EXPLORII Platform</i>	51
4.3.3. <i>Results and discussion</i>	53
5. RECOMMENDATIONS	63
6. CONCLUSIONS	66
7. REFERENCES	67
8. ANNEX	73
8.1. Annex 1: Summary of test methods used to test built elements [28]	74
8.2. Annex 2: Use type (UT) and risk categories (CR) in Portuguese law [99]	79

List of figures

Figure 1: a) Positioning b) Aerial view - of the area of interest chosen for the Chile living lab	3
Figure 2: Map of the location of species in the area of interest in Chile [25]	4
Figure 3: House inventory in Portuguese living lab	5
Figure 4: Aerial view of the area of interest for the Portuguese living lab	5
Figure 5: Photograph of the a) house on plot 105 b) vegetation on plot 34 - of the inventory given by the Portuguese stakeholders	6
Figure 6: House inventory in Canary Islands' living lab	7
Figure 7: Test module used for evaluating the fire performance of a window with SFM 12-7A-2 [29].....	9
Figure 8: Exposure conditions for radiant heat test in AS 1530.8.1 [30]	11
Figure 9: Standard configurations for glazing systems [30].....	12
Figure 10: Layout of the EXPLORII platform a) General view b) View of the exposed facade - 1: Cameras. 2: Pairs of total and radiant heat flux gauges. 3: K-type surface thermocouple 4: Radiant heat flux gauge. 5: 2D sonic anemometer. 6: 3D anemometer. 7: Go Pro. 8: Load Cell under the hedge. 9: Sampling rod for the outdoor smoke analysis	22
Figure 11: Image processing to define the descriptors of the flame geometry a) Original image b) Flame using k-means clustering.....	24
Figure 12: Photographs of the joinery a) Windows made of PVC (left), Aluminium (centre) and Wood (right) ; b) Shutters made of PVC (left), Aluminium (centre) and Wood (right).....	25
Figure 13: Photographs of the burning phases of cypress hedge a) Fire spread in wood wool; b) Hedge ignition. c) Hedge burning and d) Hedge extinction.....	26
Figure 14: Photographs of the burning phases of rockrose hedge a) Fire spread in wood wool; b) Hedge ignition. c) Hedge burning and d) Hedge extinction.....	27
Figure 15: Mass loss during the hedge burning.....	27
Figure 16: Radiant heat fluxes measured on the façade during the burning of the rockrose and cypress hedges.....	30
Figure 17: Photographs of the damage observed on the joinery a) Breakage of the exposed glass b) Blackened wood shutter c) Burnt wood shutter d) Deformed PVC shutter e) Blackened PVC shutter f) Burnt PVC shutter	31
Figure 18: Blackening and burning thresholds for wooden shutters.....	33
Figure 19: Blackening and burning thresholds for PVC shutter	33
Figure 20: Damage-free thresholds for aluminium shutter	34
Figure 21: Photographs of the hedge burning of a) rockrose b) cypress equipped with smoke analysers	36
Figure 22: Aerosol number measurements and wind speed during two experiments with a rockrose hedge	36
Figure 23: Evolution of number size distribution ($dN/\log D_p$, $1/\text{cm}^3$) for different experiments carried out with rockrose hedge.....	37

Figure 24: Number size distribution ($dN/\log D_p$, $1/\text{cm}^3$) as function of time (s) and aerodynamic diameter (μm) during a test with a cypress hedge.....	37
Figure 25: Schematic diagram of the laboratory experiments for the influence of the moisture content on the fire behaviour	43
Figure 26: Different phases of an experiment with a fuel MC of 10 % - a) Fire front spread across the wood wool bed b) Branch ignition c) Flame spread upward through the branches d) Extinction phase	45
Figure 27: Different phases of an experiment with a fuel MC of 65 % - a) Fire front spread across the wood wool bed b) Branch ignition c) Flame spread upward through the branches d) Extinction phase	45
Figure 28: Different phases of an experiment with a fuel MC of 100 % - a) Fire front across the wood wool bed b) No ignition of the branches	45
Figure 29: a) Mass loss divided by the initial wet mass b) Mass loss rate (MLR) - for three leaf MC: 25 %, 65 % and 100 %.....	46
Figure 30: a) Final mass loss of the rockrose branches calculated from the initial wet mass – b) Peak of mass loss rate for the rockrose branches – as function of the different leaf MC.....	46
Figure 31: Topography modelling: (a) Chile DTM superimposed by the parcel details, (b) Smokeview rendering of the numerical terrain implementation	49
Figure 32: Example of meshing strategy around the structures for the Chilean scenario.....	49
Figure 33: Smokeview rendering of the Portuguese scenario illustrating the boundary conditions including the wind modelling, and the vegetation.....	50
Figure 34: Smokeview representation of the numerical domain for the EXPLORII simulation cases.	52
Figure 35: Smokeview representation of the Chilean Living Lab scenarios: (a) Standard Vegetation, (b) Landscaping Management.....	54
Figure 36: Iso-surface of HRRPUV at 200 kW/m^2 predicted for the Chile scenario in extreme weather conditions: (a) Unmanaged vegetation, (b) Managed vegetation.	56
Figure 37: Iso-surface of HRRPUV at 200 kW/m^3 reaching houses façade for the Chilean Scenario: (a) at given time t , (b) at $t + 10 \text{ s}$	57
Figure 38: Thermal Dose for each sensor positioned on the façade of house number 3 and damages thresholds for wood and PVC.	58
Figure 40: Smokeview representation of the Chilean Living Lab scenarios: (a) Unmanaged Vegetation, (b) Landscaping Management	59
Figure 40: Iso-surface of HRR per unit of volume at 200 kW/m^2 predicted for the Portuguese scenario: (a) Unmanaged vegetation, (b) Managed vegetation	61
Figure 41: Thermal Dose for each sensor positioned on the façade of house n°3 superimposed with damages threshold.	62

List of tables

<i>Table 1: Timber crib dimensions in AS 1530.8.1 (based on properties for Douglas Fir) [30].....</i>	<i>11</i>
<i>Table 2: Summary of the requirements for glazing systems in AS 3959 [5].....</i>	<i>13</i>
<i>Table 3: Parameters ϕ_0 and k_0 for the calculation of the incident heat flux in Portugal [6].....</i>	<i>17</i>
<i>Table 4: Required reaction to fire for windows, skylights and shutters</i>	<i>18</i>
<i>Table 5: Required fire resistance for windows.....</i>	<i>18</i>
<i>Table 6: Description of the sensors used on the EXPLORII platform.....</i>	<i>23</i>
<i>Table 7: Range of the experimental conditions observed during the burning tests. The mean value and the standard deviation are in parenthesis.....</i>	<i>24</i>
<i>Table 8: Description of windows and shutters used for testing.....</i>	<i>25</i>
<i>Table 9: Range of the fire descriptors recorded during the hedge burning.....</i>	<i>28</i>
<i>Table 10: Summary of damage observed on the joinery</i>	<i>30</i>
<i>Table 11: Indicators for the breakage of the windows</i>	<i>35</i>
<i>Table 12. Mean particle size distributions in number and volume emitted during the hedge burning..</i>	<i>37</i>
<i>Table 13. Particle size distributions in number and volume emitted during the burning</i>	<i>38</i>
<i>Table 14: Defensible space characteristics found in regulations/guidelines worldwide</i>	<i>42</i>
<i>Table 15: Average values of the initial wet and dry mass of rockrose for the different leaf moisture contents tested.</i>	<i>44</i>
<i>Table 16: Summary of the results for all experiments: average final mass loss and peak of MLR for the different leaf moisture contents tested.</i>	<i>47</i>
<i>Table 17: Ambient conditions and vegetation moisture content for the EXPLORII test cases.</i>	<i>51</i>
<i>Table 18: Relative difference between experimental measurements and numerical predictions for the EXPLORII test cases.....</i>	<i>53</i>
<i>Table 19: Ambient conditions considered for the Chilean numerical scenario.</i>	<i>54</i>
<i>Table 20: Properties of the vegetation used for the Chilean scenarios. FE: Fuel Element approach, BF: Boundary Fuel approach. Twigs refer to particles of 0 – 2 mm</i>	<i>55</i>
<i>Table 21: Prediction of thermal exposure and material damage for the different scenarios of the Chilean living lab.</i>	<i>58</i>
<i>Table 22 Ambient conditions considered for the Portuguese numerical scenario.</i>	<i>59</i>
<i>Table 23: Properties of the vegetation used in the Portuguese scenarios. FE: Fuel Element approach, BF: Boundary Fuel approach. Twigs refer to particles of 0 – 2 mm</i>	<i>60</i>
<i>Table 24: Prediction of thermal exposure and material damage for different scenarios of the Portugal living lab simulation case.....</i>	<i>62</i>

1. INTRODUCTION

Due to climate change and rural area expansion, the severity and frequency of wildfires have dramatically increased in recent decades. These fires impact ecosystems and can cause significant damage to structures, injuries, or fatalities [1,2]. Wildland-urban interfaces (WUI) are particularly high-risk areas. In these areas, human activities increase the risk of fire ignition [3], while structures are adjacent to or intermingled with wildland vegetation. In the remainder of this report, the definition given by the Federal Register for the different types of WUI will be used [4].

The WUI interface consists of areas where three or more structures per acre (4046.9 m²) are in direct proximity to wildland vegetation. Wildland vegetation typically does not extend into the developed area. Intermixed interfaces are areas where structures (with a density greater than 1 house per 40 acres or 6.17 houses per km²) are scattered among wildland vegetation. Worldwide, fire risk prevention in WUI generally involves increasing the fire resistance of structures [5–11] and managing fuels around buildings [6,8,12–20].

In the light of recent disasters caused by forest fires [21], it appears that prevention policies have weaknesses that need to be addressed in order to make buildings in WUI resilient. This is all the more important as the number of extreme fires tends to increase in Europe and effective prevention policies need to be developed to make the territory resilient. As highlighted in the review by Filkov et al. in 2023, there is a lack of specification of fire exposure conditions in the WUI, as well as of information about the effects of fire on structures [22].

To try to fill these gaps, the work we carried out as part of the FIRE-RES project had two aims. The first was to contribute to architectural design. This encompassed an experimental study of the effects of a hedge fire on the joinery. Hedges were chosen because post-fire studies have shown that they are vectors for the spread of fire from wildland vegetation to buildings [23]. The joinery was chosen because it is a vulnerable element of the building envelope, as shown by studies of vegetation fire damage [1]. The second objective was to contribute to landscape design. This included an assessment of how landscaping can change the impact of fire on structures, in order to determine whether the fuel management recommendations made in the areas studied were sufficient to ensure their resistance to vegetation fire. To this end, an experimental study of the influence of moisture content on vegetation ignition and fire spread was conducted. A numerical study based on data coming from the Living Labs of Portugal (WUI interface) and Chili (intermixed interface) was also carried out to address this issue.

Recommendations for landscaping and architecture design in the WUI were then made based on the results of these works. Three fundamental pathways have been identified for the spread of fire in the WUI: the radiant exposure, the direct flame contact exposure and the firebrand exposure [24]. Only radiant and direct flame contact have been considered in this report. Firebrands have not been investigated as the fire prevention recommendations worldwide are generally based on fire radiation and direct flame contact. The report is divided into four parts. The first part presents the case studies in the three participating Living Labs - Chile, Portugal and the Canary Islands -, whose

Communities of Wildfire Innovation were involved in this Innovation Action. The second part presents the results on the architectural design for WUI by focusing on joinery. The third part is dedicated to the WUI landscape design results. The last part presents the recommendations for both architecture and landscape design.

2. CASE STUDY IN THE LIVING LABS

The work we proposed involved three living labs: Chile, Portugal and the Canary Islands, which were interested in increasing the resilience of their buildings in WUIs. For each of them, we asked the stakeholders to define an area of interest for our study, with dimensions of approximately 300 m × 100 m, including a maximum of 3 houses. For this area, we asked them for the following data:

- Type 1: GIS data
 - DEM and DSM model for this area
 - National Map of Vegetation for this area
 - Cadastre data for the dwellings
- Type 2: Fire data
 - Fuel maps (Fire behaviour Fuel Models)
 - Meteorological data of the area of interest during the fire season
- Type 3: Vegetation data
 - Fuel moisture content (dead and live) during the fire season
 - National Forest Inventory data
- Type 4: Other Data
 - WUI Regulations in the zone of interest
 - RTEEX fire: Historic wildfire records and house destruction
 - Information on the building materials: Type of construction, Base material, Insulation Type, Exterior cladding, Joinery material, Presence of shutters (yes/no) if yes: Shutter material, Roof material, Exposed framework (yes/no), Presence of gutters (yes/no) if yes: Gutter material.

Chile and Portugal sent us the information we requested. The Canary Islands sent only Type 4 data late, which precluded the possibility of developing the landscape design study in this Living Lab. The Canary Islands were only considered for the architectural design part.

Based on the data obtained from Types 1 to 3, and after discussion with stakeholders in Portugal and Chili, in particular on the weather conditions to be considered, scenarios for numerical simulations of a fire arriving in the areas of interest (defined by the Living Labs in the WUI) were chosen for Chile and Portugal as part of the Landscape Design study. A summary of the data for each participating Living Lab is presented in the following section.

2.1. Chile

The Chilean stakeholders have defined an area of interest approximately 2 km from the town of Rafael, a community located 20 km from Tomé, Province of Concepción, Bio-Bio Region (Figure 1.a). The GPS point of this area is as follows: 36°38'21.9"S 72°48'41.0"W. In this area, there are 4 buildings (Figure 1.b). Houses 1, 2 and 3 are wooden houses with zinc roofs. House 1 has wooden cladding. Houses 2 has Internit (fibre cement) cladding and house 3 has cement cladding. House 4 is made of Internit (fibre cement) with a roof in zinc. None of the houses has shutters. In our study we have not taken into account the secondary structures that exist around the 4 main houses, as no data was provided for them.



Figure 1: a) Positioning b) Aerial view - of the area of interest chosen for the Chile living lab

Fruit trees and ornamental vegetation are present near the buildings. In addition, the houses are surrounded by a forest composed of *Nothofagus obliqua*, *Eucalyptus globulus* and *Acacia melanoxylon* with an undergrowth composed of several species such as *Aristotelia chilensis*, *Cryptocaria alba*, *Acacia melanoxylon*, *Pinus radiata*, *Eucalyptus globulus*, *Luma apiculata*, *Gevuina avellana*, *Peumus boldus*, *Genista monspessulana*, *Rubus ulmifolius*, *Boquila trifoliolata*, *Acrisione denticulata*, *Elytropus chilensis*, *Azara integrifolia*, *Myoschilos oblogum* and *Lapageria rosea*. So this is an Intermix WUI. A report on the species present in the area of interest was provided by CORMA [25], which gave us data on the location of the species and the characteristics of the trees and undergrowth (Figure 2). The resolution of the Digital Terrain Model provided by the stakeholders is 1 m.

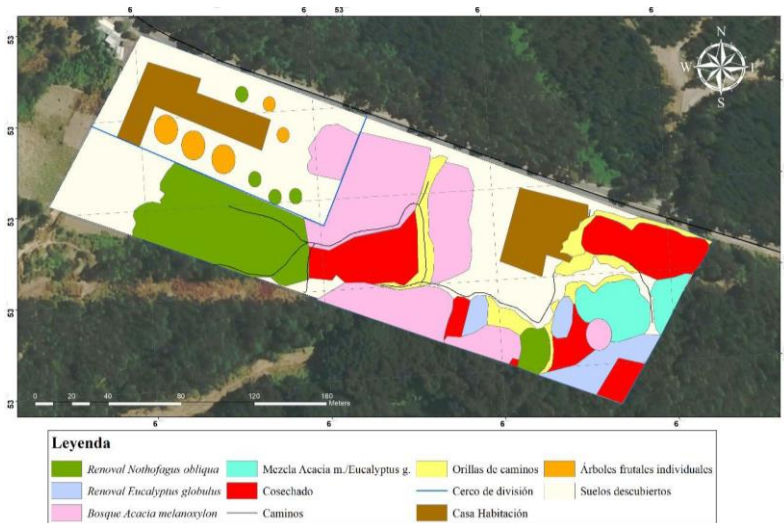


Figure 2: Map of the location of species in the area of interest in Chile [25]

2.2. Portugal

The Portuguese stakeholders selected a study area in Vale do Sousa. They gave us a digital terrain model with a resolution of 30 metres. The inventory of houses in the Portuguese Living Lab shows that the houses are mainly made of cement or stone with a ceramic tile roof (Figure 3). The joinery is mainly aluminium or aluminium and wood, and half of the windows are single glazed. 61% of the houses have shutters in aluminium or PVC. The Portuguese stakeholders did not specify any particular area of interest. However, they specified that our simulations should consider a hilly terrain that is representative of the fire-prone areas in the Portuguese Living Lab. We selected an area of interest located in the municipality of Capela (41°05'45"N 8°20'47"W), in an Interface WUI (Figure 4).

D2.3 QUALITY STANDARD FOR WUI ARCHITECTURE AND LANDSCAPE DESIGN

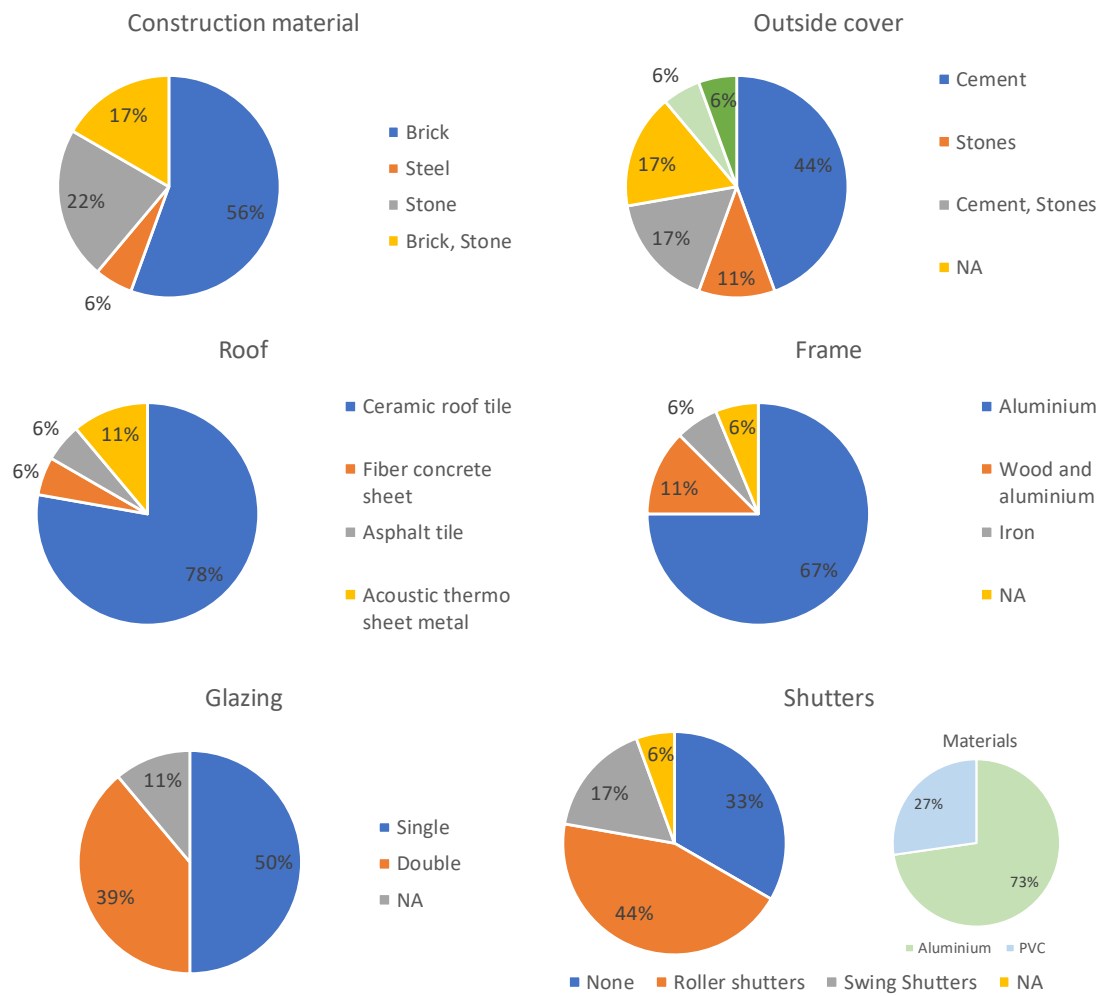


Figure 3: House inventory in Portuguese living lab

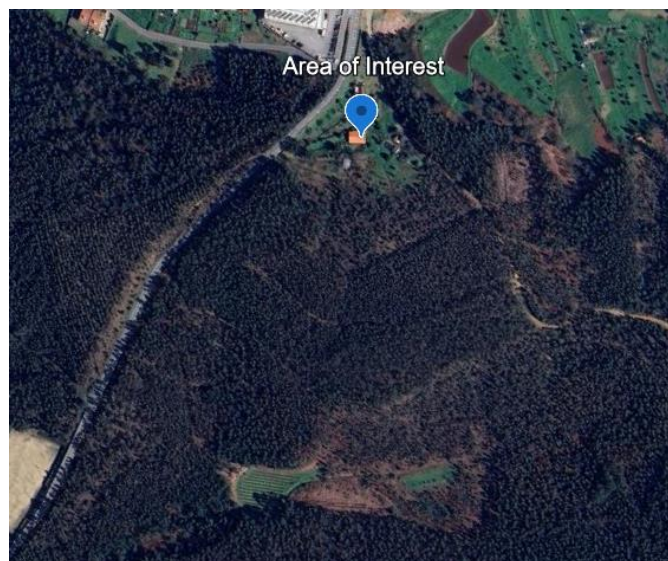


Figure 4: Aerial view of the area of interest for the Portuguese living lab

For the house, we chose the characteristics corresponding to the plot 105, as suggested by the stakeholders (Figure 5.a). This house is built of brick with cement render and has a ceramic tiled roof. It has single glazed windows with aluminium frames and PVC shutters. The house is located at the top of the slope, which contributes to increase the fire risk involved. The Portuguese stakeholders also requested to use the vegetation from plot 34 of the inventory, which corresponds to 8-year-old eucalyptus trees with an understorey of *Spartium junceum*, *Genista*, *Cytisus*, *Ulex argenteus* and herbaceous plants (Figure 5.b).



Figure 5: Photograph of the a) house on plot 105 b) vegetation on plot 34 - of the inventory given by the Portuguese stakeholders

2.3. Canary Islands

The Living Lab of Canary Islands is focused on Gran Canaria Island. However, due to a change in the composition of the consortium, the data collection was reduced to information on four typical building and information on legislation in the WUI. The inventory of houses in the Canary Islands' Living Lab shows that the houses are mainly made of cement (Figure 6). Half of the houses have tiled roofs and the other half have cement flat roofs. 75% of houses have single glazed windows and aluminum frames. 3 quarters of houses have shutters, 67% of which are wooden.

D2.3 QUALITY STANDARD FOR WUI ARCHITECTURE AND LANDSCAPE DESIGN

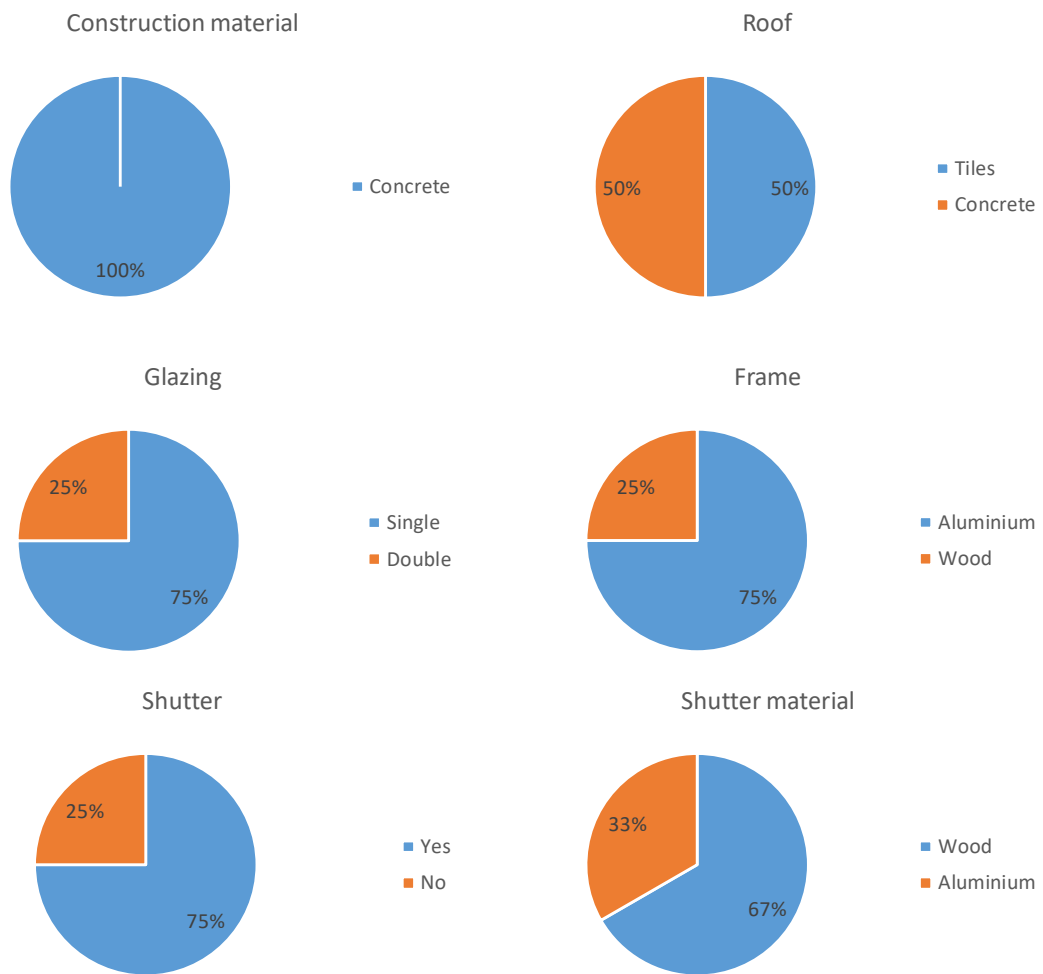


Figure 6: House inventory in Canary Islands' living lab

3. ARCHITECTURE DESIGN

This section presents the study on architectural design in WUIs carried out within the FIRE-RES project. Increasing the fire resistance of buildings, also called hardening of houses, is indeed one of the means to minimize the impact of forest fires in WUI. In this section we will summarise the different recommendations, standards and regulations that exist in the world on this subject. A sub-part has been dedicated to the case of the living labs that participated in this study. Then we will describe the experimental devices set up at house scale to study the vulnerability of windows and shutters to a hedge fire. Finally, the results are presented and discussed in order to give recommendations for joinery in WUI.

3.1. Guidelines, standards and regulations

3.1.1. Global overview

Recommendations for “hardening” buildings can be found in various fire-prone areas. Common recommendations include using non-combustible materials at the base of walls or for window sills, installing metal mesh screens over vents and chimney holes to prevent the entry of firebrands, using roof gutters made of non-combustible materials, closing or boxing open eaves with non-combustible materials, or sealing all gaps in the eaves area with caulking material [7–11,15,26,27].

Some countries also have standards for testing building materials for lessening the destruction on the built environment caused by outdoor fires. The ISO/TR 24188 provides an overview of global testing methodologies related to the vulnerability of roof assemblies, external walls and facades, windows, decks, eaves or vents to large outdoor fire exposures [28]. Annex 1 summarises the scenarios used in the different standards to model the three different exposures to the building: radiation, firebrands and direct flame contact. Except for the case of firebrands which is not considered in this study, the tests are mainly carried out using either furnaces, radiant panels or burners.

Focusing on joinery, the performance of exterior windows is tested in the United States with the SFM 12-7A-2 standard [29] and in Australia with the AS 1530.8.1 [30] and AS 1530.8.2 [31] standards. In the SFM 12-7A-2 standard [29], windows (less than 900 mm wide) are installed in a non-combustible wall. A 100 × 1000 mm diffusion burner with an output of 150 kW is placed against the wall and centered in relation to the width of the wall assembly (Figure 7). The distance from the floor to the top of the burner is 30 cm. The test is continued until flame-through occurs at the window. Flame-through may occur at the glass (glazing) and/or in the frame. To pass this test, the window and window assembly shall withstand 8 minutes of direct flame exposure without flame penetration through the window frame or glazing, or structural failure of the window frame or glazing.

For new buildings located within a Wildland-Urban Interface Fire Area, the glazing systems installed must comply the SFM 12-7A-2 standard [32]. For the other buildings in WUI, it is recommended that existing windows are replaced with double-glazed windows with tempered glass and metal frames [26]. It is also recommended to install mesh

screens with an opening of less than 1/16 inch (1.6 mm) to prevent the ingress of firebrands. Shutters are only required in hurricane areas. The installation of 1/2 inch (12.7 mm) thick plywood panels over the windows is suggested as a less expensive alternative [33].

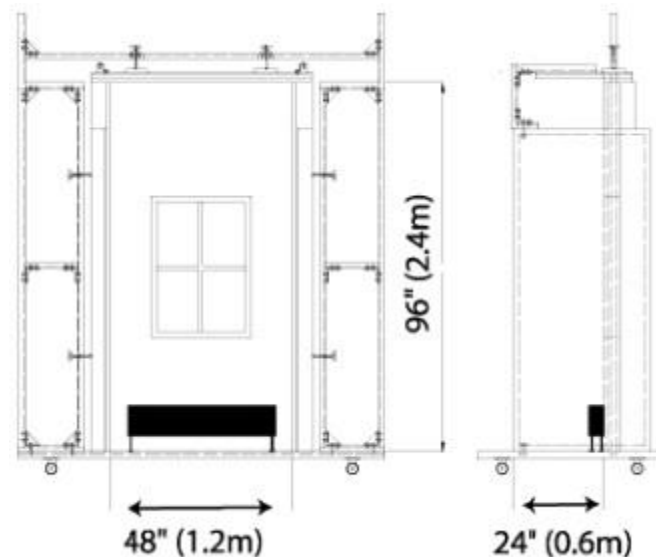


Figure 7: Test module used for evaluating the fire performance of a window with SFM 12-7A-2 [29]

The Australian Standard for the Construction of Buildings in Bushfire Prone Areas (AS 3959 [5]) specifies requirements for building materials in relation to the bushfire attack levels (BAL). There are 6 bushfire attack levels: BAL-LOW, BAL-12.5, BAL 19, BAL-29, BAL-40 and BAL-FZ. The level depends on the region, the slope, the vegetation and the distance between the building and the vegetation. The highest level is BAL-FZ and corresponds to a case with flame contact, ember attack and radiant heat of more than 40 kW/m². Table 2 gives a summary of the requirements for glazing system for the different BAL. The standard to test the building materials apply depends on whether direct flame impingement is considered (AS 1530.8.2 [31]) or not (AS 1530.8.1 [30]). The AS 1530.8.1 aims to test the performance of materials exposed to radiant heat, burning debris and burning embers without direct flame impingement [30].

Exposure to burning embers impinging on the vertical and underside of exposed horizontal surfaces is simulated by application of a small gas flame (25 mm long) to volatiles released from combustible materials. Exposure to burning debris and the collection of burning embers on the upper surface of horizontal is simulated by pre-ignited timber cribs.

There are three options for timber crib sizes (Table 1). The selection of size of the crib and position for application are based on the potential for debris to collect. The crib size Class A is representative of debris that may collect around a building with reasonable levels of housekeeping. This is the default size. Class B and C cribs simulate collections of debris that are representative of larger collections of debris, which may be more appropriate for

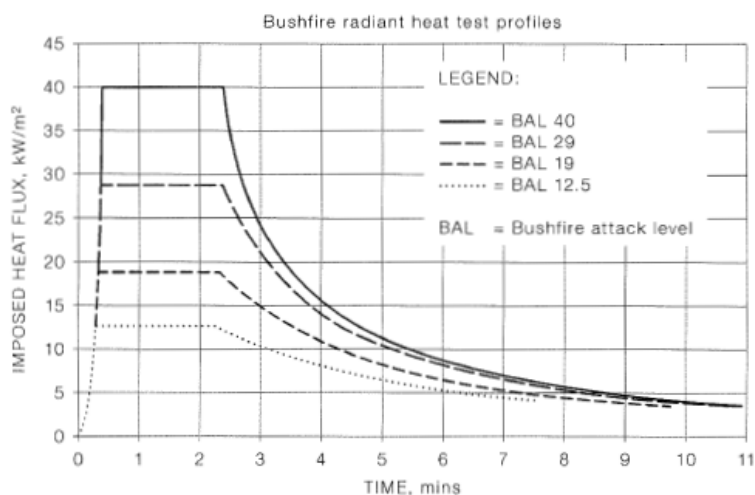
facilities and structures that are not regularly maintained or where it is expected that accumulation of debris may occur. The cribs are ignited by exposure to a gas burner for 3, 4 and 5 minutes for Class A, Class B and Class C cribs, respectively. The passage of the fire front near the structure is simulated with a radiant heat profile combined with a pilot ignition source (small gas flame to simulate embers or burning cribs to simulate debris). The radiant heat source shall be at least 3000 mm × 3000 mm high or be 400 mm wider and 400 mm higher than the construction element to be evaluated. Four profiles can be used (Figure 8): BAL 12.5, BAL 19, BAL 29 and BAL 40. The values 12.5, 19, 29 and 40 correspond to the incident radiation in kW/m². To test the windows, the glazing system is installed in a wall according to the configurations shown in Figure 9. To pass the test, the glazing system shall not allow:

- Formation of an opening from the fire-exposed face to the non-fire-exposed face of the element through which a 3 mm diameter probe can penetrate during the 60 min test period.
- Sustained flaming for more than 10 s on the non-fire side during the 60 min test period.
- Flaming on the fire-exposed side at the end of the 60 min test period.
- Radiant heat flux 365 mm from the non-fire side of the specimen in excess of 15 kW/m² from glazed and uninsulated areas during the 60 min test.
- Mean and maximum temperature rises greater than 140 K and 180 K, respectively, on the non-fire side during the 60 min test, except for glazed/uninsulated areas for which the radiant heat flux limits are applicable.
- Radiant heat flux 250 mm from the fire-exposed face of the specimen, greater than 3 kW/m² between 20 min and 60 min after the commencement of the test.
- Mean and maximum temperatures of the internal faces of construction including cavities, exceeding 250°C and 300°C respectively between 20 min and 60 min after the commencement of test.

In AS 1530.8.2 [31], in order to model the direct flame impingement from the fire, the glazing system is subjected to the standard heating regime of AS 1530.4 [34] for 30 minutes as given by:

$$T = 345 \log_{10}(8t + 1) + 20 \quad (1)$$

Where t is the time into the test, measured from the ignition of the furnace (in minute) and T is the furnace temperature at time t (in degree Celsius). The glazing system fails the test if integrity is deemed to have been lost. This occurs if the element collapses, or if a gap or fissure exceeding 6 mm × 150 mm or a hole exceeding 25 mm diameter develops in the glazing or its surrounding construction or if flaming occurs for 10 s or of longer duration.



**BUSHFIRE RADIANT HEAT TEST PROFILES—
TIME FROM START OF TEST**

Bushfire Attack Level (BAL)	Incident Radiation kW/m ²	Time from start of test (s)								
		20–140	140–180	180–240	240–300	300–360	360–420	420–480	480–540	540–600
Severe [1]	40	Min 40	24	16	12	8.5	7	5	4	3
Very high	29	Min 29	21	14	11	8	6.5	5	3.5	3
High	19	Min 19	15	11	8	7	5	4	3	3
Medium	12.5	Min 12.5	10	8	6	5	4	3	3	3

NOTES:

- 1 Refer to AS 1530.8.2 for the BAL FZ
- 2 Whilst in most applications the exposure will drop rapidly after the 2 min plateau, the extended decay phase has been added to provide a total heat load greater than that caused by a slowly approaching fire, allowing a single profile to be applied to all cases.

Figure 8: Exposure conditions for radiant heat test in AS 1530.8.1 [30]

Table 1: Timber crib dimensions in AS 1530.8.1 (based on properties for Douglas Fir) [30]

Characteristic	Class A	Class B	Class C
Thickness ¹ of stick (m)	0.02	0.02	0.02
Length of stick (m)	0.1	0.15	0.23
No. sticks per row	4	6	9
No of rows	3	3	3
Approx. mass ² (± 0.05 kg)	0.25	0.50	1.25

¹ Dimension of square cross-section

² Nominal density=500 ±50 kg/m² (sticks may be added/removed to top layer to achieve mass requirements)

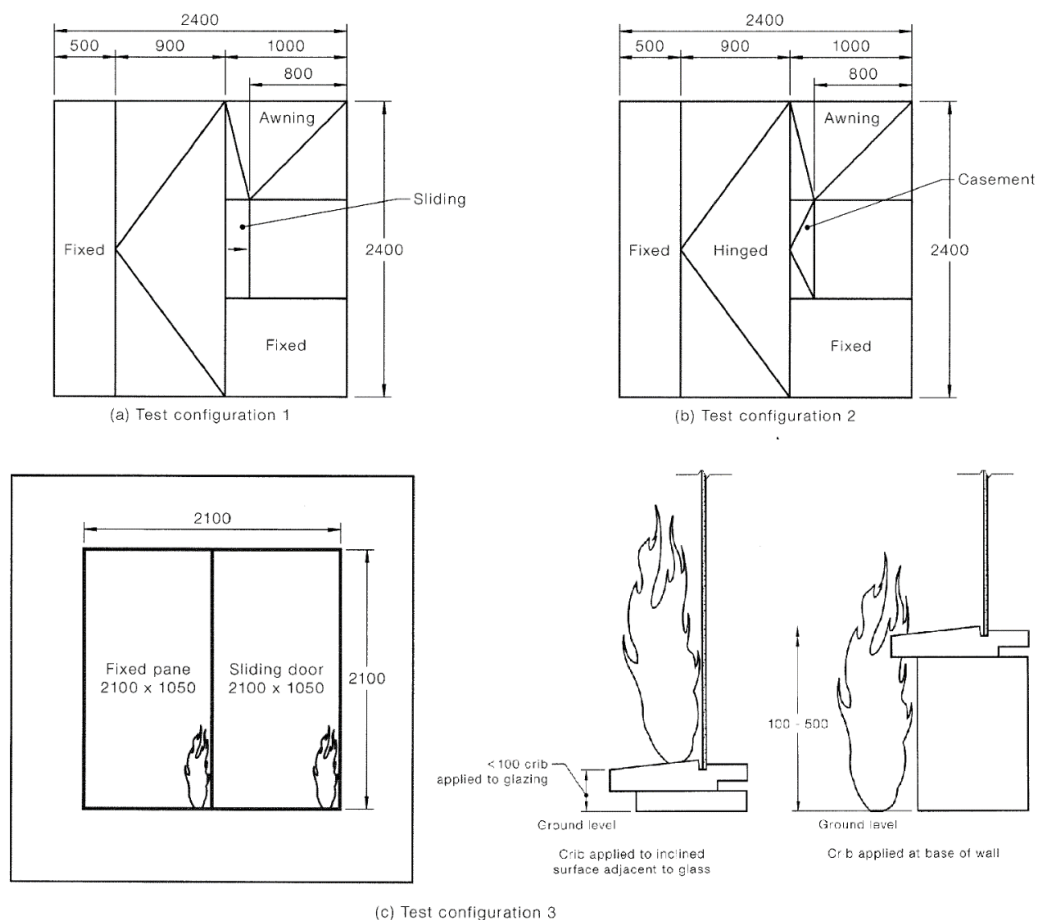


Figure 9: Standard configurations for glazing systems [30]

France does not have a specific standard for window testing. However, requirements for joinery are specified in various forest fire risk prevention plans (called Plans de Prévention des Risques Incendie de Forêt PPRIF³) [35,36]. In general, an E30 performance (integrity (E) for 30 minutes) is required for occultation devices.

³ A PPRIF is a plan for the prevention of foreseeable natural risks (Plan de Prévention des Risques Naturels prévisibles PPRN) aimed at forest fire risks. It is drawn up by the prefect in areas where fire protection requires it, in order to define the preventive measures to be taken to avoid fire risks.

D2.3 QUALITY STANDARD FOR WUI ARCHITECTURE AND LANDSCAPE DESIGN

Table 2: Summary of the requirements for glazing systems in AS 3959 [5]

	Shutter	Window
BAL-LOW	No construction requirements	
BAL-12.5	<ul style="list-style-type: none"> - Be fixed to the building and be non-removable; - When in the closed position, have no gap greater than 3 mm between the shutter and the wall, the sill or the head; - Be readily manually operable from either inside or outside; - Protect the entire window assembly; - Where perforated, have (i) uniformly distributed perforations with a maximum aperture of 3 mm when the shutter is providing radiant heat protection or 2 mm when the shutter is also providing ember protection (such as where the openable portion of the window is not screened in accordance with the requirements of the respective BAL); and (ii) a perforated area no greater than 20% of the shutter. 	<ul style="list-style-type: none"> - Shall comply with AS 1530.8.1, or - Protected by a bushfire shutter, or - Protected externally by screens with a mesh with a maximum aperture of 2 mm, made of corrosion-resistant steel, bronze or aluminium, or - Window frames and window joinery shall be made from Bushfire-resisting timber, or timber species, or metal or metal-reinforced PVC-U. When glazing is less than 400 mm from the floor, glazing shall be Grade A safety glass minimum 4 mm, or glass blocks with no restriction on glazing methods, otherwise annealed glass may be used. The openable portions of windows shall be screened with mesh with a maximum aperture of 2 mm, made of corrosion-resistant steel, bronze or aluminium.
BAL-19	<ul style="list-style-type: none"> - Made from non-combustible material or timber species⁴ or bushfire-resisting timber⁵ or a combination of the above three 	<ul style="list-style-type: none"> - Shall comply with AS 1530.8.1, or - Protected by a bushfire shutter, or - Protected externally by screens with a mesh with a maximum aperture of 2 mm, made of corrosion-resistant steel, bronze or aluminium, or - Window frames and window joinery shall be made from Bushfire-resisting timber, or timber species, or metal or metal-reinforced PVC-U. When glazing is less than 400 mm from the floor, glazing shall be toughened glass, minimum 5 mm, or glass blocks with no restriction on glazing methods, otherwise annealed glass may be used. The openable portions of windows shall be screened internally or externally with a mesh with a maximum aperture of 2 mm, made of corrosion-resistant steel, bronze or aluminium.

⁴ Wood with density of 650 kg/m³ or greater

⁵ Eucalyptus sieberi, Eucalyptus pilularis, Eucalyptus camaldulensis, Corymbia maculate, Corymbia henryi, Corymbia citriodora, Eucalyptus sideroxylon, Intsia bijuga, Syncarpia glomulifera

D2.3 QUALITY STANDARD FOR WUI ARCHITECTURE AND LANDSCAPE DESIGN

BAL-29		<ul style="list-style-type: none"> - Shall comply with AS 1530.8.1, or - Protected by a bushfire shutter, or - Window frames and window joinery shall be made from Bushfire-resisting timber, or metal or metal-reinforced PVC-U. Glazing shall be toughened glass minimum 5 mm. The openable portions of windows as well as glazing less than 400 mm from the floor shall be screened internally or externally with a mesh with a maximum aperture of 2 mm, made of corrosion-resistant steel, bronze or aluminium.
BAL-40	<ul style="list-style-type: none"> - Be fixed to the building and be non-removable; - When in the closed position, have no gap greater than 3 mm between the shutter and the wall, the sill or the head; - Be readily manually operable from either inside or outside; - Protect the entire window assembly; - Where perforated, have (i) uniformly distributed perforations with a maximum aperture of 3 mm when the shutter is providing radiant heat protection or 2 mm when the shutter is also providing ember protection (such as where the openable portion of the window is not screened in accordance with the requirements of the respective BAL); and (ii) a perforated area no greater than 20% of the shutter. - Made from non-combustible material 	<ul style="list-style-type: none"> - Shall comply with AS 1530.8.1, or - Protected by a bushfire shutter, or - Window frames shall be in metal. Glazing shall be toughened glass, minimum 5 mm. Both the openable and the fixed portions of the window shall be screened with a mesh with a maximum aperture of 2 mm, made of corrosion-resistant steel or bronze.
BAL-FZ	<ul style="list-style-type: none"> - Be fixed to the building and be non-removable; - When in the closed position, have no gap greater than 3 mm between the shutter and the wall, the sill or the head; - Be readily manually operable from either inside or outside; - Protect the entire window assembly; - Perforations are not acceptable; - Shall comply with AS 1530.8.2 	<ul style="list-style-type: none"> - Protected by a bushfire shutter, or - The openable portion of the window shall be screened with a mesh with a maximum aperture of 2 mm, made of corrosion-resistant steel or bronze; and either the window system shall have an FRL of at least -/30/-⁶; or the window system shall comply with AS 1530.8.2 when tested from the outside.

⁶ FRL is the fire resistance level [34]. A FRL of -/30/- means that the window system must maintain its integrity during 30 minutes.

3.1.2. Focus on the living labs

In Spain, the prevention of wildfires is carried out according to local regulations and guidelines, such as Catalonia [37] and Comunitat Valenciana [10]. In Catalonia, it is indeed advisable to avoid the use of synthetic materials for the exterior closures (polycarbonates, methacrylates, PVC, etc.). In Catalonia or in Comunitat Valenciana, it is recommended to protect the glass windows with shutters, to use double glazing and tempered glass and to prioritize reticulated windows. In the Canary Islands, there are no uniform regulations and guidelines at a regional level. There is only a quick mention in the Special Plan for Civil Protection and Emergency Response to Forest Fires in the Autonomous Community of the Canary Islands (INFOCA), which recommends building roofs and facades of fire-resistant materials and fire-proofing wooden facades regularly. However, several awareness campaigns are being implemented at an insular level in which some recommendations have been established for safeguarding homes against the threat of fire. For instance, the Gran Canaria Mosaico project⁷ advocates for the application of fireproof varnish to wooden windows and the removal of awnings and curtains as measures to mitigate fire vulnerability. In Chile, it is recommended to install double or triple glazed windows, avoiding PVC frames or flammable materials [15]. It is also advisable to install a fine 1/8-inch (3.175 mm) metal mesh on the windows or fire-resistant metal shutters.

In Chile, it is recommended to install double or triple glazed windows, avoiding PVC frames or flammable materials [15]. It is also advisable to install a fine 1/8-inch (3.175 mm) metal mesh on the windows or fire-resistant metal shutters.

In Portugal, for new constructions or when refurbishing or expanding buildings, owners must adopt protective measures relating to the resistance of buildings to the passage of fire [38]. The terms are defined in decree No. 8591/2022 of July 13 [6]. This decree defines 5 fire exposure classes (Classe de Exposição ao Incêndio Rural (CEIR)), which depend on:

1. The vegetation scenario around the building. There are 4 possibilities:
 - Scenario 1: herbaceous vegetation less than 20 cm high
 - Scenario 2: herbaceous vegetation and trees
 - Scenario 3: bushes alone
 - Scenario 4: bushes and trees.
2. The mean slope of area where the flames can spread. There are 4 possibilities: 10, 20, 30 and 40°.
3. The distance of horizontal separation (called DS), which is the distance between the building and the nearest vegetation.

⁷ Gran Canaria Mosaico project: <https://grancanariamosaico.com/alrededor-de-la-vivienda/>

These data allow the parameters ϕ_0 and k_0 to be determined (For new buildings or extensions with a distance of horizontal separation (DS) less than 50 m, windows, skylights and external opening closure elements shall comply with the reaction to fire class [39] indicated in Table 4 and the fire resistance [40] indicated in Table 5. The types of use (Utilização-Tipo UT) and risk categories (Categorias de Risco CR) that are mentioned in Table 4 and 5 respectively are given in Annex 2. To test the fire resistance, the windows are placed in a furnace and heated according to the standard heating regime (Eq. 1). The minimum requirement is EI 45, i.e., that the windows must withstand fire exposure for 45 min without the fire spreading to the other side in the form of flames and without the transmission of the fire in the form of heat transfer (mean temperature increase of less than 140 K on the unexposed side). The duration increases to 180 min for the extreme fire exposure class and the fourth risk category. For existing buildings, there are no regulatory requirements. However, the authorities recommend protecting windows with blinds or shutters, to use double glazing and tempered glass and to favour sliding windows [41].

Table 3). The incident heat flux ϕ (kW.m^{-2}) is then calculated using the following formula [6]:

$$\phi = \phi_0 \times DS^{-k_0} \text{ outside the APPS} \quad (2a)$$

$$\phi = 1.25 \times \phi_0 \times DS^{-k_0} \text{ inside the APPS} \quad (2b)$$

Where APPS (Áreas Prioritárias de Prevenção e Segurança) correspond to priority areas for prevention and safety. In the APPS, the fire risk is high or very high according to the rural fire risk mapping established by Decree No. 82/2021 of 13 October [38]. Finally, the fire exposure class is determined according to the value of the incident heat flux: low (between 0 and 12.5 kW.m^{-2}), medium (between 12.5 and 19 kW.m^{-2}), high (between 19 and 29 kW.m^{-2}), very high (between 29 and 40 kW.m^{-2}) and extreme (more than 40 kW.m^{-2}).

For new buildings or extensions with a distance of horizontal separation (DS) less than 50 m, windows, skylights and external opening closure elements shall comply with the reaction to fire class [39] indicated in Table 4 and the fire resistance [40] indicated in Table 5. The types of use (Utilização-Tipo UT) and risk categories (Categorias de Risco CR) that are mentioned in Table 4 and 5 respectively are given in Annex 2. To test the fire resistance, the windows are placed in a furnace and heated according to the standard heating regime (Eq. 1). The minimum requirement is EI 45, i.e., that the windows must withstand fire exposure for 45 min without the fire spreading to the other side in the form of flames and without the transmission of the fire in the form of heat transfer (mean temperature increase of less than 140 K on the unexposed side). The duration increases to 180 min for the extreme fire exposure class and the fourth risk category. For existing buildings, there are no regulatory requirements. However, the authorities recommend protecting windows with blinds or shutters, to use double glazing and tempered glass and to favour sliding windows [41].

Table 3: Parameters ϕ_0 and k_0 for the calculation of the incident heat flux in Portugal [6]

Vegetation scenario	Slope (°)	ϕ_0	k_0
Scenario 1	0°	19.838	0.99 5
	10°	26.981	1.00 0
	20°	32.852	1.00 8
	30°	45.156	1.02 4
	40°	55.444	1.04 4
Scenario 2	0°	150.22 4	0.94 5
	10°	172.86 9	0.97 5
	20°	191.28 0	0.99 3
	30°	214.53 2	1.01 7
	40°	248.89 7	1.04 9
Scenario 3	0°	100.42 3	0.97 8
	10°	120.02 1	0.99 7
	20°	152.02 7	1.00 5
	30°	196.85 1	1.02 6
	40°	257.11 0	1.07 0
Scenario 4	0°	227.00 4	0.90 1
	10°	233.77 2	0.86 3
	20°	274.66 6	0.91 6
	30°	318.75 9	0.93 9
	40°	361.46 4	0.964

Table 4: Required reaction to fire⁸ for windows, skylights and shutters

Use type (UT)	Fire exposure class (CEIR)	Requirement
I. II. III. IV. V. VI. VII. VIII. IX. X and XI	Low or medium	C-s2. d0
	High or very high	B-s2.d0
	Extreme	A1 or A2-s1.d0
XII	Low or medium	B-s2. d0
	High or very high	A1 or A2-s1.d0
	Extreme	A1

Table 5: Required fire resistance⁹ for windows

Use type (UT)	Fire exposure class (CEIR)	Risk Category (CR)			
		1	2	3	4
I. III. IV. V. VI. VII. VIII. X and XI	Low or medium	EI 45	EI 60	EI 60	EI 90
	High or very high	EI 60	EI 60	EI 60	EI 90
	Extreme	EI 60	EI 60	EI 90	EI 120
II. IX and XII	Low or medium	EI 45	EI 60	EI 120	EI 120
	High or very high	EI 60	EI 90	EI 120	EI 120
	Extreme	EI 60	EI 90	EI 120	EI 180

⁸ Reaction to fire indicates if the material supplies fuel to the fire before the flashover (Standard Test ISO 5660 [39]). This classification system is composed of seven groups ranking from A1 to F, where A1 is made up of non-combustible products and F of easily flammable products (Euroclass: A1 / A2 / B / C / D / E / F). There are two additional classification criteria – S and D. S refers to smoke production. Products classified S1, contrary to those classified S3, produce small amounts of smoke. D index refers to the generation of flaming droplets. D0 corresponds to no droplets and D2 is the least favourable.

⁹ Fire resistance is the capacity of a construction element (system) to maintain its LOAD-BEARING FUNCTION (designed by R), INTEGRITY (designed by E) and THERMAL INSULATION (designed by I) properties during a specific period given in minutes (Standard NF EN 1363-1 [40]).

3.2. Materials and methods

22 experiments were carried out to test the vulnerability of windows and shutter to hedge fires at the EXPLORII platform located in Corte, France [42]. The platform consists of a slope 10 m long and 6 m wide with an inclination of 20° and a plateau located at the top (Figure 10). A single-storey house (in concrete) 7 m long, 3.65 m high and 3.8 m wide, and a terrace, 7 m long and 3 m wide, are built on the plateau. The platform is equipped with sensors to monitor the atmospheric conditions in the vicinity of the fire, the behaviour of the fire and its impact on the building. An air temperature and relative humidity sensor is used to measure the ambient conditions. Wind conditions are measured with four sonic anemometers (WindSonic1 Gill. Campbell Scientific. Inc.; 5.a-d in Figure 10) and one 3D sonic anemometer (CSAT3B. Campbell Scientific. Inc.; 6 in Figure 10). The anemometers are sampled at a frequency of 1 Hz using a Campbell Scientific. Inc. CR9000 data logger. A wind direction of 180° corresponds to the wind along the axis of the slope (i.e., the most favourable for fire spread towards the house).

The mass loss of the burning hedge is measured with a 7 m long and 1 m wide load cell (8 in Figure 10). It is placed adjacent to the top of the slope at a distance of 3 m from the facade. The load cell is made up of 2 stainless steel plates. Each one is equipped with 2 SQB load cells (EXA), which are connected to an ENOD4 digital transmitter (Scaime) with a 4/20 mA analog output. The load cell assembly is covered with calcium silicate to protect it from heat. Its measurement range is 150 kg with 20 g accuracy. Two pairs of MEDTHERM heat flux gauges are placed on the facade at a height of 1.73 m from the surface of the terrace (2.a and 2.b in Figure 10). Each pair consists of a total heat flux gauge (MEDTHERM 64-20-18) with a measuring range of 0-200 kW.m⁻² and a radiant heat flux gauge with a sapphire window (MEDTHERM 64P-10-22) with a measuring range of 0-100 W.m⁻².

All heat flux gauges on façade are water cooled using a Cooling Water Chiller at 15°C. Two pairs of uncooled CAPTHERM heat flux gauges are also placed on the roof at a height of 2.73 m from the surface of the terrace (2.c and 2.d in Figure 10). Each pair consists of a total heat flux gauge with a measuring range of 0-200 kW.m⁻² and a radiant heat flux gauge with a measuring range of 0-100 W.m⁻². The load cell and the heat flux gauges are sampled at a frequency of 1 Hz using a Campbell Scientific. Inc. CR1000 data logger. A GoPro camera (Hero 10 Black) is mounted on a telescopic mast installed at the bottom of the slope (7 in Figure 10) to observe the rear of the fire front as it spreads up the slope towards the hedge.

Three cameras (Canon EOS 6) equipped with a Canon RF 24-105 mm f/4 lens are also placed at the top of the slope to observe the combustion at the level of the load cell. The first lateral camera (1.a in Figure 10) makes it possible to characterise the geometry of the flame front as the hedge burns. The second lateral camera (1.b in Figure 10) allows the spread of the fire in the hedge to be visualised during the test. The third camera (1.c in Figure 10) is placed on inside the wall (behind a pothole) under the central window to observe the fire front. These cameras and the GoPro take an image every second. To simplify image processing, the three devices (GoPro camera and the 3 cameras) are synchronised. The flame geometry during the hedge burning is determined by image processing with MATLAB® using the camera 1.a [43]. The visibility of the flame boundaries

is improved by using an image enhancement contrast procedure based on the Contrast-Limited Adaptive Histogram Equalization (CLAHE) [44]. The flames are then extracted from the rest of the image using a k-means clustering based image segmentation method [45]. The following definition is used to characterise the flame (Figure 11):

- The flame length (FL) is the distance between the highest point of the flame envelope (point A) and the lowest point to the left of the flame (point B).
- The flame height (FH) is the distance between the point A and point C, which is the projection of point A on the ground
- The horizontal flame extent (HFE) is the distance between the lowest point on the left of the flame (point B) and point C.
- The separation angle (β) is the angle between the direction of the flame length (FL) and the ground.

For this work, the values of flame length correspond to the maximum extensions of the visible flame front. For the separation angle, the value is an average over the flame duration. Flame duration is defined as the time interval between the ignition of the hedge and the moment when the flame height is less than 1 m.

The system designed for smoke analysis consists of two components (Table 6). The first set of instruments is focused on characterizing the source terms of smoke, which refers to the quantity and type of emissions released into the atmosphere during a vegetation fire. This set includes an ELPI+ (Electrostatic Low Pressure Impactor; Addair) for particle analysis, a Fourier-Transform Infrared Spectroscopy device (model AA-4000, Addair), and a Multiparametric QA station (Ethera) for gas analysis (CO, CO₂, CH₄, etc.). Additionally, Tenax TA Tubes (Supelco) with a pump sampling system (Gilair Plus) are used, along with offline analyses (ATD-GC/SM and FID) for the detection of VOCs and total hydrocarbons. A sampling probe is positioned on the roof of the building (Figure 10) to collect smoke during fire test, while the smoke analyzers are housed safely inside the home. Combustion products generation is quantified using emission factors, EF_i (g.kg⁻¹). Fire-integrated emission factors are calculated through a carbon and nitrogen mass balance approach, where the emission factor for a given species i is determined by the ratio of that species' mass concentration to the total carbon or nitrogen concentration emitted in the smoke [46].

$$EF_i = \frac{[C_i]}{\Sigma([C_{CO_2}] + [C_{CO}] + [C_{CH_4}] + [C_{NMOC}] + [C_a])} \times C_{fuel} \text{ for gases containing carbon} \quad (3)$$

$$EF_i = \frac{[N_i]}{\Sigma([C_{NO_2}] + [C_{NO}] + [C_{NH_3}])} \times N_{fuel} \text{ for gases containing nitrogen} \quad (4)$$

Where C_{fuel} is the mass fraction of carbon in the fuel, C_i is the mass concentration of carbon constituent i emitted during the burning, C_{NMOC} corresponds to the non-methane organic compounds and C_a refers to the aerosols, N_{fuel} is the mass fraction of nitrogen in the fuel.

The second set of devices is dedicated to measuring the smoke that entered the house, in order to evaluate indoor air quality during and after the experiment. The equipment used includes the Fidas 200 (Addair) for aerosol quantification (in terms of particle size and count), the MX6 iBrid Multigas (Industrial Scientific) for gas detection (CO, CO₂, O₂, H₂, NO_x, NH₃, HCN), and Tenax TA Tubes (Supelco) with pump sampling (Gilair Plus), paired with offline analyses (ATD-GC/SM and FID) to measure VOCs.

To ensure a repeatability between the burning experiments, the hedge is reconstructed from branches of rockrose (*Cistus monspeliensis*) or green cypress (*Cupressus sempervirens*) in welded mesh cages measuring 6 m long and 1 m wide. The hedge height for the rockrose is 2 m, while the hedge height for the cypress is 1 m. These different hedge configurations are designed to provide fire exposures with different flame intensities and durations. In order to maintain a realistic vegetation density, the branches are placed in the cages with a bulk density of approximately 6.8 kg.m⁻³ for rockrose [47] and 15 kg.m⁻³ for green cypress (corresponding to the bulk density obtained during the species characterisation using the cube method [48]). To mimic the ignition of the hedge by a fire spreading across an herbaceous layer, white pine wood wool with a load of 1 kg.m⁻² is placed in the slope over an area 5 m long and 6 m wide. The wood wool is ignited at one edge with a torch containing a gasoline/diesel mixture along the entire width of the bed. The ambient conditions (temperature, relative humidity) is measured for each test.

The Moisture Content (MC) of the rockrose leaves, cypress needles and the wood wool are determined using a desiccator at 105°C before each experience. Table 7 shows the range of the experimental conditions observed during the 22 burning tests. 12 experiments were carried out with rockrose and 10 with cypress. The study focuses on the performance of double-glazed windows with frames made of different materials: PVC, wood (fir) and aluminium. The size of the windows is 600 mm × 950 mm. Each window is installed in the centre of the wall thickness (made of brick, insulation and plaster) and can be protected with a shutter (600 mm × 980 mm) made of PVC, wood (fir) or aluminium.

Table 8 gives a description of the joinery and Figure 12 shows photographs of it. Different configurations were tested during the hedge fires, resulting in 6 exposures of aluminium shutters, 6 exposures of wooden shutters, 7 exposures of PVC shutters, 13 exposures of aluminium-framed windows (without shutters), 14 exposures of wooden-framed windows (without shutters) and 16 exposures of PVC-framed windows (without shutters).

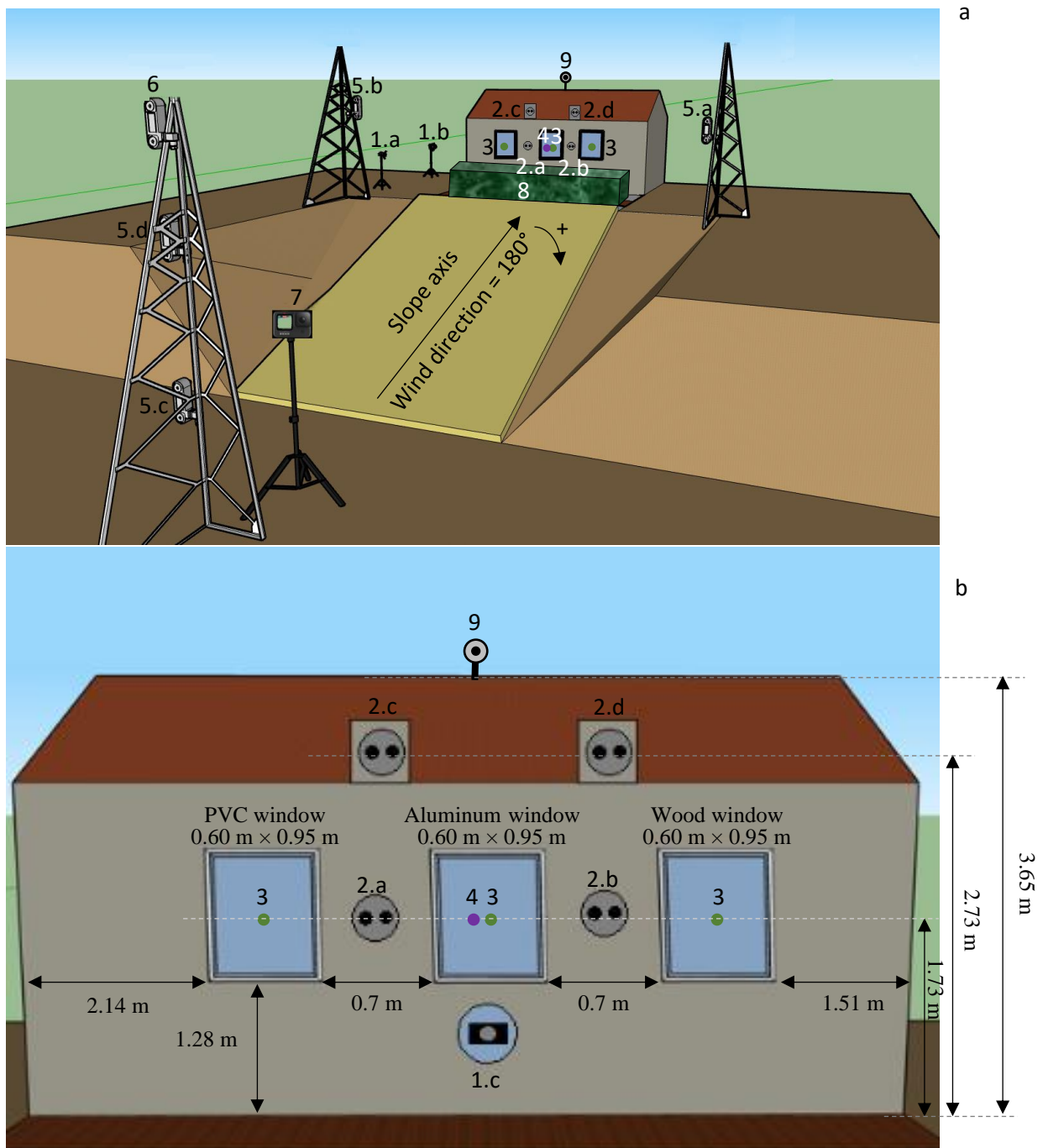


Figure 10: Layout of the EXPLORII platform a) General view b) View of the exposed facade - 1: Cameras. 2: Pairs of total and radiant heat flux gauges. 3: K-type surface thermocouple 4: Radiant heat flux gauge. 5: 2D sonic anemometer. 6: 3D anemometer. 7: Go Pro. 8: Load Cell under the hedge. 9: Sampling rod for the outdoor smoke analysis

D2.3 QUALITY STANDARD FOR WUI ARCHITECTURE AND LANDSCAPE DESIGN

Table 6: Description of the sensors used on the EXPLORII platform

Sensors	Sensor type, manufacturer and model	Variables	Measurement height range (m above the ground level)
Main mast (10 m)	3D sonic anemometer (CSAT3B, Campbell Scientific, Inc.)	u, v, w	10
	2D sonic anemometer (WindSonic1 Gill, Campbell Scientific, Inc.)	u, θ	2 and 6
Short masts (7 m)	2D sonic anemometer (WindSonic1 Gill, Campbell Scientific, Inc.)	u, θ	2
Fire behavior	Load cell (SQB load cells (EXA))	Mass	0
Flame geometry	Camera Hero 10 Black (GoPro)	Fire front shape and velocity	10
	Camera EOS 6 (Canon) equipped with a Canon RF 24-105 mm f/4 lens	Flame front geometry	1
Fire impact	Total heat flux gauge 64-20-18 (MEDTHERM)	Heat flux on the facade	1.73
	Radiant heat flux gauge 64P-10-22 (MEDTHERM)	Heat flux on the facade	1.73
	Radiant heat flux gauge 64P-5-22 (MEDTHERM)	Heat flux inside the house	1.73
	K-type surface thermocouples	Temperature	1.73
Smoke analysis outdoor	ELPI+ (Electrostatic Low Pressure Impactor; Addair)	Particles analyses	4.7
	FTIR (Fourier-Transform Infrared Spectroscopy AA-4000 model Addair)	Gas analyses	4.7
	Multiparametric QA station (Ethera)	Gas analyses	4.7
	Tenax TA Tubes (Supelco) with pump sampling (Gilair plus) for off-lines analyses with ATD-GC/MS and FID (Flame ionization detector; TVA Thermofischer)	VOC Total Hydrocarbon	4.7
Smoke analysis indoor	Fidas 200 (Addair)	Particles analyses	1
	MX6 ibrid Multigas (Industrial Scientific)	Gas analyses	1
	Tenax TA Tubes (Supelco) with pump sampling (Gilair plus) for off-lines analyses with ATD-GC/MS and FID (Flame ionization detector; TVA Thermofischer)	VOC Total Hydrocarbon	1

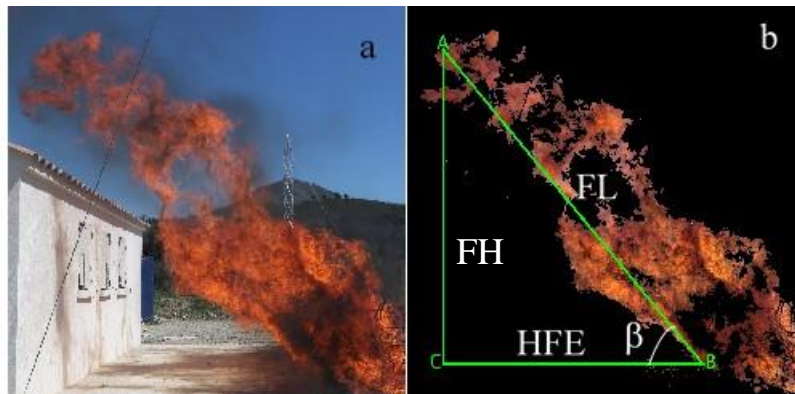


Figure 11: Image processing to define the descriptors of the flame geometry a) Original image b) Flame using k-means clustering

Table 7: Range of the experimental conditions observed during the burning tests. The mean value and the standard deviation are in parenthesis

Fuel	Rockrose	Cypress
Hedge dimension (Length (m) × width (m) × height (m))	6 × 1 × 2	6 × 1 × 1
Initial mass (kg)	90.5 ± 10.1	81.2 ± 5.3
Wind speed (m/s)	0.20-3.00 (1.09 ± 0.68)	0.58-1.87 (1.10 ± 0.37)
Wind direction (°)	133.0-283.3 (185.7 ± 49.5)	63.7-260.2 (161.6 ± 62.3)
Ambient temperature (°C)	17.0-34.0 (26.9 ± 5.1)	20.3-30.0 (25.9 ± 3.4)
Relative humidity (%)	26.0-64.6 (45.8 ± 12.8)	22.0-51.5 (39.8 ± 8.4)
Foliar moisture content (%)	2.7-47.3 (24.9 ± 14.4)	14.4-65.0 (27.4 ± 14.9)
Wood wool moisture content (%)	4.8-11.8 (8.7 ± 2.6)	1.3-11.5 (7.6 ± 2.7)

Table 8: Description of windows and shutters used for testing

Type	Material	Description	Number of tests
Window (600 mm × 950 m)	Wood (BIEBER INOVA 68 model)	Double glazing 6/20/4 with argon Frame in pine wood	14
	Aluminium (PREFAL model)	Double glazing 4/20/4 with argon Frame in white extruded aluminium (alloy 6060)	13
	PVC (PREMIO PLUS 74 RESIDENCE PVC model)	Double glazing 4/20/4 with argon Frame with a thickness of 74 mm in lead-free PVC with steel reinforcement	16
Shutter (600 mm × 980 m)	Wood (RUSTIZED model)	Made with white pine slats 90 mm wide and 27 mm thick Color: raw wood	6
	Aluminium (P30 model)	Made with closed louvered slats with a thickness of 30 mm Color: white	6
	PVC (PVCéa 24 model)	Made up of 24 mm thick PVC slats Color: white	7



Figure 12: Photographs of the joinery a) Windows made of PVC (left), Aluminium (centre) and Wood (right) ; b) Shutters made of PVC (left), Aluminium (centre) and Wood (right)

3.3. Results and discussion

3.3.1. Description of the hedge burning and flame geometry

The different burning phases are shown in Figure 13 for the cypress hedge and Figure 14 for the rockrose hedge. The top row of photos is from camera 1.a, the second row from camera 1.b, the third row from camera 1.c and the bottom row from the GoPro (number 7 in Figure 10). The time $t=0$ corresponds to the moment when the hedge ignites, as determined by the cameras. The experiments began with the propagation of the fire front

in the wood wool (Figure 13.a and Figure 14.a). The hedge was ignited by direct contact with the flame front coming from the wood wool (Figure 13.b and Figure 13.b). The fire front then spread within the hedge (Figure 13.c and Figure 14.c). Since the finest particles were in the upper part of the hedge, this zone was consumed first, followed by the lower part where the thickest particles were concentrated. After the flameout, smouldering was observed (Figure 13.d and Figure 14.d).

At the end of the experiments, it was mainly the large particles at the bottom of the fuels that remained. The mean hedge mass loss was $73.4 \pm 5.8 \%$ for cypress and $71.8 \pm 16.9 \%$ for rockrose. Figure 15 shows the hedge mass and the mass loss rate recorded during the burning of a rockrose hedge with a foliar moisture content of 16 % and that of a cypress hedge with a foliar moisture content of 22 %. At comparable moisture contents, the mass loss rate (MLR) peak was greater for the rockrose hedge, averaging 2.9 ± 1.1 kg/s for rockrose and 1.5 ± 0.4 kg/s for cypress (Table 9). However, the flame residence time was longer for cypress hedges, averaging 85 ± 28 s for cypress and 58 ± 27 s for rockrose (Table 9). During our experiments, significant variations of the MLR were observed. These variations were due to the moisture content of the hedge, which varied from experiment to experiment, and to the wind direction, which could lead to slightly off-centre ignitions, causing the fire to spread through the hedge, resulting in lower MLR peaks than if the ignition was centred.

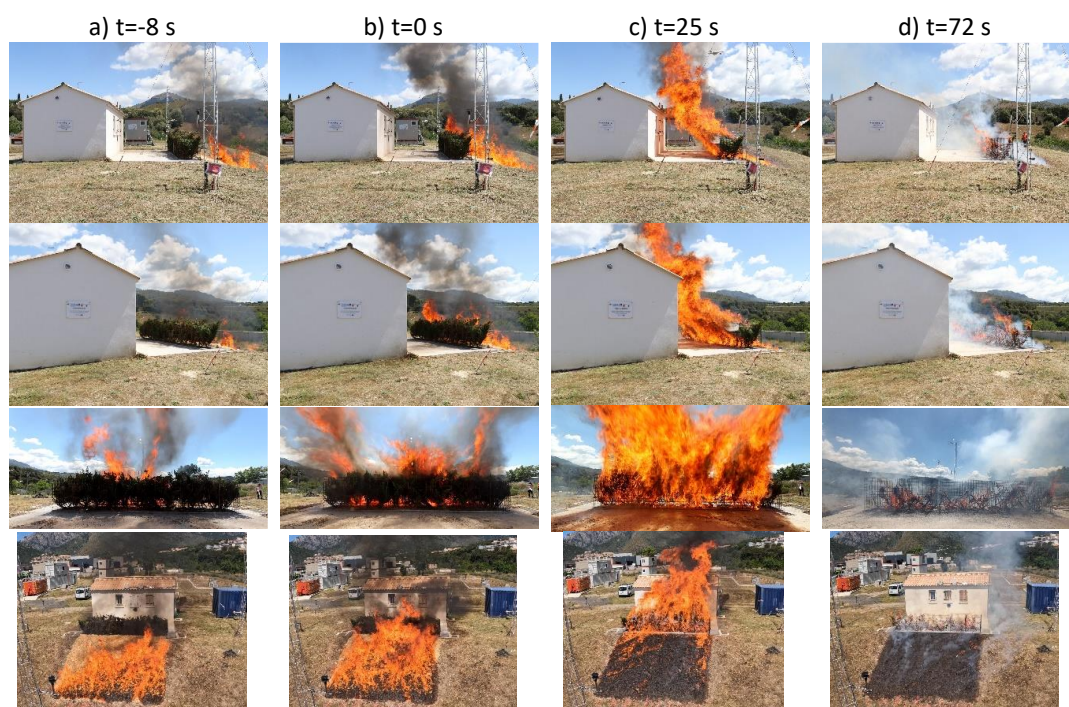


Figure 13: Photographs of the burning phases of cypress hedge a) Fire spread in wood wool; b) Hedge ignition. c) Hedge burning and d) Hedge extinction.



Figure 14: Photographs of the burning phases of rockrose hedge a) Fire spread in wood wool; b) Hedge ignition. c) Hedge burning and d) Hedge extinction.

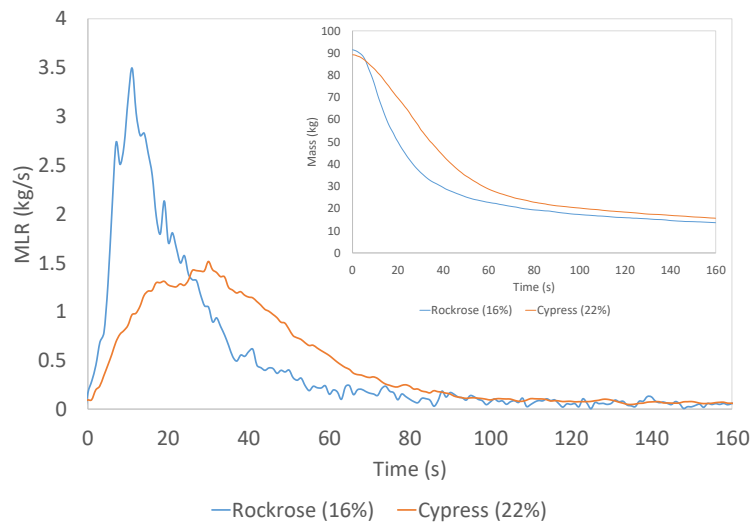


Figure 15: Mass loss during the hedge burning

Table 9: Range of the fire descriptors recorded during the hedge burning

Fuel	Rockrose	Cypress
Mass loss (%)	42.6-91.5 (71.8 ± 16.9)	63.7-84.1 (73.4 ± 5.8)
Peak of MLR (kg/s)	0.9-5.2 (2.9 ± 1.1)	0.6-1.9 (1.5 ± 0.4)
Residence time (s)	33-125 (58 ± 27)	49-146 (85 ± 28)
FH (m)	3.0-5.7 (4.8 ± 0.7)	3.8-5.6 (4.4 ± 0.5)
FL (m)	3.3-8.1 (6.1 ± 1.3)	4.1-8.9 (6.2 ± 1.6)
β (°)	46.7-123.8 (63.8 ± 19.9)	42.8-128.5 (60.9 ± 24.2)
HFE (m)	1.8-6.2 (4.2 ± 1.4)	0.6-7.5 (4.4 ± 2.1)
Peak of RHF on façade (kW/m²)	6.2-88.0 (40.5 ± 25.6)	3.9-82.6 (31.8 ± 19.2)
Peak of THF on façade (kW/m²)	11.9-200.0 (72.6 ± 48.6)	6.4-134.9 (58.0 ± 32.1)
Peak of RHF on roof (kW/m²)	10.1-117.3 (56.5 ± 31.0)	4.8-94.2 (46.2 ± 24.4)
Peak of THF on roof (kW/m²)	13.3-200 (89.0 ± 57.0)	5.7-99.8 (60.7 ± 27.5)

Table 9 shows the maximum flame height (FH), maximum flame length (FL), maximum horizontal flame extent (HFE) and mean separation angle (β) measured during the hedge burnings. The maximum flame heights ranged between 3.0 and 5.7 m for the rockrose hedges and between 3.8 and 5.6 m for the cypress hedges. On average, the maximum flame height was 4.8 ± 0.7 m and 4.4 ± 0.5 m for rockrose and cypress, respectively. Therefore, although the rockrose hedge was twice as high as the cypress hedge, the geometry of the flame was comparable between the two species. In addition, the flame front was higher than the roof ridge. For the two experiments, where the wind was not aligned with the axis of the slope (e.g. directions of 283.3 or 260.2°, corresponding to winds perpendicular to the slope), the flames were inclined backwards. Otherwise, the flame front was inclined towards the house. On average, the separation angle was 63.8° for rockrose and 60.9° for cypress. Excluding the experiments where the wind was not aligned with the slope are not taken into account, the average separation angles were $58.3 \pm 8.5^\circ$ and $53.3 \pm 9.3^\circ$. These separation angles are higher than those obtained by Graziani et al. ($45.1 (\pm 5.6)^\circ$ on average [43]), who carried out experiments without obstacles around the hedges. In our case, the presence of the house tends to limit the inclination of the flame front. This is probably due to a recirculation zone between the wall and the hedge, which straightens the flame in relation to the ground [49]. Flame

inclination induced horizontal flame extents between 1.8 and 6.2 m for rockrose and between 0.6 and 7.5 m for cypress. The average HFE was 4.2 ± 1.4 m for rockrose and 4.4 ± 2.1 m for cypress. Excluding the experiments where the wind was not aligned with the slope are not taken into account, the average HFE was 4.4 ± 1.2 m for rockrose and 4.8 ± 1.7 m for cypress. As the house was 3 m away from the hedges, the flame front often touched the façade or the roof during the experiments. Therefore, to ensure that the flames do not come into contact with buildings most of the time, a minimum distance of 5 m is should be required between façades and vegetation, especially since the tests were carried out with low winds (less than 2.9 m/s) and without taking into account other fuels (secondary structures, fences, wood piles, etc.) that could increase the fire intensity [50]. This recommended distance is greater than that required in the United States, Canada, Abruzzo in Italy, Greece, Comunitat Valenciana in Spain, the Canary Islands in Spain and France. In Tuscany and Portugal, the distance to be maintained between the vegetation and the buildings (5 m) allows contact to be avoided in most cases for such hedges. Only Australia has a defensible space (10 m between vegetation and building) that guarantees no flame contact on buildings for such hedges.

3.3.2. Heat fluxes and damage

Figure 16 shows an example of radiant heat flux measured on the building façade at 3 m from the rockrose and cypress hedges for a foliar moisture content of 35 and 23 %, respectively. Table 9 shows the ranges of the peak values of the radiant heat flux (Peak of RHF) and the total heat flux (Peak of THF) measured during the experiments on the façade and on the roof. The heat fluxes follow the same trends as the MLR. On the facade, the maximum radiant heat fluxes ranged between 6.2 and 88 kW/m² with an average of 40.5 ± 25.6 kW/m² for rockrose and between 3.9 and 82.6 kW/m² with an average of 31.8 ± 19.2 kW/m² for cypress. Total heat flux values ranged from 11.9 to 200 kW/m² with an average of 72.6 ± 48.6 kW/m² for rockrose and from 6.4 to 134.9 kW/m² with an average of 58.0 ± 32.1 kW/m² for cypress. At the edge of the roof, the average heat flux peaks were higher for rockrose: 56.5 ± 31.0 kW/m² and 89.0 ± 57.0 kW/m² for the radiant and the total heat flux, respectively. For cypress, however, the values were lower, due to the fact that the flames were lower: 46.2 ± 24.4 kW/m² and 60.7 ± 27.5 for the radiant and the total heat flux, respectively. This is because the burning of the cypress hedges produced flames that were lower and more inclined towards the ground. The heat fluxes measured in our experiments are in agreement with the data found in the literature for field-scale experiments [22]. As an example, the peak of radiant heat flux measured by Lopes et al. on the wall of the garden shed was equal to 48 kW/m² for shrubs at 0.5 m from the house walls [51]. We also compared our results with the incident heat fluxes defined in the Portuguese regulations [6]. Using Scenario 3 for shrubs (Table 3), for a zero slope at 3 m, formulas 2 give a value of 34.3 kW/m² outside the APPS and 42.9 kW/m² inside the APPS. These values are very close to the average radiant heat fluxes measured experimentally on the façade for the 2 m high rockrose hedges and the 1 m high cypress hedges (Table 9).

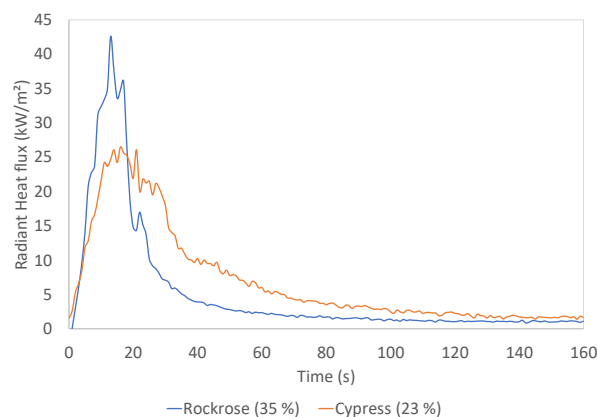


Figure 16: Radiant heat fluxes measured on the façade during the burning of the rockrose and cypress hedges

Table 10 shows the damage observed during the tests carried out. When windows were exposed to the fire, only the outer pane was damaged (Figure 17.a). The inner pane was never broken, which shows the interest in recommending the use of double glazing. The breakage of the outer glass was observed either during the heating phase, when the hedge was burning, or during the cooling phase, after the flameout. The flame front made contact with the façade in all cases where damage was observed, with the exception of the wood-framed windows. PVC framed windows suffered the most damage, with 25% of windows having their exposed glass broken during the tests, compared to less than 8% for other window types. In the absence of shutters, the radiant heat flux measured behind the window inside the house did not exceed 4.8 kW/m², showing that the double glazing acted as a thermal screen for the flame radiation.

Table 10: Summary of damage observed on the joinery

Type	Material	Damage description	Flame contact	Number
Window	Wood	No damage	No	13 (92.9%)
		Exposed glass breakage during cooling	No	1 (7.1 %)
	Aluminium	No damage	No	12 (92.3 %)
		Exposed glass breakage during heating	Yes	1 (7.7 %)
	PVC	No damage	No	12 (75 %)
		Exposed glass breakage during heating	Yes	1 (6.25 %)
Exposed glass breakage during cooling		Yes	3 (18.75 %)	
Shutter	Wood	No damage	No	1 (16.7 %)
		Blackened	Yes	2 (33.3 %)
		Burnt	Yes	3 (50 %)
	Aluminium	No damage	Both	6 (100 %)
	PVC	No damage	No	0 (0 %)
		Deformed	No	3 (42.9 %)
		Blackened	Yes	3 (42.9 %)
Burnt		Yes	1 (14.2 %)	

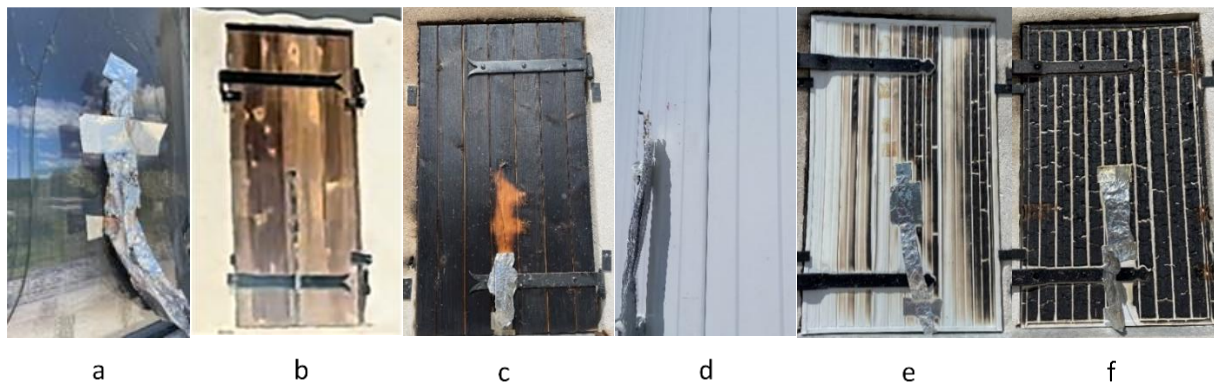


Figure 17: Photographs of the damage observed on the joinery a) Breakage of the exposed glass b) Blackened wood shutter c) Burnt wood shutter d) Deformed PVC shutter e) Blackened PVC shutter f) Burnt PVC shutter

For shutters exposed to the fire, no damage was observed to the aluminum shutters, whether or not the flame came into contact with the façade. The maximum temperature of the exposed face of the aluminium shutter did not exceed 130°C. This temperature is lower than the melting temperature (550-600°C) or the temperature at which aluminium loses its strength (50% of its strength is lost at 200°C) [52], explaining the absence of damage. The wooden shutters remained intact only when the flame front did not touch the façade. When the flames touched the house, we observed either a blackening of the shutter (Figure 17.b) or its burning (Figure 17.c). In the case of the PVC shutters, when the flames did not touch the façade, the shutters remained intact or were only deformed (Figure 17.d), i.e., the slats that make up the shutter were slightly distorted. For the deformed shutters, the maximum temperatures measured on the exposed side ranged from 92.7 to 114.2°C. These values are higher than the glass transition temperature of PVC (80°C) but remained below the decomposition temperature of PVC (290°C) [53]. This explains why only deformation was observed. When the flames reached the house, the PVC shutters were blackened (Figure 17.e) or burnt (Figure 17.f). Despite the damage to the various shutters, the windows behind them remained intact in all cases. It should also be noted that the combustion was not sustained on the shutters after the hedge stopped burning. We did not observe any self-sustaining combustion of the shutters during our experiments.

On the basis of these results, we tried to establish criteria to define whether or not the joinery would suffer damage when exposed to a vegetation fire. Firstly, as shown in Table 10, the contact of the flame with the shutter is an essential criterion that leads to significant damage such as the blackening or burning of the shutter. In fact, when there is no contact, the shutter suffers little or no damage (at worst, a slight deformation of the PVC shutter). In order to establish a criterion for distinguishing between cases leading to blackening and those leading to shutter burning, several quantities were calculated from the measurements: the peak of the radiant heat flux, the peak of the total heat flux, the total and radiant energy per square meter received (E_{tot} and E_{rad} , respectively) defined

by equations 5a and 5b and the total and radiant thermal dose (D_{tot} and D_{rad} , respectively) defined by equations 6a and 6b.

$$E_{tot} = \int_{t_0}^{t_f} \dot{q}_{total}'' dt \quad (5a)$$

$$E_{rad} = \int_{t_0}^{t_f} \dot{q}_{rad}'' dt \quad (5b)$$

$$D_{tot} = \int_{t_0}^{t_f} \dot{q}_{total}''^{4/3} dt \quad (6a)$$

$$D_{rad} = \int_{t_0}^{t_f} \dot{q}_{rad}''^{4/3} dt \quad (6b)$$

Where \dot{q}_{total}'' and \dot{q}_{rad}'' are the total and the radiant heat fluxes measured on the façade respectively, t_0 is the hedge ignition time and t_f is the time at which the damage (blackening or burning) was observed. As the time of deformation could not be determined during the test, the energy and dose for deformation were not calculated.

Figure 18 to Figure 20 show the thresholds obtained for the peak of heat fluxes, the energy and the thermal dose received by the shutters. Black color corresponds to blackening, red to burning, yellow to deformation and green to no damage. Although the exposures measured on the aluminium shutters were much higher than those measured on the wooden or PVC shutters, there was no damage to the aluminium shutters, demonstrating the robustness of this type of shutter. Below a total heat flux of 50 kW/m², there was no damage to the wooden shutters, unlike the PVC shutters, which deformed from a total heat flux of 12 kW/m². The blackening of the PVC and wooden shutters occurred above the same peak of heat flux, i.e. a total flux of 50 kW/m². However, the energy received and the thermal dose required to blacken the wood were lower (368 kJ/m² and 1219 (kW/m²)^{4/3}.s in total flux) than those required to blacken the PVC shutters (614 kJ/m² and 2109 (kW/m²)^{4/3}.s). Burning of the wooden shutters also occurred at lower thresholds than for the PVC shutters. In fact, the wooden shutters burned at total heat flux peaks above 76 kW/m² compared to 96 kW/m² for PVC shutters. The total energy received and the total thermal dose required to burn the wooden shutters were 734 kJ/m² and 2775 (kW/m²)^{4/3}.s compared to 1010 kJ/m² and 4238 (kW/m²)^{4/3}.s. Wooden shutters are therefore more fire resistant than PVC shutters at low exposure levels. This trend is reversed when the total heat fluxes received exceed about 50 kW/m².

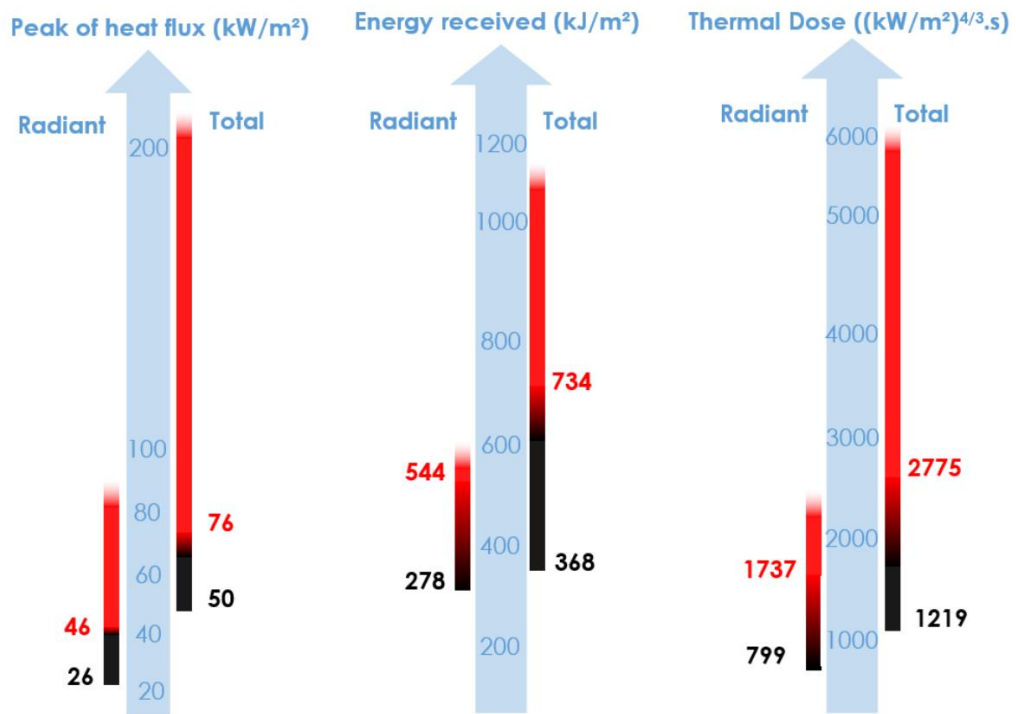


Figure 18: Blackening and burning thresholds for wooden shutters

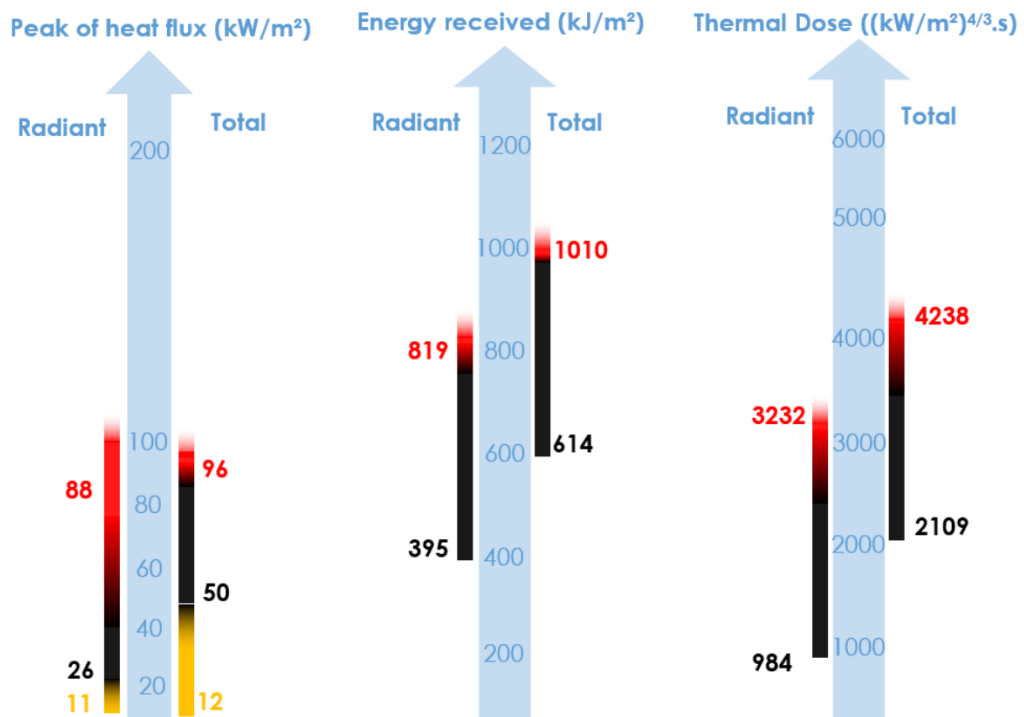


Figure 19: Blackening and burning thresholds for PVC shutter

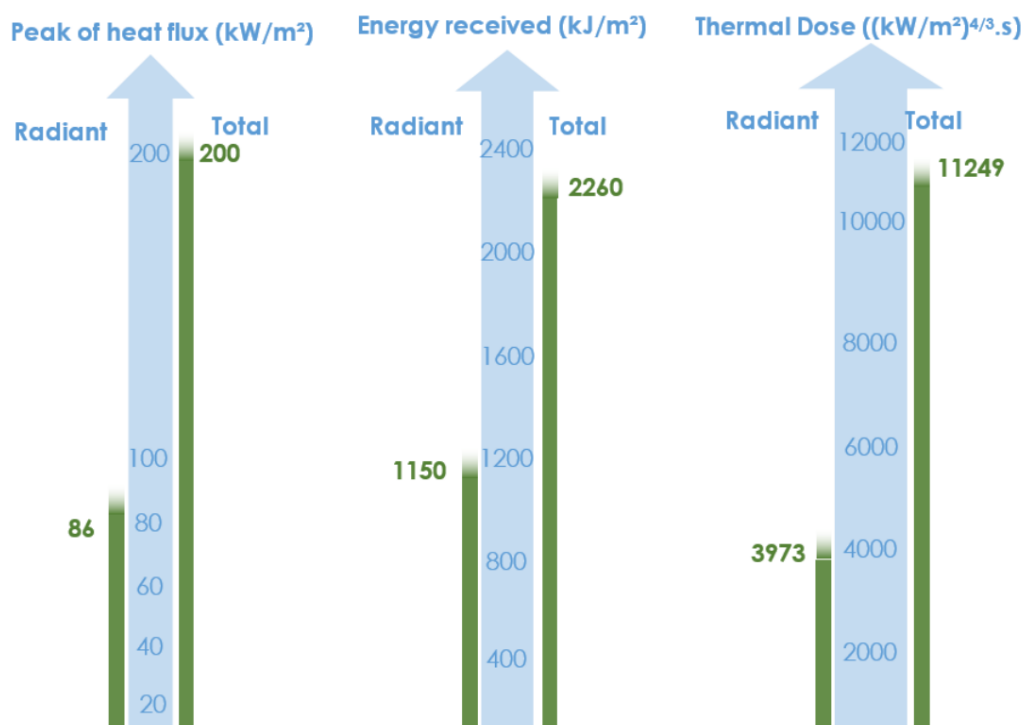


Figure 20: Damage-free thresholds for aluminium shutter

A similar analysis was done for the glass windows by adding the maximum temperature measured at the centre of the glass in the indicators (Table 11). The few cases of breakage observed make it difficult to analyse the results. However, the calculated indicators do not seem to allow the determination of thresholds for window breakage during cooling. In fact, the values obtained for intact cases are often higher than those obtained for cases of breakage during cooling. Furthermore, flame contact does not seem to be a predominant criterion, since breakages occurred with and without flame contact (Table 10). For breakage during heating, based on the 2 cases observed, only the total energy received and the temperature of the windows could be used to determine a threshold. For the PVC window, the breakage of the glass exposed to heating would occur for a total energy received between 1925.3 and 3213.4 kJ/m² and a maximum glass temperature between 75 and 140°C. For the aluminium window, the total energy received would be between 1933.3 and 2019.9 kJ/m² and the maximum glass temperature would be between 92 and 95.7°C. These values are consistent with the energies (420 and 2920 kJ/m²) and the temperature (77 and 157°C) of glass breakage found in literature [54–59]. Given the low number of breakages observed, it is difficult to recommend one type of window over another on the basis of damage thresholds. The only recommendation that can be drawn from these tests is to favour double glazing, as the second pane never broke whatever the window frame.

Table 11: Indicators for the breakage of the windows

	Wooden window		PVC window			Aluminum window	
	Intact	Breakage during cooling	Intact	Breakage during cooling	Breakage during heating	Intact	Breakage during heating
Peak of radiant heat flux (kW/m²)	3.9-60.7	38.8	6.2-70.8	34.8-82.6	41.9	7.5-61.9	34.2
Peak of total heat flux (kW/m²)	6.4-95.7	56.5	8.2-134.2	68.2-103.3	134.9	8.2-95.7	69.2
Radiant energy received (kJ/m²)	175.0-1143.7	1110.2	200.1-978.2	748.2-1434.8	1113.9	175.0-1157.1	922.8
Total energy received (kJ/m²)	395.6-2128.3	1815.1	447.2-2205.3	1264.9-1925.3	3213.4	395.6-1933.3	2019.9
Radiant thermal dose ((kW/m²)^{4/3}.s)	308.2-3727.8	2933.2	330.0-3176.7	1790.6-4823.1	3197.9	308.2-3749.3	2387.0
Total thermal dose ((kW/m²)^{4/3}.s)	961.9-7269.9	5474.8	678.8-7475.7	3670.5-6812.6	13313.4	679.9-7320.4	6678.5
Maximum temperature (°C)	43.5-87.1	90.9	35.5-75.1	71.4	140.0	45.5-92.0	95.7

3.3.3. Smoke analysis

To assess the impact of hedge burning on ambient air quality, the smoke above the roof was analysed with the outdoor system (9 in Figure 10), as was the air inside the house during 9 experiments: 5 with rockrose hedges and 4 with cypress hedges. During the experiments, the gases passing over the roof were very diluted (Figure 21). Unfortunately, this made it impossible to measure the gases with the MX4 sensors and FTIR as they lacked the sensitivity to effectively detect and quantify the diluted gases. We therefore decided to focus our study on the emitted particulate matter (PM₁₀, PM_{2.5}, and PM₁).



Figure 21: Photographs of the hedge burning of a) rockrose b) cypress equipped with smoke analysers

Figure 22 shows the evolution of the wind speed and the number concentration of aerosols measured during two tests with a rockrose hedge using the outdoor setup. Table 12 shows the mean particle size distributions in number and volume emitted during the burning of the two types of hedge. The number of particles suspended in the air near the house is on average $4.01 \times 10^6 \pm 2.14 \times 10^6$ ($1/\text{cm}^3$) for rockrose and $5.44 \times 10^6 \pm 3.00 \times 10^6$ ($1/\text{cm}^3$) for cypress. This corresponds to a mean volume concentration of these particles of $3.39 \times 10^4 \pm 1.63 \times 10^4$ ($\mu\text{m}^3/\text{cm}^3$) and $6.26 \times 10^4 \pm 2.88 \times 10^4$ ($\mu\text{m}^3/\text{cm}^3$) for rockrose and cypress, respectively. The concentration of particles is therefore higher in the smoke emitted by the burning of cypress hedges than in that of rockrose hedges.

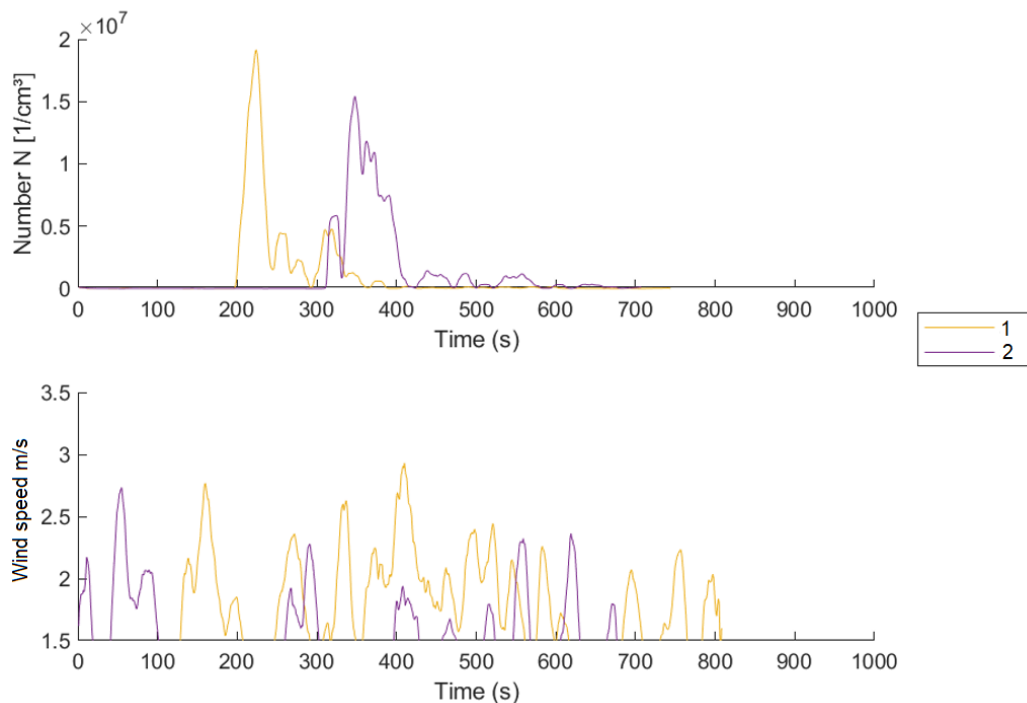


Figure 22: Aerosol number measurements and wind speed during two experiments with a rockrose hedge

Table 12. Mean particle size distributions in number and volume emitted during the hedge burning

	Number N [1/cm ³]	Volume V [μm ³ /cm ³]
Rockrose	$4.01 \times 10^6 \pm 2.14 \times 10^6$	$3.39 \times 10^4 \pm 1.63 \times 10^4$
Cypress	$5.44 \times 10^6 \pm 3.00 \times 10^6$	$6.26 \times 10^4 \pm 2.88 \times 10^4$

Figure 23 shows the evolution of the number size distribution of the particles for different experiments carried out with rockrose hedges. We observe significant repeatability between the different tests. Figure 24 shows the evolution of the particle distribution (size and number) measured in the house during an experiment carried out the VMC switched off and a cypress hedge. The finest particles around 10⁻¹ μm were the most important.

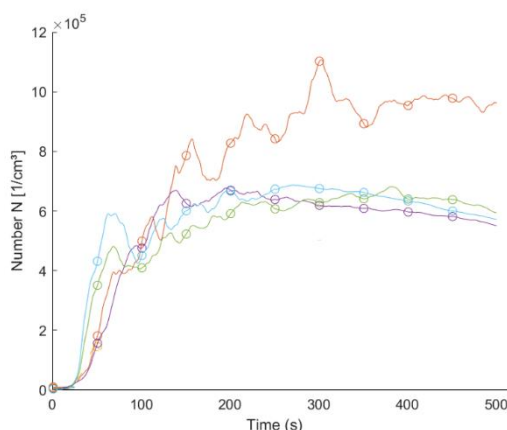


Figure 23: Evolution of number size distribution (dN/logDp, 1/cm³) for different experiments carried out with rockrose hedge

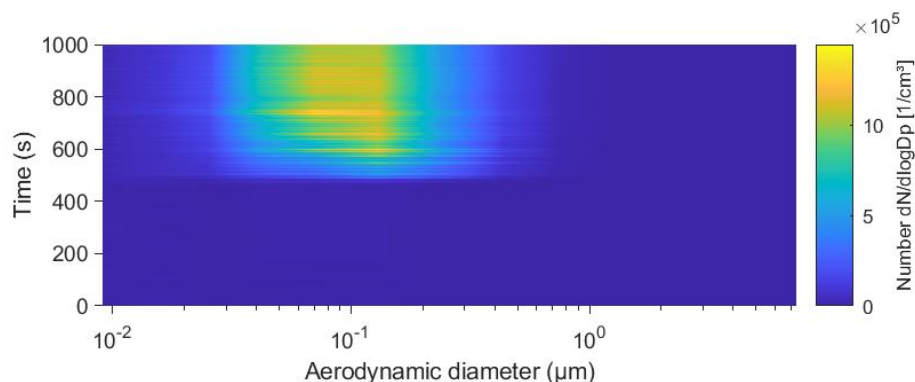


Figure 24: Number size distribution (dN/dlogDp, 1/cm³) as function of time (s) and aerodynamic diameter (μm) during a test with a cypress hedge.

Table 13 shows the mean concentration of particles in μg/m³ entering the house during the burning of cypress and rockrose hedges. Irrespective of the species, the most

abundant particles inside the house were PM₁₀ particles, followed by PM_{2.5} and finally PM₁ ultrafine particles. As with the outdoor analyses, burning the cypress hedge resulted in higher concentrations of particles inside the house than the rockrose hedge. This was probably due to a greater production of particles during the burning of this species, as the initial mass of fuel for the cypress hedge was lower than for the rockrose hedge (Table 7). This phenomenon highlights the importance of the choice of hedge species to mitigate the effects of burning on indoor air quality during a fire. Indeed, the burning of certain species, such as cypress, seems to generate a more worrying level of particulate pollution, which poses a greater risk to the health of the occupants, particularly with regard to fine and ultrafine particles, which are more likely to penetrate deep into the lungs.

Table 13. Particle size distributions in number and volume emitted during the burning

	PM _{0.1} [µg/m ³]	PM ₁ [µg/m ³]	PM _{2.5} [µg/m ³]	PM ₁₀ [µg/m ³]	Exposition time [s]
Rockrose	22.0	977.3	1092.7	1600.7	730.0
Cypress	18.2	1196.6	1756.7	2300.4	1205.0

4. LANDSCAPE DESIGN

This section presents the study on landscaping design in WUIs carried out within the FIRE-RES project. In this section we will summarise the different recommendations and regulations that exist in the world for the fuel management in WUI. Then, we will describe the experiments carried out at the laboratory scale to study the influence of the fuel moisture content on the ignition of shrubs and the fire spread through them. Finally, the numerical simulations carried out for the case studies in the Chilean and Portuguese Living Labs in order to study the effectiveness of the national regulations / recommendations will be presented.

4.1. Guidelines, standards and regulations

Fuel management in the WUI is one of the ways to prevent fire risk in these areas. It aims to limit the spread of a fire and reduce its intensity by creating horizontal and vertical discontinuities in the vegetation situated between the wildland and the buildings. There are different recommendations or regulations around the world regarding the fuel management in the WUI (Table 14). In the United States, California is the most advanced state in wildfire risk prevention. California Public Resources Code (PRC) § 4291 [60] requires that a defensible space of 100 feet must be maintained on each side of the structure, and cites the existence of 2 zones located at 5 and 30 feet (1.524 and 9.144 m) around the structure, to which is added an ember-resistant zone within 5 feet of the structure. Any tree branch within 10 feet (3.048 m) of the outlet of a chimney or stovepipe must be removed. In addition to PRC § 4291, each county's fire code goes on to describe specifics for fuel management. For example, vegetation management, as defined by Orange County [61], requires that in the immediate 5-foot (1.524 m) zone, planting must be limited to low growth (less than 2 feet (0.609 m)) and non-combustible materials such as gravel must be used instead of bark or mulch. Between 5 and 30 feet (respectively 1.524 and 9.144 m), owners must remove all tree branches or vegetation within 10 feet (3.048 m) of the chimney or stovepipe outlet. Grass must be cut to less than 4 inches (10.2 cm). In addition, property owners with vegetative-covered land must follow the guidelines for horizontal and vertical separation distances for trees and plants over 2 feet (0.609 m) in height that are within 100 feet (30.480 m) of a structure. For example, all shrubs greater than 2 feet (0.609 m) in height shall be in a maximum grouping of 3 plants and separated by a distance of 3 times the height of the tallest shrub in the group or 15 feet (4.572 m), whichever is greater.

In Canada, the national guide for wildland-urban interface fires defines priority zones for the fuel management within 100 m of buildings [14]. The priority zone 1A corresponds to the zone within 1.5 m of the building. In this zone, vegetation and combustible material including woody shrubs, trees and tree branches should be completely removed down to mineral soil. For Priority Zone 1, beyond 1.5 m and within 10 m of the building, there is no requirement for distance between vegetation and buildings. It is only advisable to remove over-mature, dead and dying trees, to remove highly flammable tree species and to thin and prune vegetation to prevent a fire from being carried towards the building.

Between 10 m and 100 m, the vegetative fuel should be reduced through selective removal of coniferous trees to maintain a horizontal separation not less than 3 m between single and grouped tree crowns. The branches located up to a height not less than 2 m from the ground should be removed from remaining trees. The accumulations of fallen branches, dry grass, and needles should be removed.

In Italy, forest fire management is defined in the law called Legge No. 353, November 21, 2000 [16]. Some regions, such as Tuscany and Abruzzo, have included the concept of defensible space in their fire prevention plans (Piano Antincendi Boscivi (AIB)). In Tuscany [62], in zone 1 located less than 10 m from buildings, trees and shrubs must be present in isolated form and possibly belong to non-flammable species (for example, deciduous trees are preferable to conifers). Trees and shrubs must not be in contact with each other (at least 2.5 meters between each plant) nor with the building (at least 5 meters). The foliage of the plants must then be kept at least 2.5 meters from the ground to avoid continuity between the ground and the foliage. Trees and bushes should not be placed in front of doors or windows and the creation of hedges without interruption or ending alongside buildings should always be avoided. For the Abruzzo regione [63], only herbaceous vegetation is allowed in zone 1, which is less than 3 m from the buildings. In zone 2, located between 3 and 10 m, no separation distance between trees is specified. It is only recommended to reduce fuel load.

The Greek government issued a ministerial decision in May 2023 to establish a uniform and mandatory framework of measures and means of fire protection for properties located in the WUI [8]. Fuel management must be carried out over a minimum width of 10 m. 3 zones are defined. In zone 1, adjacent to the building and 2 m wide, the cover must be non-combustible and free of vegetation. In zone 2 (between 2 and 5 m from the building), only low vegetation (shrubs less than 1 m high or ground cover plants) with grass is allowed. In zone 3 (between 5 and 10 m from the building), trees and large shrubs are at least 3 m apart. Trees are pruned to 3 m from the ground. Bushes are allowed provided they are not under trees.

In France, the fuel modification distance is 50 m [17]. Each county then defines by decree the rules for fuel management in this area. For Corsica [18], for a hedge less than 2 m high or a shrub less than 3 m, the distance between the vegetation and an opening or an exposed frame must be at least three times the height of the vegetation, but not less than 3 m. For trees (greater than 3 m), the distance between the crown and an opening or an exposed frame must be greater than or equal to 3 m.

In Australia, in bushfire prone areas, the Bush Fire Risk Treatment Standards must be applied [20]. The Inner Zone is within 10 m of the building. The owner or occupier of the land must clear any vegetation from the land to create a defensible space by creating a separation between flammable vegetation and the building surface. The Outer Zone includes land that is between 10 and 20 m from the building. This zone is managed to reduce the impact of a bushfire by slowing its rate of spread and suppressing the fire spread into the tree canopy. In this zone, the branches of the trees less than 2 m above the ground must be pruned. No vegetation clearance is required.

In Spain in the Comunitat Valenciana, the preventive measures in WUI are given by Decree 1/2021 [64] in accordance with Royal Decree 893/2013 of 15 November [65]. A defensible space of 30 m is required around the buildings. In the case of slopes, this distance must be increased to at least 50 m for slopes of more than 30%. Shrub and tree cover must be reduced so that it does not exceed 40% of the surface area of the plot. Contact between vegetation and buildings must be avoided. A minimum distance of 3 metres is therefore required between branches and any type of building. The use of materials and vegetation such as flammable hedges to enclose plots should be avoided.

For the Living Labs, in Canary Islands, Annex 3 of Decree 60/2014 requires a 30-metre fuel management zone around buildings for new construction [66]. This zone must be free of dry vegetation and the distance between the crowns of trees and shrubs must be at least 3 m. It is also recommended to maintain a distance of 2 m free of vegetation around buildings. Some insular initiatives, such as Gran Canaria Mosaico [27], extend these recommendations: use non-combustible species in the garden and keep them moist, avoid cypress or heather hedges, remove plant debris and clean weeds and bushes within the first 15 metres, plant crops or orchards, use non-combustible coverings in the first metres adjacent to the building (e.g. gravel, clay tiles or stone paving).

In Chile, the Ministry of Agriculture and CONAF give recommendations for the creation of self-protection zones around buildings based on 4 zones [15]. In the first zone, located between 0 and 2 m around the buildings, the herbaceous vegetation must not exceed 10 cm and combustible materials must be removed. In zone 2, between 2 and 10 m, all branches less than 3 m from the buildings must be removed and fire-resistant plant species must be selected. Branches less than 2-3 m from the ground must be pruned. The vertical distance between shrubs and tree branches should be at least three times the height of the shrub. Zone 3 is between 10 and 30 m and can extend up to 60 m depending on the slope. In this zone, tree tops should be at least 3 m apart. Bushes should be spaced 2 to 6 times their height, depending on the slope. It is also necessary to ensure vertical discontinuity as in zone 2. Zone 4, located between 30 and 60 m, is managed by the competent authorities. In this last zone, vegetation may be thinned or fuel breaks made.

In Portugal, the fuel modification distance is 50 m [38]. Around buildings, it is advisable to create a strip of non-inflammable pavement between 1 and 2 m wide around the building [19]. A 10 m strip (up to 20 m in steeper situations) of limited fuels should be established. This zone may, exceptionally, include a few isolated trees or shrubs, provided that they are located more than 5 m from the building, are irrigated and are of low flammability species and do not create horizontal and vertical continuity of the fuel. Beyond 10 m, trees must be pruned 4 m above the ground or on the lower half of the tree for trees less than 8 m. The distance between treetops should be at least 4 m or 10 m for maritime pine and eucalyptus, respectively.

Table 14: Defensible space characteristics found in regulations/guidelines worldwide

Country	Fuel modification distance (m)	Distance without fuels (except herbaceous vegetation) around building (m)	Separation distance between shrub/tree/tree branch and building (m)	References
USA (California)	30.48	1.5	3.048	[60,61]
Canada	100	1.5	-	[14]
Chile	30 to 60*	2	3	[15]
Italy (Tuscany)	30	-	5	[62]
Italy (Abruzzo)	30	3	3	[63]
Greece	10	2	2 m for shrub less than 1 m high and 5 m otherwise	[8]
France (Corsica)	50	3	For trees: minimum of 3 m For hedges and shrubs: 3 times the height of the plants with a minimum distance of 3 m	[18]
Portugal	50	2	5	[19,38]
Australia	20	10	10	[20]
Canary Island (Spain)	30	2	-	[66]

*The extension to 60 m depends on the slope

4.2. Plant moisture content

Among the environmental parameters affecting fire spread, fuel moisture content (MC) is recognised as one of the most important (along with wind and topography) [67–72]. This part presents the investigation of the influence of the moisture content on the fire behaviour of *Cistus monspeliensis* shrubs exposed to a fire front spreading over a bed of wood wool on a laboratory scale. This plant was chosen because of the work of Pellizzaro et al. [73]. They showed that the moisture content of *Cistus monspeliensis* varies is very wide throughout the year, including the range of most plants in the Mediterranean. This work has been published in Fire Safety journal [74]. The aim is to provide the ignition and spread thresholds to make recommendations on the fuel moisture content of vegetation in the WUI.

4.2.1. Materials and methods

63 burning experiments were carried out in this experimental campaign. In order to obtain the desired fuel moisture contents, the branches were air-dried in the laboratory with an ambient temperature of 20.3 (±3.5) °C and a relative humidity of 37.9 (±5.8) %. A

preliminary study was conducted in order to determine the time needed to reach a given moisture content (MC) of leaves. For example, the time required to reach a leaf MC of 40% from an initial MC of fresh leaves of 127% was 5 days. In this experimental campaign, leaf MC ranging from 10 to 100 % (on dry basis) were investigated.

For each test, rockrose branches with an initial wet mass between 2.23 and 3.84 kg, depending on the leaf moisture content, were placed in a welded mesh cage ($0.5 \times 0.5 \times 1 \text{ m}^3$) to simulate the shape of a real shrub [75]. The initial wet mass of the shrub (m_{wet}) was adjusted for each run, in order to keep a constant dry mass of leaves around 0.332 (± 0.005) kg for all experiments. Table 16 gives the initial wet mass of the shrub (m_{wet}) and the corresponding initial dry mass (m_{dry}) for each leaf moisture content tested. The cage was placed on a $1.2 \times 1.2 \text{ m}^2$ combustion bench made of aerated concrete located on a load cell (with an accuracy of 3 g and sampling rate of 1 Hz) (Figure 25). To mimic the ignition of a shrub by a flame front in an herbaceous layer, a bed of wood wool was positioned in front of the branches. The wood wool of white pine was oven-dried at 60°C for 24 hours and then was used to make a bed of 0.7 m long (including 0.2 m under the branches) by 0.6 m wide with a fuel load of $0.6 \text{ kg}\cdot\text{m}^{-2}$. This resulted in a bed thickness of 0.10 m. The wood wool bed was ignited with 3 mL of ethanol spread across the width of the bed edge. A GoPro camera was placed on the left side of the device to record the different stages of combustion. Between 1 and 4 replicates were made for each leaf moisture content.

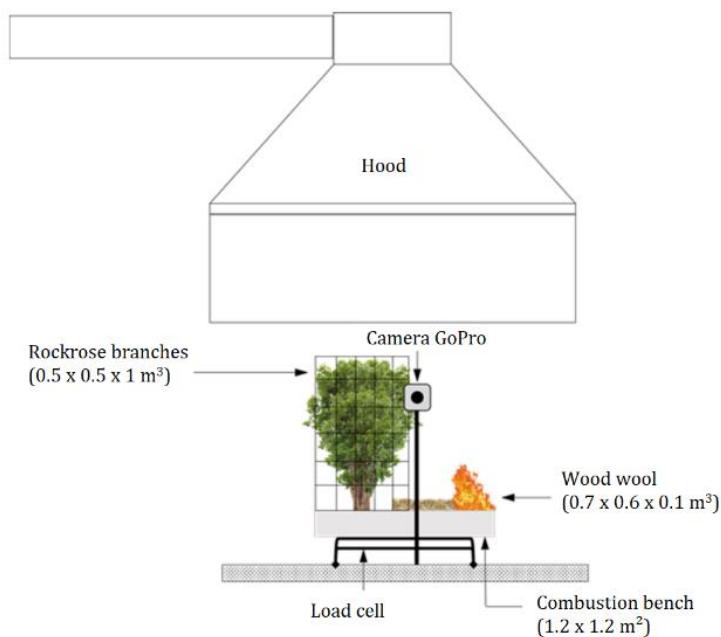


Figure 25: Schematic diagram of the laboratory experiments for the influence of the moisture content on the fire behaviour

Table 15: Average values of the initial wet and dry mass of rockrose for the different leaf moisture contents tested.

Leaf moisture content (%)	Initial wet mass (kg)	Initial dry mass (kg)
100	3.84 (± 0.20)	2.35 (± 0.03)
95	3.71 (± 0.00)	2.30 (± 0.00)
90	3.80 (± 0.00)	2.38 (± 0.00)
85	3.70 (± 0.00)	2.34 (± 0.00)
80	3.61 (± 0.25)	2.31 (± 0.00)
75	3.51 (± 0.25)	2.27 (± 0.01)
70	3.40 (± 0.25)	2.24 (± 0.01)
65	3.30 (± 0.25)	2.19 (± 0.00)
60	3.11 (± 0.14)	2.09 (± 0.14)
55	3.26 (± 0.32)	2.24 (± 0.25)
50	3.01 (± 0.35)	2.04 (± 0.40)
45	2.79 (± 0.00)	1.95 (± 0.00)
40	2.73 (± 0.32)	1.94 (± 0.10)
35	2.60 (± 0.00)	1.87 (± 0.00)
30	2.36 (± 0.30)	1.71 (± 0.20)
25	2.50 (± 0.25)	1.84 (± 0.25)
20	2.40 (± 0.25)	1.81 (± 0.00)
12.5	2.25 (± 0.10)	1.76 (± 0.04)
10	2.23 (± 0.25)	1.76 (± 0.12)

4.2.2. Results and discussion

The different stages of combustion observed during the tests are shown in Figure 26 to Figure 28 for different leaf MC values. The flame front initially spread across the wood wool bed (Figure 26.a, Figure 27.a and Figure 28.a) with a flame height of approximately 40 cm, based on observation of the cage mesh. This resulted in a slight mass loss (Figure 29.a). After 33.4 (± 7.6) s of spread, the flame front reached the branches of rockrose. Depending on the MC of the leaves, either the branches were ignited by direct contact at the base of the crown (Figure 26.b), or the rockrose branches did not ignite and only the fine particles above the flame front were burned or even scorched at the highest MC values (Figure 28.b). When no ignition of the branches occurred (i.e. above 85 %), the observed mass loss was due to the combustion of the wood wool and the dehydration of the fine particles of rockrose located above the fire front. When the rockrose branches ignited, two behaviours were observed as a function of the leaf MC. (i) For MC values below 55 %, the flame front spread over the entire crown (Figure 26.c and 25 % MC in Figure 29). Mass loss increased rapidly until the MLR reached a peak. Then the decay phase began until the flames were extinguished.

After the flameout, the thicker particles remained (Figure 26.d). Contrary to the experiments carried out by Meerpoel-Pietri et al. [76] on *Cistus monspeliensis*, the branches did not collapse at the end of the combustion, which prevented them from burning completely. (ii) For MC values between 55 % and 85 %, the flame front extinguished gradually after ignition (Figure 27.b and 65 % MC in Figure 29). The MLR showed a peak as before, but with a lower magnitude. At the flameout, there remained

many unburned particles including leaves, thin and thick twigs because the flame did not reach all the branches (Figure 27.d).

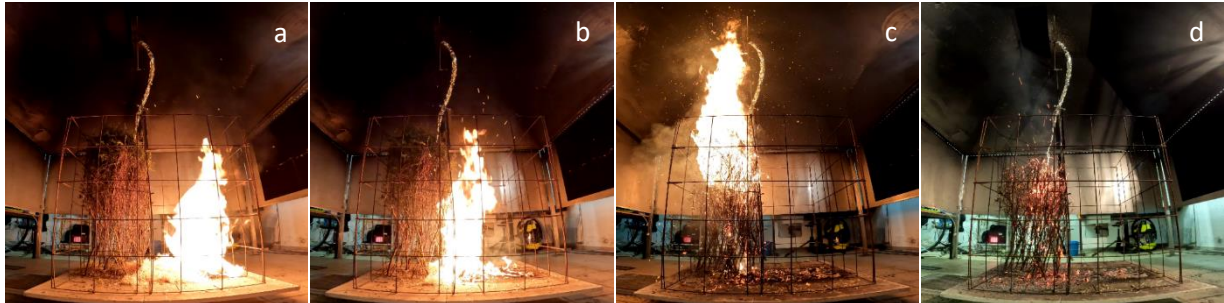


Figure 26: Different phases of an experiment with a fuel MC of 10 % - a) Fire front spread across the wood wool bed b) Branch ignition c) Flame spread upward through the branches d) Extinction phase

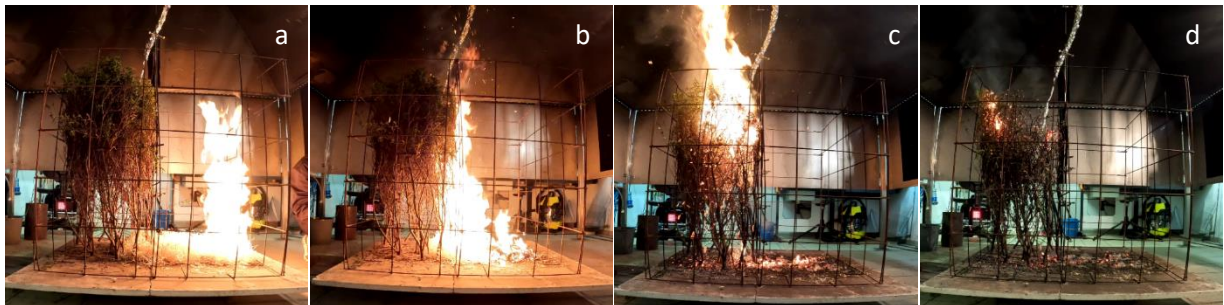


Figure 27: Different phases of an experiment with a fuel MC of 65 % - a) Fire front spread across the wood wool bed b) Branch ignition c) Flame spread upward through the branches d) Extinction phase



Figure 28: Different phases of an experiment with a fuel MC of 100 % - a) Fire front across the wood wool bed b) No ignition of the branches

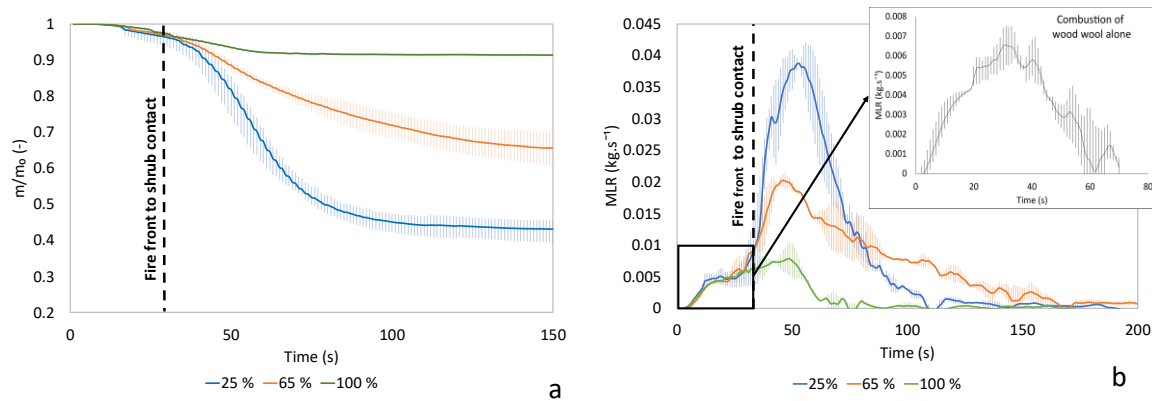


Figure 29: a) Mass loss divided by the initial wet mass b) Mass loss rate (MLR) - for three leaf MC: 25 %, 65 % and 100 %

Figure 30 shows the final mass loss and the peak of MLR for the different leaf moisture contents investigated. The values are given in Table 16. The mass loss tends to decrease as the leaf moisture content increases. This result is in agreement with the work of Dahale et al. [77]. Three behaviours can be identified as a function of the leaf moisture content:

- For moisture contents above 85%, the mean final mass loss does not exceed 15% and the mean peak of MLR is around 0.015 (± 0.001) $kg.s^{-1}$.
- For moisture contents between 85 and 55%, the mean final mass loss and the mean peak of MLR are almost constant: on average 33.90 (± 7.14) % and 0.020 (± 0.004) $kg.s^{-1}$, respectively.
- For moisture contents lower than 55%, the mean final mass loss and mean peak of MLR are the highest, varying between 45 and 55 % and between 0.031 and 0.049 $kg.s^{-1}$ respectively.

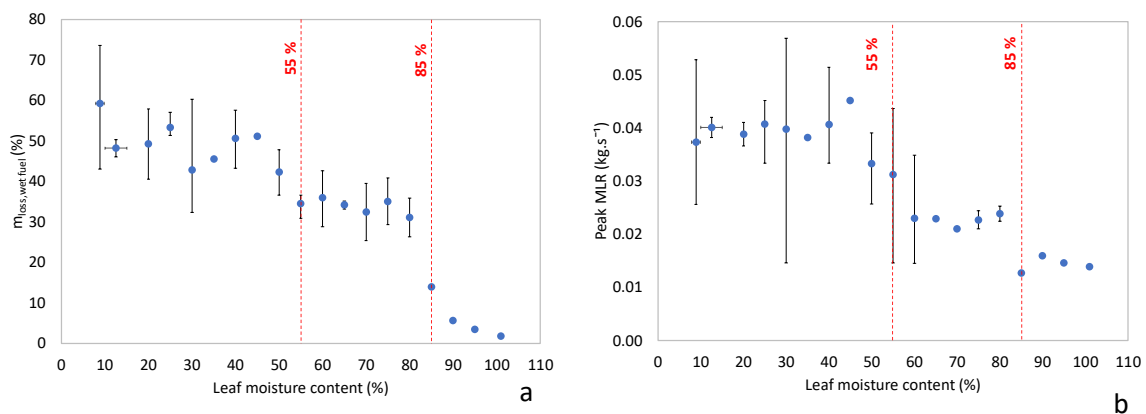


Figure 30: a) Final mass loss of the rockrose branches calculated from the initial wet mass – b) Peak of mass loss rate for the rockrose branches – as function of the different leaf MC.

Table 16: Summary of the results for all experiments: average final mass loss and peak of MLR for the different leaf moisture contents tested.

Leaf moisture content (%)	Final mass loss (%)	Peak of MLR (kg.s ⁻¹)
100	1.78 (±0.35)	0.014 (±0.000)
95	4.15 (±0.00)	0.015 (±0.000)
90	5.65 (±0.00)	0.016 (±0.000)
85	13.95 (±0.00)	0.013 (±0.000)
80	31.12 (±4.80)	0.020 (±0.005)
75	35.09 (±5.74)	0.023 (±0.002)
70	32.47 (±7.04)	0.021 (±0.000)
65	34.19 (±1.00)	0.023 (±0.000)
60	35.96 (±5.47)	0.023 (±0.008)
55	34.57 (±2.60)	0.031 (±0.012)
50	44.99 (±2.27)	0.033 (±0.006)
45	51.16 (±0.00)	0.045 (±0.000)
40	50.61 (±6.44)	0.041 (±0.007)
35	50.99 (±5.40)	0.040 (±0.001)
30	49.59 (±11.19)	0.048 (±0.010)
25	51.51 (±0.15)	0.042 (±0.001)
20	51.51 (±0.15)	0.042 (±0.001)
12.5	51.51 (±0.15)	0.042 (±0.001)
10	55.33 (±10.81)	0.036 (±0.010)

These data allowed us to identify thresholds of leaf moisture content that govern the ignition and burning of rockrose shrub when exposed to a low intensity fire. A leaf moisture content of less than 85% is required for the rockrose to ignite upon the arrival of such a fire front. Above this value, the shrubs do not ignite and the mass loss recorded is solely due to the drying of the branches caused by the heating of the fire spreading over the wood wool. For such exposure conditions, we obtained a first threshold of leaf moisture content corresponding to the ignition of the rockrose shrub, which is 85 %. A second threshold was obtained corresponding to the condition for the fire to spread through the crown, which occurred when the leaf moisture content was below 55%. The ignition threshold found in our study is in agreement with that of Thomas (90 % for pine needles [78]) and those of Chastagner (between 30 and 90 % for conifers % [79]). Regarding the spreading threshold, our value is in agreement with Santana and Marrs (between 19 and 59 % [80]) and Chastagner (between 10 and 55 % [79]), but is slightly higher than those obtained by Masinda et al. (between 9.6 and 38.9 % [81]). The ratio between our ignition and spreading thresholds is equal to 1.55. This value is within the range obtained by Masinda et al. [81]: between 0.5 and 6.4 for match ignition and between 0.6 and 3.1 for cigarette ignition.

4.3. Numerical study

The numerical simulations of the living labs fire scenarios were performed using the physics-based Computational Fluid Dynamic (CFD) code Wildland-Urban Interface Fire Dynamics Simulator (WFDS) release version 9977. This is a standalone code based on the Fire Dynamics Simulator (FDS) developed by the National Institute of Standards and Technology (NIST), specifically designed to model vegetation fires [82]. The code solves the fundamental equations of fluid mechanics, heat and mass transfer, and combustion.

The WFDS provides two types of vegetation models that can be used either independently or combined. The first is the *Boundary Fuel* approach, which solves the energy balance within the fuel layer on its own vertical computational grid. The interactions between the solid and the gas phase are limited to heat and mass fluxes at the boundary between them. This approach is only suitable for surface fuels. The second approach, designated as the *Fuel Element* approach, considers fuel particles as thermally thin, non-scattering, perfectly absorbing, fixed sub-grid elements uniformly distributed within a bulk volume (grid cell). The interactions between the gas and the solid phases are represented by bulk source/sink terms in the mass, species, energy, and momentum balance equations. This approach is applicable to raised fuels (vegetation with a height greater than the grid cell size) or surface fuels when the grid resolution is sufficiently fine [83].

The WFDS has been tested and validated in various situations either at laboratory scale [82–87] or field scale [88–90] which have made it one of the best candidate to model wildfire scenarios at WUI. However, since numerical simulations studies with WFDS involving structures and vegetation are scarce in the literature, a validation study using WFDS to reproduce experiments carried out at the EXPLORII platform was performed and will be presented in the document.

4.3.1. Materials and methods

The fire scenarios associated with the living labs in Chile and Portugal were defined and implemented using the information provided by stakeholders, e.g., data of topography, meteorological conditions, vegetation, etc. (see Section 2 for further details). In this section, the general methodology to implement the numerical scenarios is detailed, as it is common to both living labs. However, specific details will be given for Chile and Portugal living lab simulations in sections 4.3.3.1 and 4.3.3.2, respectively.

First, the numerical domain was defined based on the area of interest provided by the living lab and considering the specific characteristics of the structure's surroundings (i.e., vegetation, roads), the most probable ignition point or fire scenario and also the prevailing average wind direction. In this regard, the meteorological conditions and the fire scenario were determined based on the local weather station measurements during the fire season and historical fires (when this information was available), in order to

identify and study the most favourable conditions for wildfire propagation in agreement with the stakeholders.

The topographic data for the numerical domain was extracted from the digital terrain model (DTM) and converted into obstacle coordinates that can be interpreted by WFDS. The level of ground detail considered in the simulations depends on the resolution of the DTM. Consequently, the higher the resolution of the DTM, the greater the level of detail in the simulation. Figure 31 illustrates the DTM model and the corresponding WFDS topography for the Chile Living Lab.

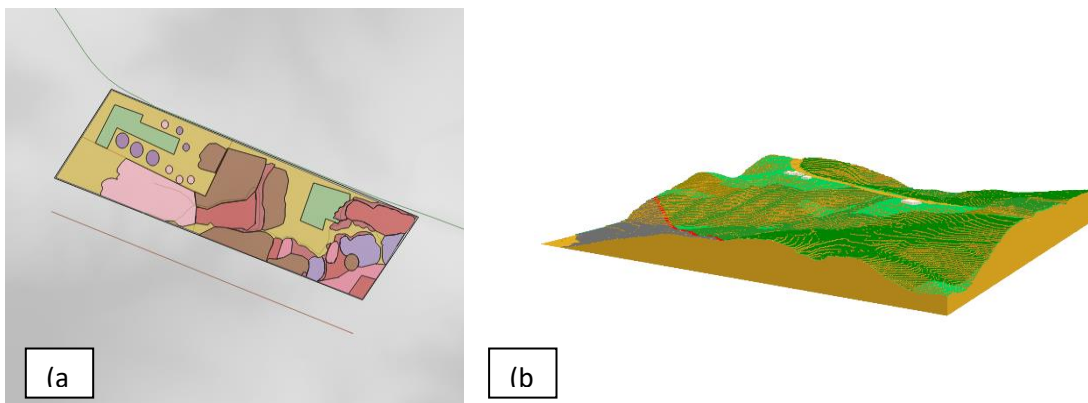


Figure 31: Topography modelling: (a) Chile DTM superimposed by the parcel details, (b) Smokeview rendering of the numerical terrain implementation

The numerical domain was divided into several discrete blocks, which were uniformly meshed with hexahedral cells. The cell size was set to 1 m, as this size resulted in the best compromise between accuracy and computational performance. Each mesh block was dimensioned to contain between 250,000 and 500,000 cells, which was found to be a suitable range for computational performance. An example of the mesh grid used around the structures for the scenario of Chile is shown in Figure 32.

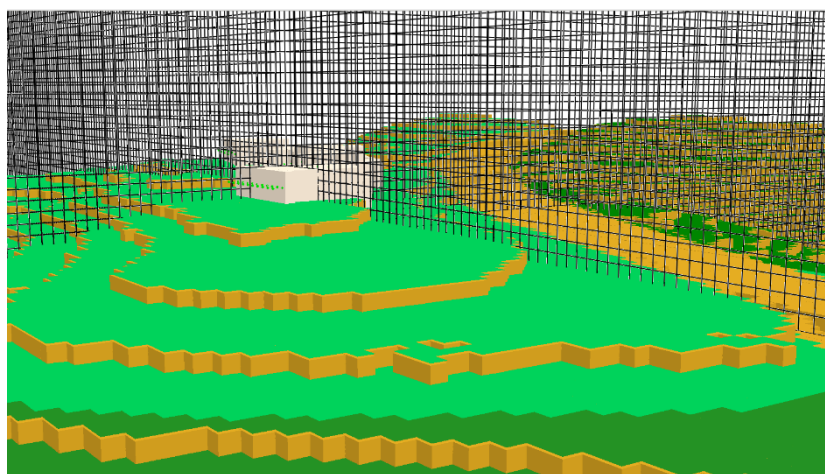


Figure 32: Example of meshing strategy around the structures for the Chilean scenario.

The incoming wind was modelled with a $1/7^{\text{th}}$ power law profile at the INLET boundary condition [91], based on the meteorological conditions previously defined. The outlet boundary condition was modelled as an OPEN boundary. The wind direction was taken into account by adjusting the (u, v) component of the velocity vector by considering the direction angle as shown in Figure 33. The rest of the boundary conditions (i.e., top and the remaining side) was also considered as OPEN to allow the fire smoke to exit the numerical domain.

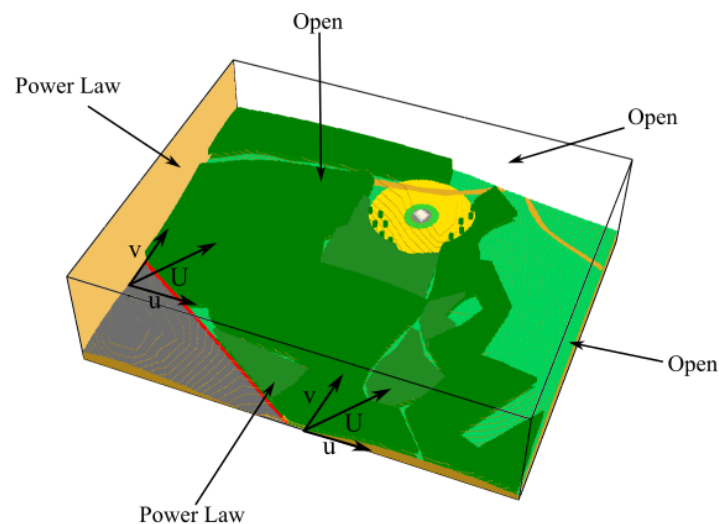


Figure 33: Smokeview rendering of the Portuguese scenario illustrating the boundary conditions including the wind modelling, and the vegetation

To implement the vegetation component of the numerical scenario, only the species and vegetation patches that were identified as the most relevant in the overall forest inventory of the plot were modelled. In accordance with the vegetation data provided by the living labs and the scale of the simulations, the grass layer and understory vegetation were modelled using the *Boundary Fuel* approach. This approach simplifies the vegetation modelling and reduces the computational resources required for the simulations. In the case of trees modelling, only the canopy was modelled, as it contains the greatest quantity of the finest particles, which are those that contribute the most to the fire spread. In this case, the *Fuel Element* approach was used to model the canopy layer taking into account only the leaves and the twigs with a diameter lower than 2 mm in order to limit the computational resources necessary to run the simulations. Thermo-physical properties for each species and particle class were gathered from both the living labs data and literature. Two types of thermal degradation models were used depending on the vegetation modelling approach used, i.e., a linear thermal degradation model that accounts for char oxidation when using the *Boundary Fuel* approach, and a three-step Arrhenius-based thermal degradation model when using the *Fuel Element* approach. The input parameters required by both approaches were taken from the literature. Figure 33 shows a Smokeview rendering for the Portugal living lab's scenario, including the vegetation.

Dwellings were modelled with INERT obstacles that approximated their geometry within the limits of the grid resolution. The grid resolution did not allow for the modelling of the openings or the gutters. The radiant and total heat fluxes received by the dwellings were measured using RADIOMETERS and GAUGE HEAT FLUXES numerical probes positioned at 1 m from the ground, on the house wall, and distributed spanwise. These types of sensors reproduce the behaviour of heat flux sensors cooled to ambient temperature and capture the radiant and total heat fluxes respectively. The vulnerability of dwelling materials was analysed by using the heat fluxes received at the façade of the structure in terms of the radiant thermal dose as described in Section 3.3.2. The numerical predictions were compared with the experimental values measured at the EXPLORII platform that led to materials damage, and that have been previously detailed in the same section.

Fire ignition was modelled by using a Heat Release Rate per Unit Area (HRRPUA) boundary condition, which was oriented to enhance the fire spread, according to the fire scenario defined with the stakeholders. The length of the ignition line varied depending on the scenario but in all cases, it was modelled as 1 m wide. The ignition was set during 30 s at 1129 kW/m^2 .

The numerical simulations were run on the ORSU computing cluster of the University of Corsica which is composed of 28 nodes, each of them equipped with 2x Intel XEON 6230R (26 cores @ 2.1GHz couple with 192 Go of DDR-4 RAM). Each mesh block defined in the WFDS input file was allocated to one CPU core of the cluster. The total number of nodes allocated for the simulation varied depending on the scenario considered. More details will be provided on Section 4.3.3.

4.3.2. Validation setup at field scale: the EXPLORII Platform

As introduced in Section 4.3, the purpose of this section is to perform a validation stage of WFDS at field scale involving a structure and vegetation in a WUI scenario, based on the EXPLORII platform experiments. To do so, experiments conducted at the platform (see section 3.2.) with a reconstructed ornamental rockrose hedge were simulated with WFDS. The experiments followed the methodology that has already been described in Section 3.2. Two sizes of reconstructed rockrose hedges ($6 \times 1 \times 1 \text{ m}^3$ and $6 \times 1 \times 2 \text{ m}^3$) were tested. The ambient conditions for these configurations are given in Table 17.

Table 17: Ambient conditions and vegetation moisture content for the EXPLORII test cases.

Hedge Size	Temperature (°C)	Air Humidity (%)	Wind Speed (m/s)	Wind Direction (°)*	Hedge FMC
$6 \times 1 \times 1 \text{ m}^3$	23.5	27	3.05	-0.95	5%
$6 \times 1 \times 2 \text{ m}^3$	28.8	55.5	3.40	-5.74	14%

*Wind direction corresponding to the angle formed between the wind and the perpendicular axis to the house facade

The platform was implemented by using a numerical domain with dimensions of $92 \times 64 \times 64 \text{ m}^3$ (Figure 34) which includes the sloped terrain, the house and a storage container of non-negligible size. The domain was composed of hexahedral cells of three different sizes. In the fire zone, which includes the slope and the house, a cell size of 12.5 cm was chosen as an optimal compromise between simulation accuracy and computational efficiency. The specified cell size was also appropriate for the implementation of a detailed particle distribution model in the numerical hedge. In regions where wind flow was the only phenomenon occurring, larger cell sizes of 25 cm and 50 cm were used to reduce the overall computational cost of the simulation. The inlet boundary condition was defined using a $1/7^{\text{th}}$ power law profile, with the velocity magnitude and the reference altitude values derived from the measurements of the anemometer located at the base of the slope (Figure 10).

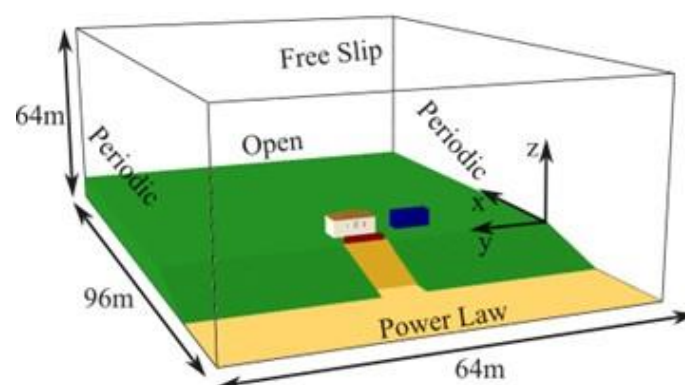


Figure 34: Smokeview representation of the numerical domain for the EXPLORII simulation cases.

In order to account for the wind direction, the side boundary conditions were set to PERIODIC. The top boundary condition was set to FREE SLIP, while the outlet was set to OPEN. Turbulence was modelled by using the synthetic eddy approach, with the root mean square value of wind velocity derived from the anemometer measurements. The wooden wool litter and the rockrose hedge were both modelled with the *Fuel Element* approach. The fuel load for the litter was 1 kg/m^2 , the surface-to-volume ratio (σ) was 10269 m^{-1} and the moisture content (FMC) was 5%. The rockrose hedge was numerically represented by six particle classes (flowers, leaves, and twigs with diameters of 0 – 2 mm, 2 – 4 mm, 4 – 6 mm, and > 6 mm) distributed across eight layers. This particle distribution was based on laboratory analysis of sampled branches of rockrose (not detailed here for brevity) and reflects the structure of an actual shrub. For an example of particle distribution modelling for raised vegetation at a laboratory scale, see the study by Meerpoel et al [84].

The thermal degradation process was modelled by a three-step Arrhenius-based model, including dehydration, pyrolysis, and char oxidation. The model coefficients for thermal degradation were obtained from the literature [85]. Numerical radiometers, heat flux gauges, and thermocouples were placed in the numerical domain at the corresponding positions of the experimental sensors of the platform. Fire ignition was modelled by using

a HRRPUA boundary condition of 191 kW/m^2 , which corresponds to the effective surface heat released by the torch.

Numerical results have been compared with experimental measurement for both cases. For conciseness, only the relative difference $\Delta\phi$ (where ϕ is the physical quantity that is compared) expressed as detailed in equation 1 are presented in Table 18.

$$\Delta\phi = \frac{|\phi_{Num} - \phi_{Exp}|}{\phi_{Exp}} \quad (7)$$

Table 18: Relative difference between experimental measurements and numerical predictions for the EXPLORII test cases.

Hedge Size	Residual Mass	Radiant Heat Fluxes Peaks	Total Heat Fluxes Peaks	Shutter Temperature Peaks
$6 \times 1 \times 1 \text{ m}^3$	3.3%	16.3%	2.6%	13.4%
$6 \times 1 \times 2 \text{ m}^3$	16.9%	13.8%	16.2%	-*

*Shutter temperature was not recorded during this test case.

As illustrated in the table, the values of the relative difference between the experimental measurement and the associated numerical predictions for the $6 \times 1 \times 1 \text{ m}^3$ hedge size are lower than 5% for the residual mass and total heat flux peaks, indicating a good agreement between the numerical model and the experimental results. The relative differences for the radiant heat flux peaks and the shutter temperature are higher but remain in an acceptable range at this scale. In comparison to the $6 \times 1 \times 1 \text{ m}^3$ hedge size, the values of the relative differences between experimental and numerical values are higher for the $6 \times 1 \times 2 \text{ m}^3$ hedge case. However, they remain within an acceptable range for both the mass loss and the radiant heat flux peaks. The relative error in the heat fluxes between the numerical simulations and the experiments can be explained by the flame orientation towards the sensors, which is slightly different. Indeed, the flame orientation is strongly influence by the upcoming turbulence in the field which is difficult to reproduce numerically. In addition, the difference in the residual mass for the $6 \times 1 \times 2 \text{ m}^3$ maybe induced by the hedge collapsing which is not reproduced experimentally as evidenced by Meerpeol *et al* at laboratory scale [84].

Given these results, it can be assumed that WFDS can be used to model WUI scenarios, provided that the results are interpreted carefully.

4.3.3. Results and discussion

4.3.3.1. Chile

The Chilean WUI scenario is an intermix type, including four houses located along a road and surrounded by forests, grasslands, and crop fields, as illustrated in Figure 1.b. A numerical domain with dimensions of $460 \times 416 \times 120 \text{ m}^3$ was defined based on the location of the houses, the fire scenario defined with the stakeholders, and the prevailing mean wind direction (Figure 35). The domain includes a significant portion of the

vegetation situated downslope from the road ahead of the houses, allowing for the fire front to fully develop before reaching these structures. Additionally, it also includes a section of the forest behind the houses in order to assess the road's ability to stop the fire propagation. The numerical domain was meshed using 80 blocks of 1 m sized hexahedral cells, with each block consisting of 287,040 cells.

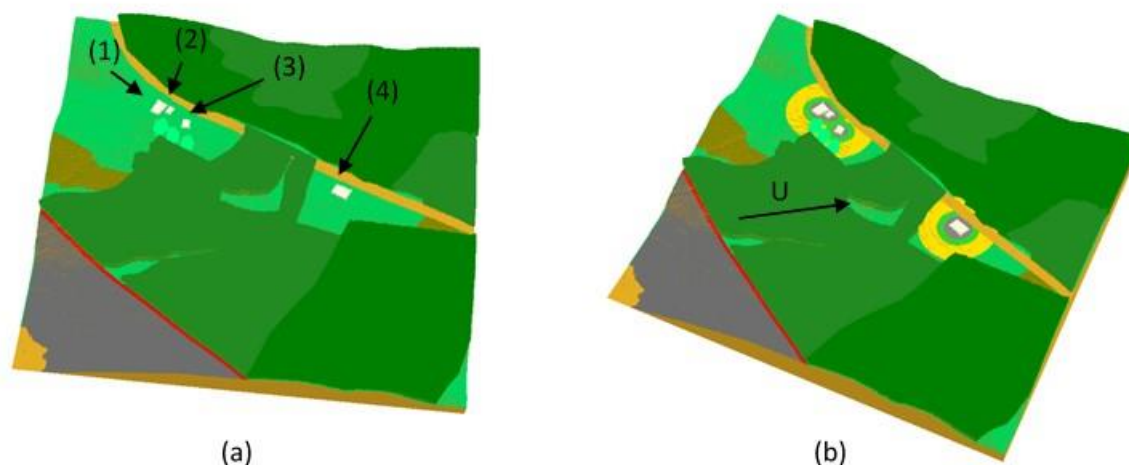


Figure 35: Smokeview representation of the Chilean Living Lab scenarios: (a) Standard Vegetation, (b) Landscaping Management.

The ambient conditions were obtained from the nearest weather station (close to the city of Tomé) for the summer seasons between 2020 and 2022. Two distinct weather scenarios were studied, as shown in Table 19. The *normal* scenario represents the average summer weather conditions, while the *extreme* scenario is representative of a warmer and drier case, taking into account the potential effects of climate change. The wind conditions remained the same in both scenarios. The wind variation induced by the wind gusts is taken into account through the u_{rms} used in the Synthetic Turbulent Eddy boundary condition utilized to model the inlet turbulence [92]. The boundary and ambient conditions for the simulation were implemented as detailed in Section 4.3.1.

Table 19: Ambient conditions considered for the Chilean numerical scenario.

Weather scenario	Temperature (°C)	Air Humidity (%)	Wind Speed (km/h)	Wind Gust (km/h)	Wind Direction (°)
Normal	24.4	45.7	16.4	26.4	191
Extreme	32.0	18.0			

The forest component was implemented by using the *Fuel Element* approach. *Eucalyptus globulus* and *Nothofagus obliqua*, identified as the primary tree species from the National

Forest Inventory data, were chosen for modelling the forest. To reduce the computational resources and time needed for the calculation, the forest was modelled by several patches of continuous canopy layers of either *Eucalyptus globulus* or *Nothofagus obliqua*, containing leaves and small twigs, instead of modelling individual trees. In addition, the detailed inventory of the plot highlighted the presence of large fruit trees close to the houses number 1 and number 2. These trees were also included in the numerical scenario but in this case as individual trees. The thermal degradation mechanisms were implemented by using literature data as described in Section 4.3.1.

For each tree species, the corresponding understory was modelled by using the Boundary Fuel approach. To this purpose, data provided by the stakeholders and data from Scott and Burgan’s SH4 fuel model were used. In addition, a patch of *Rubus ulmifolius* of a significant size in the slope towards the house number 1 was also considered and implemented in the numerical scenario as *Boundary Fuel*. Finally, a grass layer was included by using the *Boundary Fuel* and data from the literature [88].

The associated bulk density, fuel moisture content and surface-to-volume ratio for each species and particle class are given in Table 20.

Table 20: Properties of the vegetation used for the Chilean scenarios. FE: Fuel Element approach, BF: Boundary Fuel approach. Twigs refer to particles of 0 – 2 mm

Fuel modelling approach - Vegetation species - particle class	Bulk Density (kg/m ³)	FMC in Normal Conditions (%)	FMC in Extreme Conditions (%)	Surface to Volume Ratio (m ⁻¹)	Source
FE - Eucalyptus globulus - leaves	0.072	60	50	4200	[88,93-95]
FE - Eucalyptus globulus - twigs	0.036	60	50	5000	
FE - Nothofagus obliqua - leaves	0.020	60	50	4003	
FE - Nothofagus obliqua - twigs	0.010	60	50	4000	
FE - Fruit trees - leaves	0.144	60	50	4200	
FE -Fruit trees - twigs	0.072	60	50	4200	
BF - Eucalyptus globulus - understorey	1.096	32	25	4805	
BF - Nothofagus Obliqua - understorey	1.418	30	25	5524	
BF - Rubus ulmifolius	1.273	32	25	5000	
BF - Grassland	1.368	32	5	9770	

Two vegetation management cases were set up. The unmanaged case refers to the actual vegetation distribution in the study area according to the inventories provided by the

stakeholders, while the Managed vegetation case refers to a landscape design that follows the current fire safety regulations available in Chile, which considers three zones:

- Zone 1 (Grey in Figure 36b) from 0 to 2 m: No vegetation.
- Zone 2 (Green in Figure 36b) from 2 to 10 m: Grass up to 10 cm high with high FMC.
- Zone 3 (Yellow in Figure 36b) from 10 to 30 m: Grass up to 10 cm high with low FMC.

It is worth noting, that the standard case was specifically chosen by stakeholders since it is not in compliance with the actual regulations in terms of vegetation management at WUI in Chile.

The two vegetation configurations were simulated in both normal and extreme weather conditions. Figure 36 shows the iso-surfaces of heat release rate per unit of volume (HRRPUV) at 200 kW/m^2 for both studied cases, where it can be observed the fire front propagation towards the houses' façade.

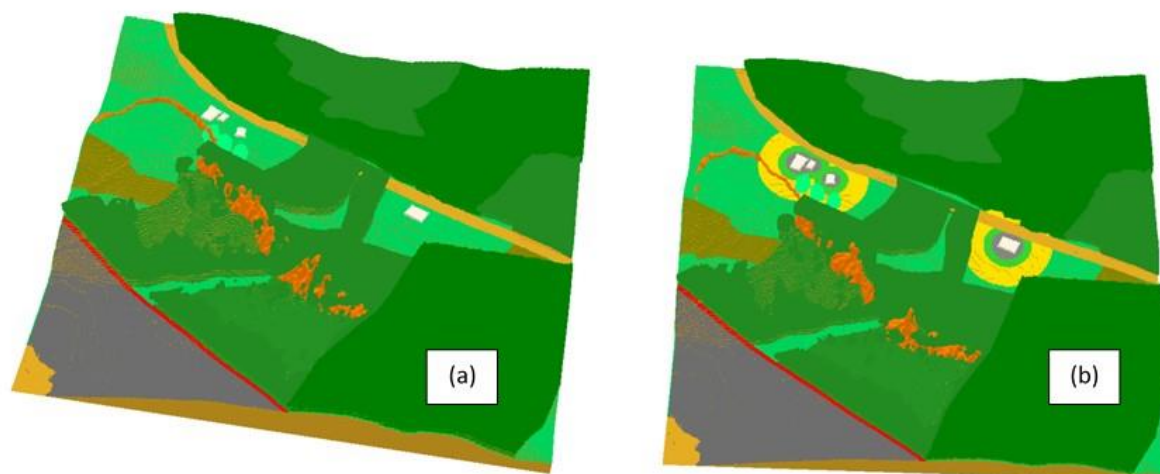


Figure 36: Iso-surface of HRRPUV at 200 kW/m^2 predicted for the Chile scenario in extreme weather conditions: (a) Unmanaged vegetation, (b) Managed vegetation.

In the unmanaged case, direct contact between the flames and the houses' façade is observed according to the simulation results. However, the number of houses impacted by the fire varies depending on the weather scenario. Under normal weather conditions, only the houses number 1, 3 and 4 experience direct flame contact. The fire front does not reach the house number 2 due to its position on a downslope terrain, that induces a reduction of the fire intensity until the fire extinction before its arrival to the location of this house (see Figure 37). However, in the case of the extreme weather scenario, the fire impacts all the houses, as the intensity of the fire is higher. The simulation results demonstrate that when managing the vegetation, the fire front extinguishes in the zone 2 (i.e., from 2 to 10 m from the houses) for both weather scenarios. This prevents the

direct flame contact with the houses' façades and thus reduces the heat flux received by the structures which in turn reduces their vulnerability.

The resulting thermal exposure has been subsequently evaluated for the four cases, and the results are presented in both Table 21 and Figure 38. As indicated in Table 21, the unmanaged vegetation cases results in a thermal exposure of the houses façades that lasts between 20 and 40 seconds, with radiant heat peaks between 80 and 160 kW/m², and total heat peaks between 100 and 180 kW/m², depending on the location of the house and the orientation of the fire front. The radiant heat dose, as illustrated in Figure 38, indicates that the thermal exposure is significantly high, thereby increasing the risk of damage for the wood and PVC materials. Indeed, the level of radiant heat dose reaches the experimental thresholds measured on the EXPLORII platform for the blackening of wood and PVC, in the case of normal weather conditions, while exceeding the burning threshold for the wood in the case of extreme weather conditions. As expected, the simulations of the unmanaged vegetation case in both weather conditions predict significant material damage in the event of an incoming wildfire under the studied conditions.

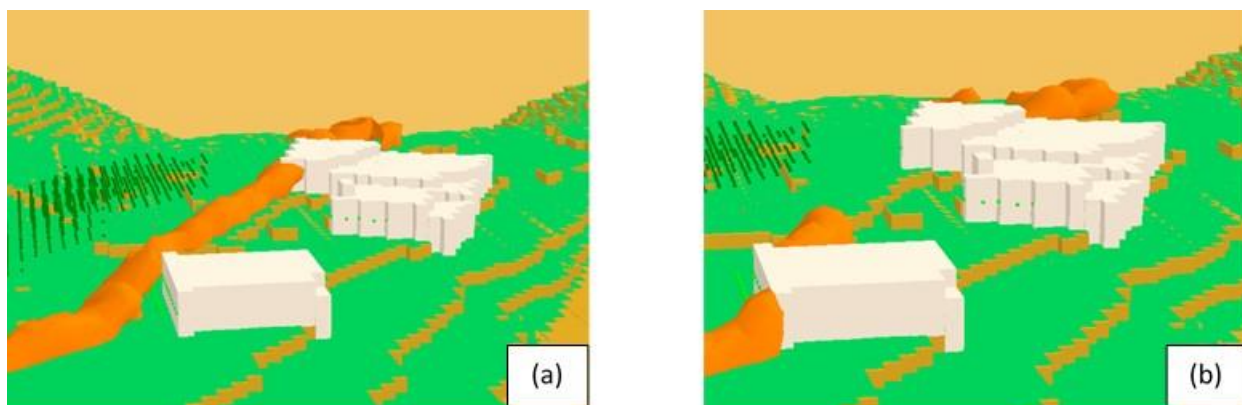


Figure 37: Iso-surface of HRRPUV at 200 kW/m³ reaching houses façade for the Chilean Scenario: (a) at given time t, (b) at t + 10 s

On the other hand, the managed vegetation cases result in a significant reduction of the houses thermal exposure induced by the incoming wildfire for both weather scenarios, as shown in Table 21. In fact, the fire extinguishes itself within the defensible zone 2, so that the heat flux received at the façades does not exceed 7 kW/m² and therefore does not result in a significant peak of heat exposure, nor in a relevant exposure time. This results in radiant heat doses that are considerably below the established experimental thresholds. Consequently, no significant material damages are predicted for the studied configurations (Figure 38) if the vegetation is managed in full compliance with the current regulations in Chile.

Table 21: Prediction of thermal exposure and material damage for the different scenarios of the Chilean living lab.

Vegetation	Weather	Total Exposure Time (s)	Radiant Heat Flux Peak (kW/m ²)	Total Heat Flux Peak (kW/m ²)	House Impacted	Wood Damage	PVC Damage
Unmanaged	Normal	20-40	80-160	100-180	n° 1,3,4	Yes	Yes
Managed	Normal	-	0.9-5	0.9-5	None	No	No
Unmanaged	Extreme	20-30	80-140	100-160	n°1,2,3,4	Yes	Yes
Managed	Extreme	-	1.7-7	1.8-7	None	No	No

The simulation results for the Chilean Living Lab show the effectiveness of the fire safety recommendations for homes exposed to wildfire in both standard and extreme weather conditions for this specific scenario.

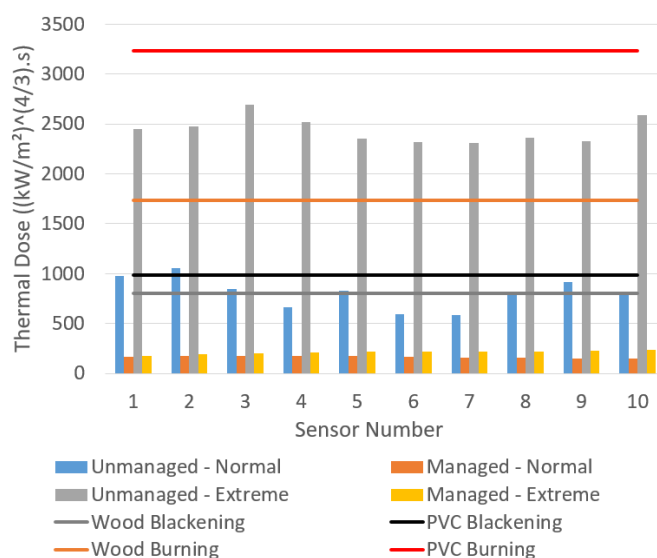


Figure 38: Thermal Dose for each sensor positioned on the façade of house number 3 and damages thresholds for wood and PVC.

4.3.3.2. Portugal

The Portuguese scenario was developed by using data from the Living Lab, as outlined in section 2.2 of this document. As illustrated in Figure 4, the WUI scenario is an interface type, including a single house positioned on the top of a hill and facing a forest. A road and an urban area are located on the north side of the house (not considered for the simulation). A numerical domain with dimensions of 460×370×120 m³ was defined based on the locations of the houses and the vegetation, as illustrated in Figure 39. The domain encompasses a significant portion of the vegetation situated downslope, allowing for the fire front to fully develop before reaching the houses. Topographic coordinates were

extracted from a digital terrain model with a 30-metre resolution. The numerical domain was meshed using 50 blocks of 1 m sized hexahedral cells, with each block consisting of 408480 cells.

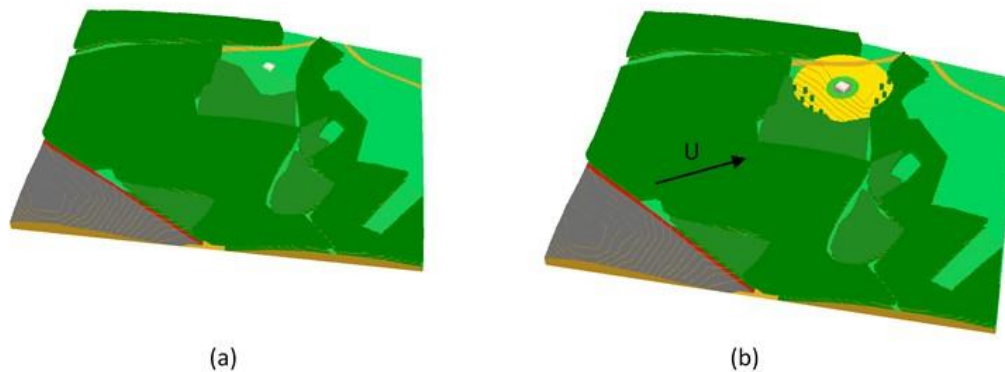


Figure 39: Smokeview representation of the Chilean Living Lab scenarios: (a) Unmanaged Vegetation, (b) Landscaping Management.

The ambient conditions were obtained from the weather station at Porto Airport for the summer seasons from 2020 to 2023. Two distinct weather scenarios were defined, as shown in Table 22. The *normal* scenario reflects the average summer weather conditions, while the *extreme* scenario represents a warmer and drier situation. Wind conditions remained the same in both scenarios. The boundary and ambient conditions for the simulations were set according to the parameters and methodology described in section 4.3.

Table 22 Ambient conditions considered for the Portuguese numerical scenario.

Case	Temperature (°C)	Air Humidity (%)	Wind Speed (km/h)	Wind Gust (km/h)	Wind Direction (°)
Normal	23.0	71	14	41	206
Extreme	38.0	35			

The vegetation modelling was based on plot n°34 of the forest inventory provided by the Portuguese stakeholders. This plot is mainly composed of an 8-years old forest of *Eucalyptus globulus* with an understorey composed of 1.5 m height shrubs. The *Fuel Element* approach was chosen to model the *Eucalyptus globulus* forest canopy. To simplify the simulation inputs and save computational resources, the forest model was reduced to a continuous canopy layer consisting of leaves and twigs, and thus focusing only on the particle classes that contribute most significantly to the fire spread. Thermal degradation of each particle class was treated as described in section 4.3.1.

The associated understorey was modelled with the *Boundary Fuel* approach by using the data from the M-EUC combustible model provided by the stakeholders [93]. The grass

layer was also modelled with a *Boundary Fuel* approach for which data was taken from the literature [88].

Associated bulk density, fuel moisture content and surface to volume ratio for each species and particle class are given in Table 23.

Table 23: Properties of the vegetation used in the Portuguese scenarios. FE: Fuel Element approach, BF: Boundary Fuel approach. Twigs refer to particles of 0 – 2 mm

Fuel modelling approach - Vegetation species - particle class	Bulk Density (kg/m ³)	FMC in Normal Conditions (%)	FMC in Extreme Conditions (%)	Surface to Volume Ratio (m ⁻¹)	Source
FE - <i>Eucalyptus globulus</i> - leaves	0.072	60	50	4200	[88,93-95]
FE - <i>Eucalyptus globulus</i> - twigs	0.036	60	50	5000	
BF - <i>Eucalyptus globulus</i> Understorey	1.096	32	25	4805	
BF - Grassland	1.368	32	5	9770	

Two vegetation management cases were set up. The unmanaged case corresponds to the actual vegetation distribution in the study area as characterized by the inventory data provided by the stakeholders. The managed vegetation case refers to a landscape design that follows the current fire safety regulations in Portugal which define three zones:

- Zone 1 (Grey in Figure 40b) from 0 to 2 m: No vegetation.
- Zone 2 (Green in Figure 40b) from 2 to 10 m: Grass up to 20 cm high with no shrubs or trees.
- Zone 3 (Yellow in Figure 40b) from 10 to 50 m: Grass up to 20 cm high with the *Eucalyptus globulus* trees spaced 10 m from each other.

Both managed and unmanaged vegetation cases were simulated for both standard and extreme weather scenarios. Figure 40 shows the iso-surfaces of HRR per unit of volume at 200 kW/m³ for both vegetation configurations, corresponding to the propagation of the fire front in the direction of the house's façade.

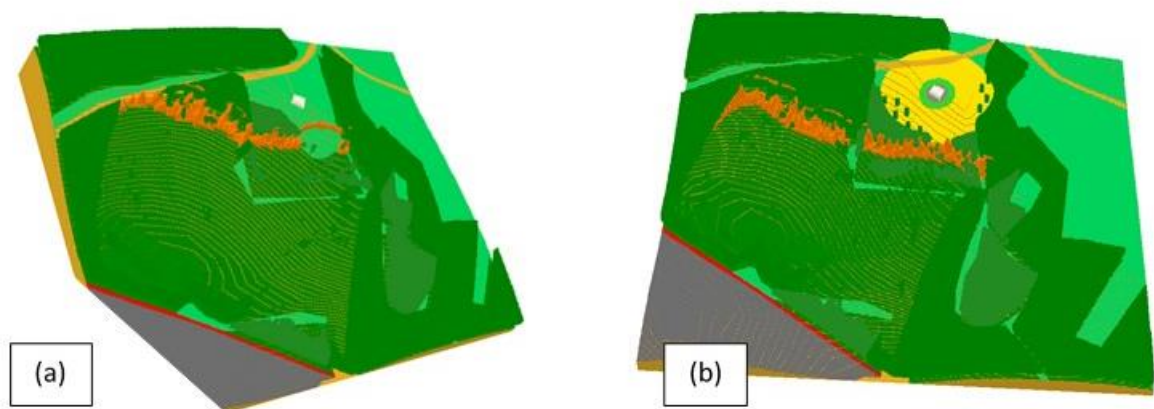


Figure 40: Iso-surface of HRR per unit of volume at 200 kW/m^2 predicted for the Portuguese scenario: (a) Unmanaged vegetation, (b) Managed vegetation

The simulations for the unmanaged vegetation case in both weather conditions result in the propagation of an active crown fire towards the house. The results of the thermal exposure induced by the fire are presented in Table 24. According to these results for the normal weather scenario, the house is exposed between 20 to 40 seconds to a radiant heat flux with maximum values ranging between 60 and 80 kW/m^2 . For the extreme weather scenario, the exposure time is shorter, ranging from 15 to 30 seconds, with a higher radiant heat flux peak, ranging from 80 to 120 kW/m^2 . In both weather conditions, the potential for material damage has been assessed by using the radiant heat dose. The results, presented in Figure 41, demonstrate that for both weather conditions the thresholds for wood and PVC damage have been exceeded for blackening, as well as the wood burning threshold. These results suggest a considerable risk of damage to openings, gutters, the roof of the house and to secondary structures that could be located close to the house.

In contrast, the thermal exposure of the house predicted by the model for the managed vegetation case, shows a significantly lower level of the heat flux peak and exposure time for both weather conditions, as reported in Table 24. In normal weather conditions, the fire front extinguished in zone 3 (i.e., between 10 to 50 m from the house), thus the house is not exposed to a significant thermal impact. This is also evidenced when computing the radiant thermal dose which is considerably lower than the damage thresholds, as shown in Figure 41. However, the results differ slightly with regard to the case of the extreme weather conditions. It can be observed that, despite the presence of defensible zones, the fire front reaches zone 1, where it extinguishes due to the lack of vegetation or combustible fuel. Since the fire reaches the immediate surroundings of the house, the level of heat exposure is higher than in the case of normal weather conditions. The radiant heat flux peaks between 10 to 30 kW/m^2 , with an exposure time ranging from 10 to 15 seconds, depending on the sensor location on the façade. As it can be observed in Figure 41, this heat exposure is not sufficient to damage the wood or PVC materials of the house or secondary elements.

Table 24: Prediction of thermal exposure and material damage for different scenarios of the Portugal living lab simulation case.

Vegetation	Weather	Total Exposition Time (s)	Radiant Heat Flux Peak (kW/m ²)	Total Heat Flux Peak (kW/m ²)	House Impacted	Wood Damage	PVC Damage
Unmanaged	Normal	20-40	60-80	80-100	Yes	Yes	Yes
Managed	Normal	-	0.1-0.8	0.1-0.8	No	No	No
Unmanaged	Extreme	15-30	80-120	90-140	Yes	Yes	Yes
Managed	Extreme	10-15	10-30	10-35	No	No	No

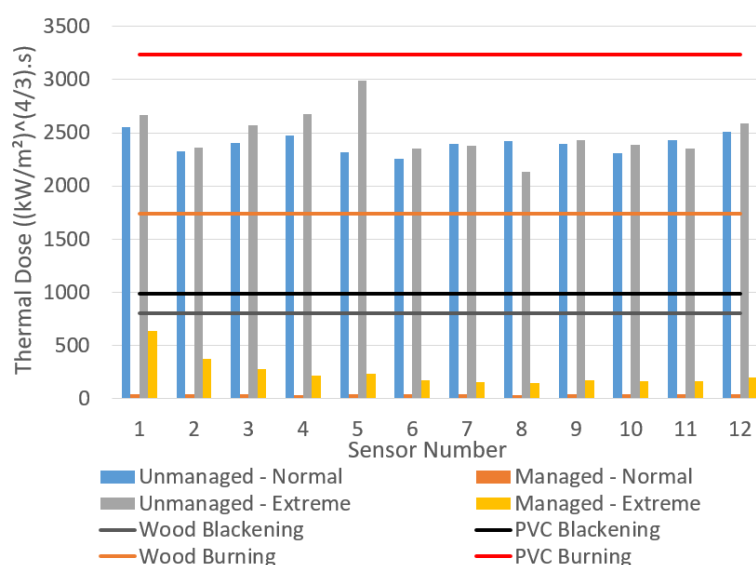


Figure 41: Thermal Dose for each sensor positioned on the façade of house n°3 superimposed with damages threshold.

The results of the simulations conducted for the Portugal Living Lab demonstrate the effectiveness of the fire safety regulations for residential properties located in wildfire prone areas, under normal meteorological conditions. However, although the simulations results indicate that there would be no structural damage to the house for the managed vegetation case in extreme weather conditions, the fire spreads to the immediate surroundings of the house despite the presence of the defensible zone.

4.3.3.3. Conclusions on numerical simulations

Numerical simulations performed for both Living Labs scenarios at WUI scale have demonstrated the importance of the current fire safety regulations in both countries. The obtained numerical results have allowed the characterization and quantification of the thermal exposure of dwellings as well as the prediction of the potential damage of

materials based on the experimental results of the experiments carried out at the EXPLORII platform. Among others, the simulation results of the studied cases have highlighted the following points:

1. When vegetation in the immediate surrounding of the houses is not in compliance with the actual regulations for the considered scenarios, the fire front spreads towards the houses and it impacts the façades in both living labs, regardless of the weather conditions tested.
2. The flame contact with the dwelling façade induces material damage for PVC and wood, essentially blackening but burning can occur.
3. Chilean landscaping regulation efficiently reduces the fire intensity, since the fire extinguishes once in the Zone n°2 (i.e., between 2 to 10 m away from the façade) in both normal and extreme weather conditions. Thus, the dwellings thermal exposure is reduced and no material damage thresholds are exceeded.
4. Portuguese landscaping regulation also reduces the thermal intensity of the fire. For normal weather conditions, the fire extinguishes when reaching zone n°2 (i.e., between 2 to 10 m from the house façade), while for the extreme weather conditions the fire extinguish in zone n°1, very close to the house façade (i.e., between 0 – 2 m). Though, no material damage threshold is exceeded.

5. RECOMMENDATIONS

In addition to the usual recommendations for wildland fire-prone areas, such as using non-combustible materials at the base of walls or for window sills, installing metal mesh screens over vents and chimney holes to prevent the entry of firebrands, closing or encasing open eaves with non-combustible materials, or sealing all gaps around the eaves with caulk [7–11,15,26,27], it is important to pay particular attention to the choice of joinery. These elements have been identified as weak points in buildings exposed to WUI fires [1]. Thanks to our house scale experiments, we were able to learn about the vulnerability of windows and shutters exposed to vegetation fires. In addition, the numerical simulations made it possible to test the effectiveness of the fuel management recommendations or regulations of Chile and Portugal. These data allow us to make the following recommendations:

1. Windows must be double glazed with a minimum glass thickness of 4mm. In our tests, we only observed breakage of the exposed glass of double-glazed windows. This prevented the fire from entering the house, which would not have been the

case with single glazing. We therefore recommend that authorities encourage people living in WUI to change their windows if they have single glazing. The inventory carried out during the project showed that this was the case in 50% and 75% of the homes in the Living Labs of Portugal (Figure 3) and the Canary Islands (Figure 6) respectively. For Chile, there was no information on glazing in the inventory

2. Shutters should be installed on windows to prevent glass breakage. This practice is common in Portugal and the Canary Islands, where more than 60% of the houses in these Living Labs have shutters (Figure 3 and Figure 6). However, it is less common in Chile, where none of the houses in the study area had shutters. In order to increase the fire resistance of Chilean houses, it would therefore be interesting for the authorities to encourage this practice.
3. Aluminium shutters are preferable to wood or PVC shutters, as we have never experienced any damage with this type of shutters in our tests. Aluminium shutters predominate in Portugal, where they account for 73% of the shutters in the living laboratory studied (Figure 3). In the Canary Islands, on the other hand, the shutters are mainly made of wood (Figure 6). This type of shutters prevents the glass from breaking. However, it can blacken or catch fire. When renovating, it would be interesting for the authorities to encourage their replacement with aluminium shutters to increase the fire resistance of the buildings in WUI. For Chile, residents of WUI should be encouraged to install shutters, preferably aluminium.
4. Gutters and roof overhangs must be made of non-combustible materials. Gutters must also be cleaned to prevent plant debris from catching fire. Our experiments have shown that a 1-metre-high hedge at a distance of 3 metres from a house, can produce flames that can reach the façade and roof.
5. To reduce the risk of damage, the contact of the flames with the façade or the roof must be avoided. We therefore recommend that trees and bushes over 1 m in height are kept at least 5 m away from buildings. In addition, fuel management regulations should encourage the creation of a fuel-free zone around buildings to avoid direct flame contact with flames. A distance of 2 m seems to be effective based on the numerical cases tested during the project.
6. The vegetation around buildings in WUI should be chosen from plants that are not easily ignited and have a low combustibility. It is therefore necessary to avoid conifers such as cypresses. In fact, our experiments have shown that a 1-metre-high cypress hedge causes fires comparable to a 2-metre-high cistus hedge (Table 9).
7. The foliar moisture content of vegetation should be kept above 55% to prevent the spread of fire to the plants. Ideally, a foliar moisture content above 85% will prevent ignition. We therefore recommend that the vegetation is kept well watered.

8. Finally, to prevent the spread of fire from wildland to buildings, a sufficient distance between trees must be maintained in the managed area. For eucalyptus, a distance of 10 m seems to be effective based on the numerical cases tested during the project.

6. CONCLUSIONS

The work carried out during the FIRE-RES project provided scientific data on the vulnerability of buildings to wildfire in the wildland-urban interface. The fire resilience tests were carried out on the EXPLORII Platform, which makes it possible to reproduce an operational environment. In addition, the project has allowed the transition from laboratory scale numerical cases to numerical simulations that reproduce a fire reaching a WUI with several dwellings and their surrounding vegetation, corresponding to an operational environment. Therefore, thanks to experimental and numerical studies carried out at field scale, the technology readiness level has moved from TRL 4 - Technology validated in a lab - to TRL 7 - System prototype demonstration in an operational environment.

These studies considered fire radiation and direct contact with flames, but embers effect was not investigated. They provided recommendations on the choice of joinery and the effectiveness of fuel management measures to prevent the risk of wildfire in these areas. However, this type of study needs to be continued. Future studies should take into account the firebrands that can cause the destruction of buildings in the WUI [96–98]. The work carried out here considers a hedge as a fire source and did not take into account the agglomeration of other fuels that could be found nearby, such as secondary structures, fences, wood piles, etc. Such elements could increase the intensity and duration of the fire [50] and may increase the recommended distances and hardening instructions.

7. REFERENCES

- [1] Laranjeira J, Cruz H. Building vulnerabilities to fires at the wildland urban interface. *Advances in forest fire research*, Imprensa da Universidade de Coimbra; 2014, p. 673–84.
https://doi.org/10.14195/978-989-26-0884-6_76.
- [2] Haynes K, Short K, Xanthopoulos G, Viegas D, Ribeiro LM, Bianchi R. Wildfires and WUI Fire Fatalities. In: Manzello SL, editor. *Encyclopedia of Wildfires and Wildland-Urban Interface (WUI) Fires*, Cham: Springer International Publishing; 2020, p. 1–16.
https://doi.org/10.1007/978-3-319-51727-8_92-1.
- [3] Ganteaume A, Camia A, Jappiot M, San-Miguel-Ayanz J, Long-Fournel M, Lampin C. A Review of the Main Driving Factors of Forest Fire Ignition Over Europe. *Environmental Management* 2013;51:651–62. <https://doi.org/10.1007/s00267-012-9961-z>.
- [4] USDA, USDI. Urban wildland interface communities within vicinity of Federal lands that are at high risk from wildfire. *Federal Register* 2001;66:751–77.
- [5] Standards Australia Committee. Australian standard—construction of buildings in bushfire-prone areas AS 3959-2009 2009.
- [6] Diário da República Portuguesa. Despacho n.º 8591/2022, Requisitos para adoção de medidas de proteção relativas à resistência do edifício à passagem do fogo, a constar em ficha de segurança ou projeto de especialidade no âmbito do Regime Jurídico de Segurança contra Incêndio em Edifícios. 2022.
- [7] République Française. Note technique du 29 juillet 2015 relative à la prise en compte du risque incendie de forêt dans les documents de prévention et d'aménagement du territoire. vol. NOR : DEVP1515741N. n.d.
- [8] Greek Government Gazette. Ministerial Decision 3475/2023; Regulation for Fire Protection of Properties within or in Proximity to Forest Areas. 2023:60.
- [9] Federal Emergency Management Agency (FEMA). Home Builder's Guide to Construction in Wildfire Zones. US Department of Homeland Security; 2008.
- [10] Generalitat Valenciana. Guía Metodológica de Actuaciones de Prevención, Defensa y Autoprotección en la Interfaz Urbano-Forest. 2014.
- [11] Standards Association of Australia, Standards Association of Australia, Standards Association of Australia. Committee FP-020 C of B in B-PA. Construction of buildings in bushfire-prone areas. North Sydney, N.S.W.: Standards Australia; 2011.
- [12] International Code Council I. 2021 International Wildland-Urban Interface Code. 2020.
- [13] California Code. California Public Resources Code (PRC) 4291. vol. California Public Resources Code (PRC) 4291. 2022.
- [14] Bénichou N, Adelzadeh, M, Singh J, Goma I, Elsagan N, Kinateder M, et al. National guide for wildland-urban interface fires. National Research Council Canada, issuing body.; 2020.
- [15] Alvarado Ojeda A, Haltenhoff Duarte H, Katelman Villirillo T, Rojo Almarza A, Saballa Espinoza P. Cómo preparo mi casa y entorno frente a los incendios forestales ? Manual de prevención de incendios forestales. Corporación Nacional Forestal Gerencia de Protección Contra Incendios Forestales Departamento de Prevención de Incendios Forestales Sección Silvicultura Preventiva y Comunidad; 2015.
- [16] Stato Italiano. Legge 21 novembre 2000, n. 353 - "Legge-quadro in materia di incendi boschivi." 2000.
- [17] République Française. Code Forestier - « Section 3 : Débroussaillage (Articles L131-10 à L131-16-1) ». 2023.
- [18] Direction départementale des territoires 2B. Arrêté DDT2B/SEBF/FORET/N° 2B-2022-04-05-00006 relatif au débroussaillage légal. vol. Arrêté DDT2B/SEBF/FORET/N° 2B-2022-04-05-00006. 2022.
- [19] Gestão de combustíveis para protecção de edificações. Autoridade Florestal Nacional; 2008.

- [20] Western Australia. Bush Fire Risk Treatment Standards 2020. 2023.
- [21] San-Miguel-Ayaz J, Durrant T, Boca R, Maianti P, Liberta G, Jacome FelixOom D, et al. Advance report on Forest Fires in Europe, Middle East and North Africa 2023. Luxembourg: Publications Office of the European Union; 2024.
- [22] Filkov AI, Tihay-Felicelli V, Masoudvaziri N, Rush D, Valencia A, Wang Y, et al. A review of thermal exposure and fire spread mechanisms in large outdoor fires and the built environment. *Fire Safety Journal* 2023;140:103871. <https://doi.org/10.1016/j.firesaf.2023.103871>.
- [23] Ganteaume A. Role of the ornamental vegetation in the propagation of the Rognac fire, 2016. *Proceedings of the Fire Continuum-Preparing for the future of wildland fire*, vol. Proceedings RMRS-P-78, Missoula: Hood, Sharon M.; Drury, Stacy; Steelman, Toddi; Steffens, Ron, [eds.]; 2018, p. 272–6.
- [24] Caton SE, Hakes RSP, Gorham DJ, Zhou A, Gollner MJ. Review of Pathways for Building Fire Spread in the Wildland Urban Interface Part I: Exposure Conditions. *Fire Technol* 2017;53:429–73. <https://doi.org/10.1007/s10694-016-0589-z>.
- [25] Soto Paredes P, Torres Ordenes D. Informe de Reconocimiento de Especies Área de Interés N°1 de la Comuna de Tomé. CORMA; 2023.
- [26] Orange County Fire Authority Authority. Home Hardening. OCFA Website 2024. <https://ocfa.org/RSG/HomeHardening>.
- [27] Gran Canaria Mosaico. Medidas preventivas. GrancanariamosaicoCom 2024. <https://grancanariamosaico.com/medidas-preventivas/>.
- [28] ISO. ISO/TR 24188:2022 - Large outdoor fires and the built environment — Global overview of different approaches to standardization 2022.
- [29] California Building Standards Code. SFM Standard 12-7A Materials and construction methods for exterior wildfire exposure. n.d.
- [30] Australian Standard. Australian Standard AS 1530.8.1 - Methods of fire tests on building materials, components and structures. Part 8.1: Tests on elements of construction for buildings exposed to simulated bushfire attack - Radiant heat and small flaming sources. 2018.
- [31] Australian Standard. Australian Standard AS 1530.8.2 - Methods of fire tests on building materials, components and structures. Part 8.2: Tests on elements of construction for buildings exposed to simulated bushfire attack - Large flaming sources. n.d.
- [32] International Code Council, INC. 2019 California Building Code, California Code of Regulations, Title 24, Volumes 1 and 2 of Part 2. 2019.
- [33] Fire Safe Marin. Fire-Resistant Windows. FiresafemarinOrg n.d. <https://firesafemarin.org/harden-your-home/fire-resistant-windows/>.
- [34] Australian Standard. AS 1530.4 - Methods for fire tests on building materials, components and structures - Part 4: Fire-resistance test of elements of construction. 2005.
- [35] Prefet de la Haute Corse. Plan de prévention des risques naturels prévisibles “incendies de forêt” Commune de Lucciana -Règlement. Direction départementale des territoires et de la mer; 2013.
- [36] Préfet du Var. Commune de Frejus - Plan de prévention des risques naturels prévisibles d’incendies de foret (P.P.R.I.F) - Règlement intégrant les modifications prescrites par l’arrêté du 19 avril 2012 portant sur les articles 1 et 3 du titre V. 2006.
- [37] Generalitat de Catalunya. Protegeos de los incendios forestales. 2024.
- [38] Diário da República. Consolidação Decreto-Lei n.º 82_2021 de 13 de outubro, Sistema de Gestão Integrada de Fogos Rurais no território continental. 2021.
- [39] AFNOR. Standard Test ISO 5660 - Reaction-to-fire tests - Heat release, smoke production and mass loss rate - Part 1: Heat release rate (cone calorimeter method) and smoke production rate (dynamic measurement) 2020.
- [40] AFNOR. Essais de résistance au feu - Partie 1 : exigences générales. 2020.

- [41] Safe Communities Portugal. Protect your house against rural fires. WwwSafecomunitiesportugalCom 2024. <https://www.safecomunitiesportugal.com/wp-content/uploads/2021/02/Protect-your-House-against-Rural-Fires-ICNF-v-2018-English.pdf>.
- [42] Tihay-Felicelli V, Barboni T, Morandini F, Santoni PA, Pieri A, Luciani C, et al. Overview of the platform for experimentation and awareness-raising on fire risks at wildland urban interfaces (EXPLORII platform). *International Journal of Disaster Risk Reduction* 2023;96:103980. <https://doi.org/10.1016/j.ijdrr.2023.103980>.
- [43] Graziani A, Tihay-Felicelli V, Santoni P-A, Perez-Ramirez Y, Morandini F, Pieri A, et al. Effect of wind turbulences on the burning of a rockrose hedge. *Experimental Thermal and Fluid Science* 2024;150:111036. <https://doi.org/10.1016/j.expthermflusci.2023.111036>.
- [44] Zuiderveld K. Contrast Limited Adaptive Histogram Equalization. *Graphics Gems* 1994:474–85.
- [45] Arthur D, Vassilvitskii S. K-Means++: The Advantages of Careful Seeding. *SODA '07: Proceedings of the Eighteenth Annual ACM-SIAM Symposium on Discrete Algorithms* 2007:1027–35.
- [46] Tihay-Felicelli V, Santoni PA, Gerandi G, Barboni T. Smoke emissions due to burning of green waste in the Mediterranean area: Influence of fuel moisture content and fuel mass. *Atmospheric Environment* 2017;159:92–106. <https://doi.org/10.1016/j.atmosenv.2017.04.002>.
- [47] Morandini F, Santoni PA, Tramoni JB, Mell WE. Experimental investigation of flammability and numerical study of combustion of shrub of rockrose under severe drought conditions. *Fire Safety Journal* 2019;108:102836. <https://doi.org/10.1016/j.firesaf.2019.102836>.
- [48] Ganteaume A, Jappiot M, Lampin C, Guijarro M, Hernando C. Flammability of Some Ornamental Species in Wildland–Urban Interfaces in Southeastern France: Laboratory Assessment at Particle Level. *Environmental Management* 2013;52:467–80. <https://doi.org/10.1007/s00267-013-0067-z>.
- [49] Hedayati F, Stansell C, Gorham D, Quarles SL. *Wildfire Research Near-Building Noncombustible Zone*. Insurance Institute for Business & Home Safety; 2018.
- [50] Maranghides A, Link ED, Hawks S, McDougald J, Quarles SL, Gorham DJ, et al. *WUI Structure/Parcel/Community Fire Hazard Mitigation Methodology*. National Institute of Standards and Technology; 2022.
- [51] Lopes RFR, Modarres M, Rodrigues JPC, Almeida M. Experimental demonstration test of damages in houses caused by wildland-urban interface fires. *Fire Safety Journal* 2023;141:103934. <https://doi.org/10.1016/j.firesaf.2023.103934>.
- [52] O'Connor DJ. The Building Envelope: Fire Spread, Construction Features and Loss Examples. In: Hurley MJ, Gottuk D, Hall JR, Harada K, Kuligowski E, Puchovsky M, et al., editors. *SFPE Handbook of Fire Protection Engineering*, New York, NY: Springer New York; 2016, p. 3242–82. https://doi.org/10.1007/978-1-4939-2565-0_86.
- [53] Hurley MJ. *SFPE Handbook of Fire Protection Engineering Fifth Edition Volume I*. Springer. 2016.
- [54] Shields TJ, Silcock GWH, Flood MF. Performance of a single glazing assembly exposed to enclosure corner fires of increasing severity. *Fire and Materials* 2001;25:123–52. <https://doi.org/10.1002/fam.764>.
- [55] Wang Y, Wang Q, Wen JX, Sun J, Liew KM. Investigation of thermal breakage and heat transfer in single, insulated and laminated glazing under fire conditions. *Applied Thermal Engineering* 2017;125:662–72. <https://doi.org/10.1016/j.applthermaleng.2017.07.019>.
- [56] Wang Y, Li K, Su Y, Lu W, Wang Q, Sun J, et al. Determination of critical breakage conditions for double glazing in fire. *Applied Thermal Engineering* 2017;111:20–9. <https://doi.org/10.1016/j.applthermaleng.2016.09.079>.
- [57] Mowrer FW. *Window Breakage Induced by Exterior Fires*. National Institute of Standards and Technology; 1998.

- [58] Harada K, Enomoto A, Uede K, Wakamatsu T. An Experimental Study On Glass Cracking And Fallout By Radiant Heat Exposure. *Fire Saf Sci* 2000;6:1063–74. <https://doi.org/10.3801/IAFSS.FSS.6-1063>.
- [59] Skelly MJ, Roby RJ, Beyler CL. An Experimental Investigation of Glass Breakage in Compartment Fires. *Journal of Fire Protection Engineering* 1991;3:25–34. <https://doi.org/10.1177/104239159100300103>.
- [60] CA Pub Res Code. Public Resources Code - PRC Division 4. Forests, Forestry and range and forage lands. Part 2 - Protection of ofrest, range and forage lands. Chapter 3. Mountainous, Forest-, Brush- and Grass-Covered Lands § 4291. 2022.
- [61] Orange County Fire Authority Authority. Vegetation Management Maintenance Guidelines for Property Owners. 2022.
- [62] Regione Toscana. Piano AIB 2023-2025. Regione Toscana Settore Forestazione. Agroambiente, Risorse idriche nel settore agricolo. Cambiamenti climatici.; 2023.
- [63] Regione Abruzzo. Piano AIB - Piano regionale de previsione, prevenzione e lotta attiva contro gli incendi boschivi 2023-2025. genzia Regionale di Protezione Civile; 2023.
- [64] Comunitat Valenciana. Decreto Legislativo 1/2021, de 18 de junio, del Consell de aprobación del texto refundido de la Ley de ordenación del territorio, urbanismo y paisaje. 2021.
- [65] Ministerio del Interior. Real Decreto 893/2013, de 15 de noviembre, por el que se aprueba la Directriz básica de planificación de protección civil de emergencia por incendios forestales. vol. BOE-A-2013-12823. 2013.
- [66] Órgano Consejería de Economía, Hacienda y Seguridad. Decreto 60/2014, de 29 de mayo, por el que se aprueba el Plan Especial de Protección Civil y Atención de Emergencias por Incendios Forestales de la Comunidad Autónoma de Canarias (INFOCA). 2014.
- [67] Hawley LF. Theoretical Considerations Regarding Factors which Influence Forest Fires. *Journal of Forestry* 1926;24:756–63. <https://doi.org/10.1093/jof/24.7.756>.
- [68] Richards LW. Effect of certain chemical attributes of vegetation on forest inflammability. *Journal of Agricultural Research* 1940;833–8.
- [69] Fons WL. Analysis of Fire Spread in Light Forest Fuels. *Journal of Agricultural Research* 72 (3): 92-121 1946;72:92–121.
- [70] Rothermel RC. A mathematical model for predicting fire spread in wildland fuels. Res Pap INT-115 Ogden, UT: US Department of Agriculture, Intermountain Forest and Range Experiment Station 40 p 1972;115.
- [71] Plucinski MP, Anderson WR, Bradstock RA, Gill AM. The initiation of fire spread in shrubland fuels recreated in the laboratory. *International Journal of Wildland Fire* 2010;19:512–20.
- [72] Possell M, Bell T. The influence of fuel moisture content on the combustion of Eucalyptus foliage. *International Journal of Wildland Fire* 2013;22:343–52. <https://doi.org/10.1071/WF12077>.
- [73] Pellizzaro G, Duce P, Ventura A, Zara P. Seasonal variations of live moisture content and ignitability in shrubs of the Mediterranean Basin. *Int J Wildland Fire* 2007;16:633–41.
- [74] Luciani C, Tihay-Felicelli V, Martinent B, Santoni PA, Morandini F, Barboni T. Influence of fuel moisture content on the burning of cistus shrubs exposed to a low-intensity fire. *Fire Safety Journal* 2024;146:104168. <https://doi.org/10.1016/j.firesaf.2024.104168>.
- [75] Morandini F, Santoni PA, Tramoni JB, Mell WE. Experimental investigation of flammability and numerical study of combustion of shrub of rockrose under severe drought conditions. *Fire Safety Journal* 2019;108:102836. <https://doi.org/10.1016/j.firesaf.2019.102836>.
- [76] Meerpoel-Pietri K, Tihay-Felicelli V, Graziani A, Santoni P-A, Morandini F, Perez-Ramirez Y, et al. Modeling with WFDS Combustion Dynamics of Ornamental Vegetation Structures at WUI: Focus on the Burning of a Hedge at Laboratory Scale. *Combustion Science and Technology* 2023;195:3181–211. <https://doi.org/10.1080/00102202.2021.2019235>.

- [77] Dahale A, Ferguson S, Shotorban B, Mahalingam S. Effects of distribution of bulk density and moisture content on shrub fires. *International Journal of Wildland Fire* 2013;22:625–41.
- [78] Thomas JC. Improving the understanding of fundamental mechanisms that influence ignition and burning behavior of porous wildland fuel beds. Ph.D. University of Edinburgh, 2017.
- [79] Chastagner G. Factors affecting the moisture levels of cut Christmas trees. IAAI Annual General Meeting 2001.
- [80] Santana VM, Marrs RH. Flammability properties of British heathland and moorland vegetation: Models for predicting fire ignition. *Journal of Environmental Management* 2014;139:88–96. <https://doi.org/10.1016/j.jenvman.2014.02.027>.
- [81] Masinda MM, Sun L, Wang G, Hu T. Moisture content thresholds for ignition and rate of fire spread for various dead fuels in northeast forest ecosystems of China. *J For Res* 2021;32:1147–55. <https://doi.org/10.1007/s11676-020-01162-2>.
- [82] Mell W, Jenkins MA, Gould J, Cheney P. A physics-based approach to modelling grassland fires. *Int J Wildland Fire* 2007;16:1. <https://doi.org/10.1071/WF06002>.
- [83] Mell W, Maranghides A, McDermott R, Manzello SL. Numerical simulation and experiments of burning douglas fir trees. *Combustion and Flame* 2009;156:2023–41. <https://doi.org/10.1016/j.combustflame.2009.06.015>.
- [84] Meerpoel-Pietri K, Tihay-Felicelli V, Graziani A, Santoni P-A, Morandini F, Perez-Ramirez Y, et al. Modeling with WFDS Combustion Dynamics of Ornamental Vegetation Structures at WUI: Focus on the Burning of a Hedge at Laboratory Scale. *Combustion Science and Technology* 2022:1–31. <https://doi.org/10.1080/00102202.2021.2019235>.
- [85] Perez-Ramirez Y, Mell WE, Santoni PA, Tramonì JB, Bosseur F. Examination of WFDS in Modeling Spreading Fires in a Furniture Calorimeter. *Fire Technol* 2017;53:1795–832. <https://doi.org/10.1007/s10694-017-0657-z>.
- [86] Sánchez-Monroy X, Mell W, Torres-Arenas J, Butler BW. Fire spread upslope: Numerical simulation of laboratory experiments. *Fire Safety Journal* 2019;108:102844. <https://doi.org/10.1016/j.firesaf.2019.102844>.
- [87] Terrei L, Lamorlette A, Ganteaume A. Modelling the fire propagation from the fuel bed to the lower canopy of ornamental species used in wildland–urban interfaces. *Int J Wildland Fire* 2019;28:113. <https://doi.org/10.1071/WF18090>.
- [88] Moinuddin KAM, Sutherland D, Mell W. Simulation study of grass fire using a physics-based model: striving towards numerical rigour and the effect of grass height on the rate of spread. *Int J Wildland Fire* 2018;27:800. <https://doi.org/10.1071/WF17126>.
- [89] Moinuddin KAM, Sutherland D. Modelling of tree fires and fires transitioning from the forest floor to the canopy with a physics-based model. *Mathematics and Computers in Simulation* 2020;175:81–95. <https://doi.org/10.1016/j.matcom.2019.05.018>.
- [90] Mueller E, Mell W, Simeoni A. Large eddy simulation of forest canopy flow for wildland fire modeling. *Can J For Res* 2014;44:1534–44. <https://doi.org/10.1139/cjfr-2014-0184>.
- [91] McGrattan K, Hostikka S, McDermott R, Floyd J, Weinschenk C, Overholt K. Fire dynamics simulator technical reference guide volume 1: mathematical model. NIST Special Publication 2013;1018:175.
- [92] Jarrin N. Synthetic Inflow Boundary Conditions for the Numerical Simulation of Turbulence. n.d.
- [93] Fernandes P, Loureiro C. Modelos de combustível florestal para Portugal - Documento de referência, versão de 2021. 2022.
- [94] Nunes L, Pasalodos-Tato M, Alberdi I, Sequeira AC, Vega JA, Silva V, et al. Bulk Density of Shrub Types and Tree Crowns to Use with Forest Inventories in the Iberian Peninsula. *Forests* 2022;13:555. <https://doi.org/10.3390/f13040555>.
- [95] Scott J H, Burgan R E. Standard Fire Behavior Fuel Models: A Comprehensive Set for Use with Rothermel’s Surface Fire Spread Model. USDA Forest Service; 2005.

- [96] Maranghides A, Mell W. A Case Study of a Community Affected by the Witch and Guejito Wildland Fires. *Fire Technology* 2011;47:379–420. <https://doi.org/10.1007/s10694-010-0164-y>.
- [97] Westhaver A. Why Some Homes Survived: Learning from the Fort McMurray Wildland/urban Interface Fire Disaster. ICLR Research Paper Series - Number 56 2017.
- [98] Leonard J, Blanche R. Investigation of bushfire attack mechanisms involved in house loss in the ACT Bushfire 2003. Bushfire CRC Report CMIT-2005-377(Melbourne) 2005.
- [99] Diário da República. Decreto-Lei n.º 220/2008, de 12 de novembro. 2008.

8. ANNEX

8.1. Annex 1: Summary of test methods used to test built elements [28]

Tested structural element	Country	Method	Radiative effect scenario	Firebrands scenario	Wind effect scenario	Others
Roofs	Japan	ISO 12468-1	No	Cribs placed on roof surface. of different types according to a building protection zone criteria (FPZ. QFPZ. “Low-flame-spread”)	No	—
	USA / Canada	CAN/ULC-S107 ASTM E108 UL 790 NFPA 276	Flames from a calibrated burner	Burning standard brands. Intermittent / cyclic flame exposure test	Yes. The spread of flame test is conducted at a 5.4 m/s (12 mph) wind speed.	
	France	CEN TS 1187 (test 3)	Exposure to a radiant panel of 10-12.5 kW/m ² (includes slope angle effect of the roof) during 30 min	Standard cribs placed on roof surface	In some extent. using a blower: for fire propagation on roof only. not for hot gases	—
Exterior walls Facades	Japan	ISO 834 Fire resistance	Yes Based on interior fire exposure	No	No	Adapted for long-duration exposure scenarios

D2.3 QUALITY STANDARD FOR WUI ARCHITECTURE AND LANDSCAPE DESIGN

Tested structural element	Country	Method	Radiative effect scenario	Firebrands scenario	Wind effect scenario	Others
		JIS A 1310 Reaction to fire for façades	Main façade: 1.8 m × 4.1 m. wing façade (option- al): 0.9 m × 4.1 m Opening in main façade: 0.9 m × 0.9 m Fire source: propane (approx. 900 kW). test duration: 20 min.	No	No	
	USA / Canada	USA – ASTM E119 or UL 263 Canada – CAN/ ULC-S101	Yes – USA – Fire resistance can be based on interior or exterior fire exposure. Yes – Canada – Fire resistance based on interior fire exposure only	No	No	Internal fire aggression. Adapted for long-duration exposure scenarios
	USA	SFM 12-7A-1 ASTM E2707	Yes 10 min exposure to 150 kW fire. reflective of plants. trash. deck. etc. beside the wall	—	—	External fire aggression. Adapted for short-duration exposure scenarios
	France	ISO 834 EN 1363-2	General ignition-resistant material. internal fire. Based on interior fire exposure	No	No	Adapted for long-duration exposure scenarios

D2.3 QUALITY STANDARD FOR WUI ARCHITECTURE AND LANDSCAPE DESIGN

Tested structural element	Country	Method	Radiative effect scenario	Firebrands scenario	Wind effect scenario	Others
			General ignition-resistant material. external fire. Based on exterior fire exposure (reaching 660 °C after 30 min)	No	No	Adapted for long-duration exposure scenarios
		Facades LEPIR2	A two-level facade. with fire starting in the lower compartment (fire of 600 kg of wood cribs). and openings at the two levels (no glass in the generic setup). A 30 min fire exposure is performed	No	No	—
	Australia	AS 1530.8.1 AS 1530.8.2	4+1 scenarios: - Direct flame impingement. based on interior fire exposure - 4 scenarios of distant flame impingement: radiant panel (or radiation produced from furnace) at exposures of 12.5. 19. 29. or 40 kW/m ² for 10 min	Burning debris simulated by standard wood cribs placed beside the wall.	No	Specific to wildland fires exposure.
Vents	USA	ASTM E2886	No	Firebrand generator (fan)	No	Also contains flame intrusion test using different test procedures

D2.3 QUALITY STANDARD FOR WUI ARCHITECTURE AND LANDSCAPE DESIGN

Tested structural element	Country	Method	Radiative effect scenario	Firebrands scenario	Wind effect scenario	Others
Decks	USA	SFM 12-7A- 4 ASTM E2632 ASTM E2736	Flame of 80 kW for 3 min. for 2 scenarios of deck ignited by firebrands accumulation: under or over the deck	Standard burning brand placed over the deck. with a fan blowing an air flow of approximately 5.4 m/s (12 mph) over the specimen for 40 min	No in ASTM E 2736 / SFM 12-7A-4 Yes in ASTM E2632	Adapted for short-duration exposure scenarios
Eaves Eaves and soffits	USA / Canada	SFM 12-7A- 3 ASTM E2957 CAN/ULC-S114. CAN/ULC-S135	Flame of 300 kW for 10 min Regulated based on combustibility of materials	No	No	Adapted for short-duration exposure scenarios
Windows	USA	SFM 12-7A- 2	150 kW. 100 mm × 1 000 mm diffusion burner under the target window. The specimen is exposed to the flame for 8 min	No	No	—
	Australia	AS 1530.8.1 AS 1530.8.2	Similar to exterior walls			
Other provisions – reaction-to-fire	USA	SFM 12-7A- 5	2 burners of 88 kW for 10 min	No	No	Ignition-resistant material Steiner Tunnel test method ASTM E84

D2.3 QUALITY STANDARD FOR WUI ARCHITECTURE AND LANDSCAPE DESIGN

Tested structural element	Country	Method	Radiative effect scenario	Firebrands scenario	Wind effect scenario	Others
	France	EN 13501-1 M- Classification	Similar to requirements for enclosures	No	No	—

8.2. Annex 2: Use type (UT) and risk categories (CR) in Portuguese law [99]

1. Type use I - Residential
 - **Risk category 1** (reduced risk): height less than or equal to 9m and number of floors below the reference plane less than or equal to 1;
 - **Risk category 2** (moderate risk): height less than or equal to 28m and number of floors below the reference plane less than or equal to 3;
 - **Risk category 3** (high risk): height less than or equal to 50m and number of floors below the reference plane less than or equal to 5;
 - **Risk category 4** (very high risk): height greater than 50m and number of floors below the reference plane greater than 5;

2. Use type II - Parking lots
 - **Risk category 1** (reduced risk): height less than or equal to 9 m. gross area less than or equal to 3200m² and number of floors below the reference plane less than or equal to 1;
 - **Risk category 2** (moderate risk): height less than or equal to 28 m. gross area less than or equal to 9600m² and number of floors below the reference plane less than or equal to 3;
 - **Risk category 3** (high risk): height less than or equal to 28 m. gross area less than or equal to 32000m² and number of floors below the reference plane less than or equal to 5;
 - **Risk category 4** (very high risk): height greater than 28 m. gross area greater than 32000 m² and number of floors below the reference plane greater than 5;

3. Use type III - Administrative Buildings
 - **Risk category 1** (reduced risk): height less than or equal to 9m. workforce less than or equal to 100 people;
 - **Risk category 2** (moderate risk): height less than or equal to 28 m. workforce less than or equal to 1000 people;
 - **Risk category 3** (high risk): height less than or equal to 50 m. workforce less than or equal to 5000 people;
 - **Risk category 4** (very high risk): height greater than 50 m. workforce exceeding 5000 people;

4. Use type IV - School Buildings and Use type V - Nursing Homes and Hospitals
 - **Risk category 1** (reduced risk): height less than or equal to 9 m. staff of less than or equal to 100 people and staff in risk D or E locations¹⁰ of less than or equal to 25 people;
 - **Risk category 2** (moderate risk): height less than or equal to 9 m. staff of less than or equal to 500 people and staff in risk D or E locations of less than or equal to 100 people;

• ¹⁰ Risk location D: location of an establishment where people are bedridden or intended to receive children aged no more than six years or people with limited mobility or ability to perceive and react to an alarm; Risk location E: location of an establishment intended for overnight stays, where people do not have the limitations indicated in risk locations D;

- **Risk category 3** (high risk): height less than or equal to 28 m. staff of less than or equal to 1500 people and staff in risk D or E locations of less than or equal to 400 people;
 - **Risk category 4** (very high risk): height greater than 28m. staff exceeding 1500 people and staff in risk D or E locations exceeding 400 people;
5. Use type VI – Shows and Use type IX- Sports and Leisure Spaces
- **Risk category 1** (reduced risk): height less than or equal to 9 m. no floor below the reference plane and a workforce of less than or equal to 100 people. Or if it is outdoors. a workforce of less than or equal to 1000 people;
 - **Risk category 2** (moderate risk): height less than or equal to 28 m. at most one floor below the reference plane and a workforce of less than or equal to 1000 people. Or if it is open-air. a workforce of less than or equal to 15.000 people;
 - **Risk category 3** (high risk): height less than or equal to 28 m. a maximum of two floors below the reference plane and a workforce of less than or equal to 5000 people. Or if it is open-air. a workforce of less than or equal to 40.000 people;
 - **Risk category 4** (very high risk): height greater than 28 m. more than two floors below the reference plane and staff exceeding 5000 people. Or if it is outdoors. a workforce of more than 40.000 people;
6. Use type VII - Restaurants and Hotels
- **Risk category 1** (reduced risk): height less than or equal to 9 m. staff equal to or less than 100 people and a maximum of 50 people in risk E locations;
 - **Risk category 2** (moderate risk): height less than or equal to 9 m. staff equal to or less than 500 people and a maximum of 200 people in risk E locations;
 - **Risk category 3** (high risk): height less than or equal to 28 m. staff equal to or less than 1500 people and a maximum of 800 people in risk E locations;
 - **Risk category 4** (very high risk): height greater than 28 m. workforce exceeding 1500 people. more than 800 people in risk E locations;
7. Use type VIII - Commercial Buildings
- **Risk category 1** (reduced risk): height less than or equal to 9 m. no floor below the reference plane and a workforce of less than or equal to 100 people;
 - **Risk category 2** (moderate risk): height less than or equal to 28 m. at most one floor below the reference plane and a workforce of less than or equal to 1000 people;
 - **Risk category 3** (high risk): height less than or equal to 28 m. a maximum of two floors below the reference plane and a workforce of less than or equal to 5000 people;
 - **Risk category 4** (very high risk): height greater than 28 m. more than two floors below the reference plane and staff exceeding 5000 people;
8. Use type X - Museums and Art Galleries
- **Risk category 1** (reduced risk): height less than or equal to 9m. workforce less than or equal to 100 people;
 - **Risk category 2** (moderate risk): height less than or equal to 28m. workforce less than or equal to 500 people;
 - **Risk category 3** (high risk): height less than or equal to 28m. workforce less than or equal to 1500 people;
 - **Risk category 4** (very high risk): height greater than 28m. staff exceeding 1500 people;

9. Use type XI - Libraries and Archives

- **Risk category 1** (reduced risk): height less than or equal to 9m. no floor below the reference plane. staff of less than or equal to 100 people and modified fire load not exceeding 5000MJ/m²;
- **Risk category 2** (moderate risk): height less than or equal to 28m. up to one floor below the reference plane. staff of less than or equal to 500 people and modified fire load not exceeding 50000MJ/m²;
- **Risk category 3** (high risk): height less than or equal to 28m. up to two floors below the reference plane. staff of less than or equal to 1500 people and modified fire load not exceeding 150000MJ/m²; **Risk category 4** (very high risk): height greater than 28m. more than two floors below the reference plane. staff exceeding 1500 people and modified fire load exceeding 150000MJ/m²;

10. Type XII use - Industrial. Workshops and Warehouses

- **Risk category 1** (reduced risk): modified fire load not exceeding 500MJ/m². no floor below the reference plane. If outdoors. modified fire load not exceeding 1000MJ/m²;
- **Risk category 2** (moderate risk): modified fire load not exceeding 5000MJ/m². at most one floor below the reference plane. If outdoors. modified fire load not exceeding 10000MJ/m²;
- **Risk category 3** (high risk): modified fire load not exceeding 15000MJ/m². at most one floor below the reference plane. If outdoors. modified fire load not exceeding 30000MJ/m²;
- **Risk category 4** (very high risk): modified fire load greater than 15000MJ/m². more than one floor below the reference plane. If outdoors. modified fire load greater than 30000MJ/m²;



FIRE-RES